

THE ECOLOGY OF DEEP-SEA CHEMOSYNTHETIC
HABITATS, FROM POPULATIONS TO
METACOMMUNITIES

A Dissertation
Submitted to
the Temple University Graduate Board

In Partial Fulfillment
of the Requirements for the Degree
DOCTOR OF PHILOSOPHY

by
Alanna G. Durkin
May 2018

Examining Committee Members:

Erik E. Cordes, Advisory Chair, Biology

Amy Freestone, Biology

Rachel Spigler, Biology

Amanda Demopoulos, External Member, United States Geological Survey

©
Copyright
2018

by

Alanna G. Durkin
All Rights Reserved

ABSTRACT

Chemosynthetic ecosystems are habitats whose food webs rely on chemosynthesis, a process by which bacteria fix carbon using energy from chemicals, rather than sunlight-driven photosynthesis for primary production, and they are found all over the world on the ocean floor. Although these deep-sea habitats are remote, they are increasingly being impacted by human activities such as oil and gas exploration and the imminent threat of deep-sea mining. My dissertation examines deep-sea chemosynthetic ecosystems at several ecological scales to answer basic biology questions and lay a foundation for future researchers studying these habitats.

There are two major varieties of chemosynthetic ecosystems, hydrothermal vents and cold seeps, and my dissertation studies both. My first chapter begins at cold seeps and at the population level by modeling the population dynamics and lifespan of a single species of tubeworm, *Escarpia laminata*, found in the Gulf of Mexico. I found that this tubeworm, a foundation species that forms biogenic habitat for other seep animals, can reach ages over 300 years old, making it one of the longest-lived animals known to science. According to longevity theory, its extreme lifespan is made possible by the stable seep environment and lack of extrinsic mortality threats such as predation. My second chapter expands the scope of my research from this single species to the entire cold seep community and surrounding deep-sea animals common to the Gulf of Mexico. The chemicals released at cold seeps are necessary for chemosynthesis but toxic to non-adapted species such as cold-water corals. Community studies in this area have previously shown that seeps shape community assembly through niche processes. Using

fine-scale water chemistry samples and photographic mapping of the seafloor, I found that depressed dissolved oxygen levels and the presence of hydrogen sulfide from seepage affect foundation taxa distributions, but the concentrations of hydrocarbons released from these seeps did not predict the distributions of corals or seep species. In my third chapter I examine seep community assembly drivers in the Costa Rica Margin and compare the macrofaunal composition at the family level to both hydrothermal vents and methane seeps around the world. The Costa Rica seep communities have not previously been described, and I found that depth was the primary driver behind community composition in this region. Although this margin is also home to a hybrid “hydrothermal seep” feature, this localized habitat did not have any discernible influence on the community samples analyzed. When vent and seep communities worldwide were compared at the family-level, geographic region was the greatest determinant of community similarity, accounting for more variation than depth and habitat type.

Hydrothermal vent and methane seeps are two chemosynthetic ecosystems are created through completely different geological processes, leading to extremely different habitat conditions and distinct sets of related species. However, at the broadest spatial scale and family-level taxonomic resolution, neutral processes and dispersal limitation are the primary drivers behind community structure, moreso than whether the habitat is a seep or a vent. At more local spatial scales, the abiotic environment of seeps still has a significant influence on the ecology of deep-sea organisms. The millennial scale persistence of seeps in the Gulf of Mexico shapes the life history of vestimentiferan

tubeworms, and the sulfide and oxygen concentrations at those seeps determine seep and non-seep species' distributions across the deep seafloor.

ACKNOWLEDGMENTS

My unending gratitude goes out to my advisor Erik Cordes and my committee members Amy Freestone, Rachel Spigler, and Amanda Demopoulos. I am forever indebted to these brilliant scientists for guiding my work, helping me reach my potential as a researcher, and most of all for believing that I could finish this project when I did not believe in myself. They have supported me with an endless supply of guidance and mentorship, and Erik has also demonstrated an endless supply of patience despite my best attempts to find its limit. Besides inspiring me to appreciate all that science has to offer, Erik also gave me one of the greatest gifts of my life: the opportunity to work at sea.

Of those working at sea, I must first thank the crew members of the *R/V Atlantis*, *R/V Pisces*, and *R/V Ronald Brown* along with the vehicle teams that maintain and pilot the *DSV Alvin*, *AUV Sentry*, and *ROV Jason II*. Without their skillful efforts, the data in this dissertation would never have been collected! I am also extremely privileged to have collaborated with so many phenomenal scientists and engineers on cruises. Working together on a ship inevitably bonds people together, and everyone I have spent time with at sea taught me invaluable skills and encouraged me to soar ever higher in life. These people include but are not limited to Jennifer Le, Kris Krasnosky, Ian Vaughn, Caitlin Adams, Charlotte Seid, Ben Moran, Greg Rouse, Shana Goffredi, Victoria Orphan, Sean Mullin, Kat Dawson, Lily Simonson, Erin Henning, Rachel Simister, Helen White, Fanny Girard, Jennifer Vaccaro, Sean Kelley and Andy Billings. I also owe special thanks to anyone who has every measured or extracted a tubeworm!

On land, Temple University has been a bastion of support in so many areas of my development. The biology department has always provided a welcoming atmosphere thanks not just to the faculty but also to the dedicated office staff that keep everything running and make sure the graduate students are taken care of. All of the members of the Cordes Lab have created an amazing team I was proud to be a part of. Jay Lunden, Andrea Quattrini, and Sam Georgian set the bar high for graduate student success and were always willing to lend a hand to help us achieve the same. I am so grateful to Danielle Deleo, Carlos Gomez, Alexis Weinnig, Steve Auscavitch, April Stabbins, and Veronica Radice for the companionship they brought to the lab to help me through difficult challenges. Besides my lab members, I was thrilled to learn alongside many other amazing fellow graduate students including but not limited to Nichole Rigby, Nicole Mazouchova, Janne Pfeiffenberger, Carlee MacPherson Cunningham, Sarah DeVaul Princiotta, Elizabeth Rielly, and Katharine Papacostas.

During my time at Temple, I learned how to be an educator in addition to a researcher. Thank you to all those who taught me to teach, including Evelyn Vleck, Sheryl Love, Dan Spaeth, and the Center for the Advancement of Teaching.

Outside of the biology department, I am thankful I availed myself to Temple's other resources for graduate students through the writing groups and writing retreats offered by the Writing Center as well as the dissertation support group offered through Tuttleman's Counseling Center. These places gave me the opportunity to exchange ideas and make lifelong friends across disciplines, including Diane Evitts, Margaret Janz,

Leslie Allison, Amanda Milena Alvarez, Lorraine Savage, Brittany Webb, Diane Garbow, and my roommate Steffi Kasperek.

Finally, I need to thank my family. Without my mom and dad encouraging me throughout my academic career to pursue my interests, I never would have made it this far. My mom Karen instilled in me a love of reading and language that made spelling hundreds of taxonomic names correctly the easiest part of my research, and I was able to absorb some of my dad Steve's gifts for public speaking and presence in the classroom. My sister Katie has always been there for me, from when we explored the outdoors and collected bugs as children to all of her support as an adult. Moving to Philadelphia brought us closer together geographically and emotionally, and I can't thank her enough for all the meals, kitten parties, and social support from her and her circle of friends and husband Scott! I must also thank my loving ex-husband John Opatz for the support he provided throughout all but the home stretch of my graduate education.

I made it through many trying times thanks to the emotional support of all the animals in my life. Although I don't own my own pets, I know an abundance of wonderful pet owners who let me borrow their animals! Thank you to everyone who has ever let me pet sit for them, and thank you to the stray cats of Temple's campus.

This research would not have been possible without funding from the National Science Foundation, the Bureau of Ocean Energy Management, TDI Brooks International, NOAA's Office of Ocean Exploration and Research and National Oceanographic Partnership Program, and of course Temple University, which funded me through teaching assistantships and the dissertation completion grant.

TABLE OF CONTENTS

	Page
ABSTRACT.....	iii
ACKNOWLEDGMENTS	vi
LIST OF TABLES	xii
LIST OF FIGURES	xiii
CHAPTER	
1. INTRODUCTION	1
1.1 The ecology of deep-sea environments.....	1
1.2 Chemosynthesis in the deep sea.....	4
1.3 From cold seeps to hot vents: the spectrum of chemosynthetic habitats	5
1.3.1 Hydrothermal vents.....	5
1.3.2 Methane seeps	6
1.3.3 Connections between vents and seeps	7
1.4 Tubeworms as an essential foundation species.....	8
1.5 The influence of seeps on the surrounding deep sea.....	10
1.6 Objectives	11
2. EXTREME LONGEVITY IN A DEEP-SEA VESTIMENTIFERAN TUBEWORM AND ITS IMPLICATIONS FOR THE EVOLUTION OF LIFE-HISTORY STRATEGIES	13
2.1 Abstract.....	13

2.2 Introduction.....	14
2.3 Methods.....	16
2.3.1 Collection and <i>in situ</i> growth measurement.....	16
2.3.2 Growth model and individual simulations.....	17
2.3.3 Population simulations.....	21
2.4 Results.....	23
2.5 Discussion.....	27
3. FINE-SCALE HABITAT MAPPING OF THE INFLUENCE OF COLD SEEPS ON DEEP GULF OF MEXICO COMMUNITIES.....	30
3.1 Abstract.....	30
3.2 Introduction.....	31
3.3 Methods.....	35
3.3.1 AUV survey design and data collection.....	35
3.3.2 Photo annotation and data analysis.....	38
3.4 Results.....	40
3.5 Discussion.....	44
4. CHARACTERIZATION OF A HYBRID HYDROTHERMAL SEEP COMMUNITY AND COMMUNITY ASSEMBLY OF CHEMOSYNTHETIC HABITATS.....	49
4.1 Abstract.....	49
4.2 Introduction.....	50
4.3 Methods.....	52

4.3.1 Study site description.....	52
4.3.2 Community sample collection from the Costa Rica margin and analysis	54
4.3.3 Global comparison to published community collections.....	57
4.4 Results.....	60
4.4.1 Regional comparison among Costa Rica margin sites.....	60
4.4.2 Global quantitative analysis	63
4.4.3 Global qualitative analysis.....	67
4.5 Discussion.....	69
5. CONCLUSIONS.....	73
 BIBLIOGRAPHY.....	 76
 APPENDICES	
A. ADDITIONAL GULF OF MEXICO HABITAT MAPS.....	89
B. COSTA RICA MARGIN COMMUNITY ANALYSIS DATA.....	97
C. PERMISSION FOR INCLUSION OF COPYRIGHTED MATERIAL	119

LIST OF TABLES

Table	Page
2.1 Individual simulation results.....	25
2.2 Population simulation results.....	26
3.1 Details of Sentry survey locations	36
3.2 Summary of the presence and absence of each photo category across each site	41
3.3 Summary of GLMM results for each foundation taxa using data from all dives	42
3.4 Summary of GLMM results for each foundation taxa using only data from dives that measured hydrocarbon concentrations.....	42
4.1 Costa Rica Margin community sample locations	55
B1 Costa Rica Margin community sample collection information	97
B2 Costa Rica Margin community sample species abundance data.....	98
B3 Costa Rica Margin community sample species presence-absence data.....	102
B4 Sites included in global family-level community analysis.....	107

LIST OF FIGURES

Figure	Page
2.1 Photograph of stained <i>E. laminata</i> tubes	18
2.2 Relationship between tube size and one year's growth for <i>E. laminata</i> and <i>L. luymesii</i>	19
2.3 Individual growth simulation results	20
3.1 A map of the sites surveyed by <i>Sentry</i> in the Northern Gulf of Mexico	36
3.2 Map of <i>Sentry</i> 's track during a single dive's photo survey	37
3.3 Examples of photo annotation categories	39
3.4 An example from Dive 236 at GC234 showing the habitat mapping process.....	43
4.1 A map of the community collection sites along the Costa Rica Margin	54
4.2 A map of all sites from which comparable family abundance data were collected and used in a quantitative global analysis of seep and vent communities.....	58
4.3 A map of all community samples included in the global analysis and compared using the presence-absence data of families visible in video analysis	59
4.4 A boxplot displaying the range of depths from which communities were sampled for each analysis and habitat type	61
4.5 NMDS of Costa Rica quantitative community samples using distances calculated with Bray-Curtis dissimilarity index	62
4.6 NMDS of Costa Rica qualitative community samples overlaid with a vector representing the correlation between depth and community dissimilarity as fit by R's envfit function.....	63
4.7 NMDS plot of Bray-Curtis distances between global quantitative samples overlaid with a vector representing the correlation of depth with community ordination as fit by R's envfit function	64
4.8 The same NMDS plot of Bray-Curtis distances between all global quantitative samples as Figure 4.7 also overlaid with 95% confidence intervals for each geographic region	65

4.9 NMDS plot of Jaccard distances between all global qualitative samples overlaid with a vector representing the correlation of depth with community ordination as fit by R's envfit function	68
A1 Three maps of Site AT357 showing the dissolved oxygen anomalies, redox potential, and taxa distribution across the site.....	89
A2 Four maps of Site GB535 showing the dissolved oxygen anomalies, hydrocarbon concentrations, redox potential, and taxa distribution across the site	90
A3 Four maps of Site GB903 showing the dissolved oxygen anomalies, hydrocarbon concentrations, redox potential, and taxa distribution across the site	91
A4 Four maps of Site GC266 showing the dissolved oxygen anomalies, hydrocarbon concentrations, redox potential, and taxa distribution across the site	92
A5 Four maps of Site GC354 showing the dissolved oxygen anomalies, hydrocarbon concentrations, redox potential, and taxa distribution across the site	93
A6 Four maps of Site MC751 showing the dissolved oxygen anomalies, hydrocarbon concentrations, redox potential, and taxa distribution across the site	94
A7 Three maps of Site VK826 showing the dissolved oxygen anomalies, redox potential, and taxa distribution across the site.....	95
A8 Three maps of Site VK906 showing the dissolved oxygen anomalies, redox potential, and taxa distribution across the site.....	96

CHAPTER 1

INTRODUCTION

1.1 The ecology of deep-sea environments

The deep sea is commonly defined as all ocean deeper than 200m below sea surface because this is the depth beyond which, depending on water clarity and seasonal variation, photosynthesis is no longer possible (Thistle, 2003). This biome makes up the majority of the ocean and 95% of all habitable volume on the planet (Ramirez-Llodra et al., 2010). Below this designated border, depth continues to be the single most important variable for shaping species distributions and ecological interactions. Although the deep open ocean seems to be a homogenous ecosystem, many environmental variables change in predictable ways with depth and challenge organisms' ability to adapt their physiology to these changing conditions. In many ways, the depth below the surface in the ocean is analogous to the effects of elevation in terrestrial ecosystems.

One similarity with elevation on land is that temperature is tightly linked to depth in the ocean as colder, denser water sinks to the bottom of the water column (Angel, 2003). Temperature drops steadily with depth and reaches temperatures within a few degrees of freezing at abyssal depths. With no seasonal variation to speak of at these depths, deep-sea organisms adapt to a narrow range of environmental conditions (Somero, 1995). Most species cannot survive small changes in temperature and pressure that occur just a few hundred meters shallower or deeper in the same geographic location (McClain & Hardy, 2010).

Another environmental variable that changes with depth is oxygen. Generally oxygen levels decrease to a minimum level around the thermocline at the bottom of the photic zone and then increase slightly with depth to the seafloor (Angel, 2003). The physical limit of oxygen saturation state is primarily determined by temperature with gases dissolving more readily in colder water. There are biological controls that can depress oxygen levels below the saturation state, however. Oxygen is consumed in the water column by aerobic organisms' respiration and replenished through photosynthesis or mixing with the atmosphere at the surface (Angel, 2003). This balance can be pushed to extremes in deep water areas below highly productive surface waters (Ramirez-Llodra et al., 2010). Phytoplankton blooms can create biomass so rapidly in some coastal upwelling areas around the world that much of this productivity gets exported to deeper waters at higher rates than average. The consumption of this matter below the photic zone depletes oxygen levels and creates an oxygen minimum zone (OMZ). OMZs intersect with benthic habitats over more than a million square kilometers of the seafloor, accounting for 0.35% of the seafloor globally (Helly & Levin, 2004). Other local features such as methane seeps can also locally depress the levels of dissolved oxygen by releasing subsurface waters depleted in oxygen (Tunnicliffe, Juniper, & Sibuet, 2003).

Similar to the effects of elevation in terrestrial ecosystems, depth zonation creates vertical dispersal barriers within the ocean. Species' distributions are limited to vertical ranges not only because of their narrow physiological tolerances, but also due to physical oceanography (Brown & Thatje, 2014). Two depth ranges in the same geographic area may have no exchange of propagules because density profiles keep the two water masses

from mixing with one another (Angel, 2003; A. M. A. M. Quattrini, Baums, Shank, Morrison, & Cordes, 2015; Radice, Quattrini, Wareham, Edinger, & Cordes, 2016). Conversely, two sites on the opposite ends of an ocean basin may have a dispersal connection if they are within the same depth range and found within the same water mass (E. E. Cordes, Carney, et al., 2007; Karine Olu et al., 2010).

The most important biological factor that changes with depth is food input. Because photosynthesis cannot be performed in the deep sea, food webs are limited to the productivity that trickles down from the surface (Thistle, 2003). Surface productivity is consumed by organisms in the water column during its downward journey, causing pelagic biomass to decrease by an order of magnitude from the surface to 1000m depth and then by another order of magnitude down to 4000m (Angel, 2003). Only about 10% of all photosynthetic productivity escapes the photic zone and just 1% reaches the abyssal seafloor (Buesseler et al., 2007; Gage, 2003). Benthic standing stock and biodiversity are shaped by this decreasing energy input with depth (Gage, 2003; Rex & Etter, 2010).

Community composition in the deep benthos is also driven by an essential habitat factor independent of depth: substrate . The vast majority of deep seafloor habitat is wide expanses of soft muddy sediment. This monotonous environment is home to many diverse infaunal communities of smaller sediment-dwelling organisms. Most sessile suspension feeders such as corals and sponges however, cannot live on the mud. They require a hard, rocky substrate to anchor to, and prefer taller formations that offer vertical relief as a way to capture more food particles from the currents flowing above the seafloor (J. M. Roberts, Wheeler, Freiwald, Cairns, & Brooke, 2009). Habitat models

have consistently found hard substrate to be the top predictor of cold-water coral species' distributions across different deep-sea environments when their niche is modeled at a fine enough resolution (Freiwald, Wilson, & Henrich, 1999; Samuel E. Georgian, Shedd, & Cordes, 2014; Guinan, Brown, Dolan, & Grehan, 2009).

1.2 Chemosynthesis in the deep sea

Forty years ago, researchers found an exception to the trend of increasing food limitation with depth when they discovered a vibrant deep sea community with unprecedented densities of animals at the first known hydrothermal vent (Lonsdale, 1977; Van Dover, 2000). The hydrothermal vent could support a high biomass of animals because these organisms were utilizing chemosynthesis, an alternative energy source to photosynthesis (Cavanaugh, Gardiner, Jones, Jannasch, & Waterbury, 1981). Bacteria at the site use reducing chemicals from the fluids flowing out of the seafloor to fix carbon. These primary producers release the food web from dependence on sunlight and surface energy input, allowing animals to thrive in the dark depths of the bottom of the ocean (Carney, 1994).

Chemosynthetic bacteria can be free-living in the environment or living in symbiotic relationships with adapted animal species (Dubilier, Bergin, & Lott, 2008). The microbes can use a number of reducing chemicals to power chemosynthesis including hydrogen sulfide, methane, and hydrogen. A few metazoan taxa that have evolved complex symbioses with bacteria serve as the foundation species for chemosynthetic habitats (Kiel, 2010; Van Dover, 2000). Mytilid mussels and vesicomid clams host bacteria in specialized cells in their gills to ensure a steady supply of oxygen

and hydrogen sulfide (or in the case of the mussels, hydrogen sulfide or methane) to their microbial partners (Taylor & Glover, 2010). The symbiosis with siboglinid tubeworms is so highly derived that these animals have no gut as adults and instead hosts large populations of sulfide-oxidizing symbionts in a specialized organ called the trophosome (Bright & Lallier, 2010). The other primary consumer macrofauna at these sites that don't host chemosynthetic symbionts gain their nutrition by grazing on free-living bacteria. Even the non-chemosymbiotic fauna found at chemosynthetic ecosystems are still highly adapted to these harsh environments and often endemic to them (Bachraty, Legendre, & Desbruyères, 2009; E. E. Cordes, Bergquist, & Fisher, 2009).

1.3 From cold seeps to hot vents: the spectrum of chemosynthetic habitats

The harsh qualities of these habitats always include exposure to reducing chemicals, but other physical conditions vary depending on the geological origin of the habitat.

1.3.1 Hydrothermal vents

The first deep-sea chemosynthetic habitats discovered were hydrothermal vents at the Galapagos Ridge in 1977 (Lonsdale, 1977). At this mid-ocean spreading center, heated seawater laden with minerals and chemicals leached from subsurface magma spewed out of the seafloor (Van Dover, 2000). The chimneys formed by minerals precipitated from the fluids create a bare rock habitat where the water containing dissolved, toxic metals can reach temperatures up to 401°C (Webber, Roberts, Murton, & Hodgkinson, 2015). Despite these extreme conditions, researchers found large communities dominated by the giant vestimentiferan tubeworm *Riftia pachyptila*, large

vesicomylid clams, and bathymodiolin mussels along with many other animals adapted to the local environment (Lonsdale, 1977; Van Dover, 2000).

Since that first discovery, hundreds more vent sites have been discovered around the world in every ocean basin (Beaulieu, Baker, German, & Maffei, 2013). These habitats occur at mid-ocean spreading centers and back-arc basins where seawater has the ability to flow into the crust and interact with magma (Beaulieu et al., 2013; Van Dover, 2000). As scientists have discovered more vent locations, they've found biogeographic variability in the communities that live there (Bachraty et al., 2009). Vestimentiferan tubeworms including *R. pachyptila* and other related species dominate vents across the eastern Pacific from the Juan de Fuca ridge down to the Southern East Pacific Rise. Tubeworms are completely lacking from the Atlantic, however, and vents along the Mid-Atlantic ridge are dominated by alvinocarid swarming shrimp instead. In another variation, the most abundant fauna at vent fields of the southeast Pacific in the region of the Lau Spreading Center are “hairy” snails of the genus *Alviniconcha* that cultivate chemosynthetic bacterial populations on projections on their shells. Bivalves of the genus *Bathymodiolus* have cosmopolitan range. More than 600 species have been described from vent communities, 70% of which are endemic to these habitats (Daniel Desbruyères, Segonzac, & Bright, 2006; Ramirez-Llodra et al., 2010).

1.3.2 Methane seeps

A decade after hydrothermal vents were discovered in the Pacific, vestimentiferan tubeworms and other vent-like taxa were collected from the Gulf of Mexico (Paull et al., 1984). These animals also gained nutrition from chemosynthetic bacteria, but without

spreading centers or potential hot vents in the area researchers knew there must be different geological forces providing reducing chemicals (Paull, Jull, Toolin, & Linick, 1985). Similar to vents, reducing chemicals were being released from discrete sites along the seafloor, but in this case the flow rate was much lower and the fluids were not heated above ambient temperature above the seafloor, leading to the designation of these new sites as “cold seeps.” Instead of the dramatic smoking chimneys created at mid-ocean spreading centers, fluids here were slowly seeping through conduits in the kilometer-thick layer of salt that underlays the Gulf of Mexico (Aharon, Roberts, & Snelling, 1992; Kennicutt, McDonald, Comet, Denoux, & Brooks, 1992). Many bacteria at seeps rely directly on the oxidation of methane for chemosynthesis, and through the actions of a consortium of microbes, the hydrocarbons released at these sites are also converted to hydrogen sulfide (Boetius, Ravensschlag, & Schubert, 2000; Joye et al., 2004).

Seeps have since been discovered at passive and active margins around the world and are caused by a range of geologic forces (Sibuet & Olu, 1998). These sites have a similar community structure to vents at the family level with the dominant macrofauna consisting of vestimentiferan tubeworms, bathymodiolin mussels, or vesicomylid clams (Kiel, 2010).

1.3.3 Connections between vents and seeps

Due to the starkly different geological conditions that give rise to seeps and vents, there is little taxonomic overlap between these two habitats at the species level. Of all the currently described species known from deep-sea chemosynthetic ecosystems, less than

10% are shared globally between seeps and vents (Tunnicliffe et al., 2003). This overlap is higher when the vent and seep communities are located in closer geographic proximity to one another, reaching shared species of up to 28% at the vents and seeps of Japan (Watanabe, Fujikura, Kojima, Miyazaki, & Fujiwara, 2010). Recent studies have also found that sedimented vents serve as a critical middle ground between hydrothermal vents and cold seeps (Kiel, 2016; Portail et al., 2015). Sedimented vents create a similar physical habitat to seeps with their predominantly soft mud substrate, in contrast to the hard basaltic substrate colonized by animals at typical vents. Community similarity was higher than predicted between neighboring sedimented vents and seeps in the Guaymas Basin because of this driving factor of substrate (Portail et al., 2015). A unique instance of co-existence between seep and vent species was found in the recently discovered “hydrothermal seep” site of the Costa Rica Margin (L. a. Levin et al., 2012). The existence of seeps along the Costa Rica margin has been known for more than two decades, and there are more than 100 likely seep sites in this region (Bohrmann, Heeschen, Jung, Weinrebe, Baranov, Cailleau, Heath, Hühnerbach, et al., 2002; Sahling et al., 2008a). The hybrid site Jaco Scar appeared initially to be another tubeworm-dominated seep site until researchers observed heated, shimmering water flowing from the base of a tubeworm bush and recognized vent-endemic species among the seep community members (L. a. Levin et al., 2012).

1.4 Tubeworms as an essential foundation species

Many vents and seep communities are dominated by vestimentiferan tubeworms (Bright & Lallier, 2010). These animals not only provide a nutritional link between their

intracellular chemosynthetic symbionts and the food web species that consume their tissues, but they also create biogenic habitat with their tall, slender chitinous tubes (E. E. Cordes, Becker, Hourdez, & Fisher, 2010; E. Cordes, Hourdez, Predmore, Redding, & Fisher, 2005). At methane seeps, tubeworm species such as *Lamellibrachia luymesii* also serve as ecosystem engineers (E. E. Cordes et al., 2009). Their posterior “roots” facilitate a microbial consortium that recycles sulfur species, allowing the seep community to persist after seepage has ceased, and raises the local alkalinity to allow for the precipitation of authigenic carbonate rocks (Boetius et al., 2000; E. E. Cordes, Arthur, Shea, Arvidson, & Fisher, 2005).

One tubeworm species adapted to life at vents, *R. pachyptila*, is remarkable for being one of the fastest growing animals on the planet, enabling it to take advantage of these rapidly changing, ephemeral habitats (Lutz et al., 1994). In the more temporally stable environment of seeps, *L. luymesii*, broke a different record. This seep tubeworm became famous as the longest-lived non-colonial animal (at the time its lifespan was estimated) (DC Bergquist, Williams, & Fisher, 2000). Based on *in situ* growth rates and model predictions, *L. luymesii* was estimated to reach ages of 250 years (DC Bergquist et al., 2000). Since then the growth rates of another species of seep tubeworm, *Seepiophila jonesii*, have also been studied and shown this species to reach ages of 250-300 years using similar methods (E. E. Cordes, Bergquist, Redding, & Fisher, 2007).

These two species dominate seeps of the upper slope of the Gulf of Mexico, but a third species that dominates seeps deeper than 1000m in the Gulf of Mexico, *Escarpia laminata*, is relatively unstudied and nothing is known about the ages this tubeworm

reaches (E. E. Cordes et al., 2009). It is expected to reach lifespans at least as old as *L. luymesi* and *S. jonesi* and has the potential to be older given that it occupies deeper habitats at colder temperatures.

The lifespans of these foundation species are essential to our understanding of seeps to give us an idea of the continuity these habitats experience over centuries. The extraordinary ages of these animals also raise basic biological questions about the evolution of longevity (Williams, 1957).

1.5 The influence of seeps on the surrounding deep sea

Although seeps represent a unique oasis of productivity in the food-poor desert of the deep sea, they are not isolated from the surrounding environment (Carney, 1994; Lisa Ann Levin et al., 2016). The productivity can get exported to background community through mechanisms such as migratory species feeding at seeps or the buoyant bubble plumes that can deliver hydrocarbons to the overlying water column (Lisa Ann Levin et al., 2016). The authigenic carbonates produced at seeps become valuable hard substrate for surrounding species after seepage has ceased (Baco, Rowden, Levin, Smith, & Bowden, 2010; Samuel E. Georgian et al., 2014; Guinan et al., 2009).

New seeps in the Gulf of Mexico release fluids with enough hydrogen sulfide to keep away non-endemic species that can't tolerate the toxicity. As the seeps age, the authigenic carbonates produced at the seep begin to block off seepage and reduce the sulfide concentrations in the water column (D. C. Bergquist et al., 2003; E. E. Cordes et al., 2006; E. Cordes et al., 2005). At the oldest vestimentiferan-dominated seeps, sulfide is completely absent from the water column, and the tubeworms themselves are only able

to persist through their posterior “roots” they’ve anchored deep in the sediment (E. E. Cordes et al., 2006; E. Cordes et al., 2005). These roots are home to a consortium of microbes that couple the anaerobic oxidation of methane with sulfate reduction to replenish the pool of hydrogen sulfide utilized by the tubeworm’s symbionts (E. E. Cordes et al., 2005; E. E. Cordes, Bergquist, Shea, & Fisher, 2003).

In addition to hundreds of known seep sites, the Gulf of Mexico is home to many deep-sea background fauna including extensive cold-water coral reefs (E. E. Cordes et al., 2008; Samuel E. Georgian et al., 2014; Mienis et al., 2012; A. M. Quattrini, Gómez, & Cordes, 2017). Most corals and coral-associated species are found away from seep sites, likely due to their intolerance of sulfide or high concentrations of hydrocarbons, but one octocoral species, *Callogorgia delta*, has been demonstrated to prefer habitats closer to seeps (Evans, 1967; A. M. Quattrini et al., 2013, 2017). Although there is a clear difference between seep and non-seep communities, it is unknown how far seep influence extends from the center of the seep and what environmental factors most influence community composition.

1.6 Objectives

This dissertation aims to address the questions raised here about deep-sea chemosynthetic habitats at multiple ecological scales, from population biology to global biogeography.

The first chapter of this dissertation investigates the basic biology of a single species: the seep tubeworm *E. laminata*. Using *in situ* growth rates and models similar to those applied to previous seep tubeworm aging studies, the age of *E. laminata* is

estimated with both individual and, for the first time, population-wide growth simulations.

The second chapter expands its scope from one seep foundation species to the whole community by examining multiple cold seeps across the Gulf of Mexico. The aim of this study is to determine which chemical properties of seep environments drive the niche processes behind community assembly in this region. The habitat of both the seeps and neighboring benthic habitat are mapped at a fine scale using paired downward-looking photos and water chemistry data. This comprehensive dataset is able to answer questions about how far the barrier of a seep extends beyond the center of seepage and which habitat factors act as environmental filters and best predict the distributions of seep and non-seep species.

In the third chapter, seep communities in another region, the Costa Rica Margin, are characterized for the first time. Again questions concerning community assembly are addressed by analyzing how community composition changes in response to environmental conditions. The temperature and proximity of each community to the hydrothermal seep at Jaco Scar are compared to community structure to determine whether this feature and/or depth influence species composition in this region. The scope then expands to incorporate community samples from vents and seeps around the world to examine drivers of community assembly across all biogeographic regions and chemosynthetic habitat types.

CHAPTER 2

**EXTREME LONGEVITY IN A DEEP-SEA VESTIMENTIFERAN TUBEWORM
AND ITS IMPLICATIONS FOR THE EVOLUTION
OF LIFE-HISTORY STRATEGIES**

2.1 Abstract

The deep sea is home to many species that have longer life spans than their shallow-water counterparts. This trend is primarily related to the decline in metabolic rates with temperature as depth increases. However, at bathyal depths, the cold-seep vestimentiferan tubeworm species *Lamellibrachia luymesii* and *Seepiophila jonesi* reach extremely old ages beyond what is predicted by the simple scaling of lifespan with body size and temperature. Here we use individual-based models based on *in situ* growth rates to show that another species of cold-seep tubeworm found in the Gulf of Mexico, *Escarpia laminata*, also has an extraordinarily long lifespan, regularly achieving ages of 100-200 years with some individuals older than 300 years. The distribution of results from individual simulations as well as whole population simulations involving mortality and recruitment rates support these age estimates. The low 0.67% mortality rate measurements from collected populations of *E. laminata* are similar to mortality rates in *L. luymesii* and *S. jonesi* and play a role in evolution of the long lifespan of cold seep tubeworms. These results support longevity theory, which states that in the absence of extrinsic mortality threats, natural selection will select for individuals that senesce slower and reproduce continually into their old age.

2.2 Introduction

Within the depths of the ocean, there are extraordinarily long-lived animals including the octopus *Graneledone boreopacifica*, found up to 2000 m deep, with the longest brooding period known for any animal (Robison, Seibel, & Drazen, 2014) and black corals (Antipatharia) more than 4000 years old (Roark, Guilderson, Dunbar, Fallon, & Mucciarone, 2009). Rockfish, a group with closely related species distributed across a broad depth gradient, show a trend of increasing lifespan from 12 to 205 years with increasing maximum depth of occurrence from 37 to 874 m depth (Cailliet et al., 2001). A similar trend of slower growth rates with depth is apparent in the octocorals (Andrews, Cordes, & Mahoney, 2002). The slower pace of life at depth can be explained best by the effects of temperature on metabolism as ambient temperature decreases steadily in deep waters (McClain, Allen, Tittensor, & Rex, 2012).

One of the longest-lived animals on the planet, the cold-seep vestimentiferan tubeworm *Lamellibrachia luymesii* (Polychaeta: Siboglinidae), exhibits lower mortality rates and a longer lifespan than predicted by metabolic scaling according to body size and temperature alone (McClain et al., 2012). Even in a study that created universal scaling laws specifically for deep-sea organisms across the globe using the Metabolic Theory of Ecology, the data from *L. luymesii* were recognized as outliers (McClain et al., 2012). Another Gulf of Mexico cold seep tubeworm, *Seepiophila jonesii*, would also have appeared as an outlier in the study had its lifespan been included in the dataset (E. E. Cordes, Bergquist, et al., 2007). The question remains how widespread these life history

traits are among the cold-seep vestimentiferans, and if longevity continues to increase with depth in this group.

Evolutionary theories offer an alternative approach to understanding lifespan beyond unifying equations that scale with body mass and environmental factors. The premise of longevity theory is that senescence is allowed to evolve because natural selection has only a weak influence on genes that contribute to deterioration with aging. Selection has only a weak effect on these genes because most members of natural populations are killed before they can reach old age and experience the detrimental effects of these genes (Kirkwood & Austad, 2000; Williams, 1957). If extrinsic mortality threats are reduced, however, selection on these genes is stronger and the organisms that possess genes that allow them to live longer and reproduce viable offspring later in life become the most successful (Austad, 1993). The deep sea offers a more stable environment and generally has fewer large predators than other biomes, decreasing the frequency of mortality events.

Cold seeps provide an additional level of stability beyond that provided by the majority of the deep sea through the steady release of fluids from the seafloor for thousands of years at a single seep (E. E. Cordes et al., 2009; Ingram, Meyers, Brunner, & Martens, 2010; H. H. Roberts & Aharon, 1994). These fluids are rich in methane and/or hydrogen sulfide and bring a reliable energy source to the microbes inhabiting the seeps, whether they be free-living or in symbiosis (E. E. Cordes et al., 2009; Paull et al., 1985). Cold-seep tubeworms are entirely reliant on internal bacterial symbionts for their nutrition and live an effectively autotrophic lifestyle (Charles R. Fisher, 1990). In

addition to the geological stability of the cold seep's sulfide supply, tubeworms biologically enhance this source of sulfide by facilitating microbially-mediated sulfur recycling (E. E. Cordes et al., 2005). Microbes in the sediment couple anaerobic methane oxidation to sulfate reduction using sulfate released from the tubeworms' posterior "roots," and this process produces hydrogen sulfide to be taken up by the tubeworm and used by its symbionts (E. E. Cordes et al., 2003; Dattagupta, Miles, Barnabei, & Fisher, 2006). When mediated by *L. luymesii*, this sulfide-replenishing process has been modeled to supply the tubeworm's metabolic needs for at least 250 years (E. E. Cordes et al., 2005). Given this stable energy supply, it is possible for *L. luymesii* to reach lifespans over 250 years and *S. jonesii* over 300 years (DC Bergquist et al., 2000; E. E. Cordes, Bergquist, et al., 2007). *Escarpia laminata* is another chemosynthetic bacteria-hosting vestimentiferan tubeworm of the Gulf of Mexico that inhabits seeps between approximately 1000 m and 3300 m depth, but little is known about this species and its life history. This study aims to estimate the lifespan of *E. laminata* and determine if this deeper-dwelling tubeworm species exhibits longevity similar to its shallower relatives.

2.3 Methods

2.3.1 Collection and in situ growth measurement

To investigate age and life history, the growth of *E. laminata* tubeworms was measured *in situ* using methods developed for *L. luymesii* (DC Bergquist et al., 2000). Six aggregations of *E. laminata* were stained with Acid Blue #158 (Figure 2.1) and seven different unstained aggregations were sampled with the Bushmaster Jr. collection device

(D. C. Bergquist et al., 2003) in June 2006. In June 2007, the six stained aggregations were located again and collected. The total length of each tubeworm was measured from the anterior end of the tube to the posterior portion that tapered to 2mm in diameter. The white anterior portion of the tube (new growth above the blue dye line) was measured as the growth between staining and collection, approximately one year's growth. In total, six populations were collected from Atwater Valley 340 (27.64° N, 88.36° W, 2180 m), two from Alaminos Canyon 818 (26.18° N, 94.62° W, 2745 m), one from Alaminos Canyon 601 (26.39° N, 94.51° W, 2425 m), and four from Green Canyon 852 (27.11° N, 91.19° W, 1410 m). Growth was measured from 356 total stained tubeworms and standardized to an annual growth rate based on staining and collection dates, and all 13 Bushmaster-collected aggregations including an additional 1,046 unstained tubeworms were used as reference populations for the population simulations. In addition to the stained tubeworms, five *E. laminata* individuals banded with zip ties and ID tags in 1992 at Alaminos Canyon 645 were found alive in 2007 and re-imaged to calculate their average annual growth rate over 15 years by dividing all new growth by 15 years.

2.3.2 Growth model and individual simulations

The measured growth rates from the stained *E. laminata* individuals were fit to the negative exponential equation $g = ae^{-bL}$ derived from *L. luymesii* growth rates in the program JMP (DC Bergquist et al., 2000; E. E. Cordes, Bergquist, et al., 2007; SAS Institute Inc., n.d.). In this model, g is annual growth (cm year⁻¹), L is length (cm), and a and b are constants that were calculated during the regression ($a = 2.401$ and $b = 0.0367$). To create an error term for the model, another nonlinear regression was performed on the positive residuals from the growth equation. The residuals were best fit by another



Figure 2.1 – Photograph of stained *E. laminata* tubes The tubes visible in the left half of the picture are unstained, natural *E. laminata*, and the tubes on the right show the conspicuous Acid Blue #158 stain that was applied to distinguish new growth.

negative exponential equation $\varepsilon = ce^{-dL}$, where c and d are constants ($c = 2.102$ and $d = -0.0294$). The probability of whether or not an individual would grow in a given year was also found to be correlated to the size of the tubeworm, similar to the cold seep tubeworm species *Seepiophila jonesi* (E. E. Cordes, Bergquist, et al., 2007). After calculating proportions of *E. laminata* showing nonzero growth in bins of 20 individuals (ordered by size), the probability of annual growth was best fit by the equation $p_g = x + ye^{-zL}$ where x , y , and z are constants ($x = 0.264$, $y = 3.751$, and $z = -0.0880$). If a uniformly-distributed random number between zero and one was greater than the probability p_g , the individual tubeworm in simulation would increase its length by the size-dependent amount $g + N(0, \varepsilon)$ cm that year.

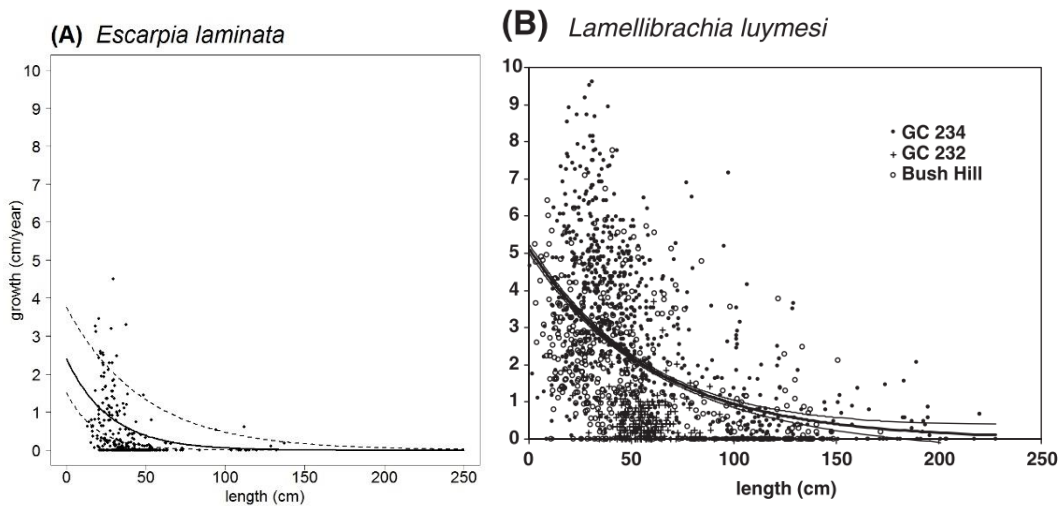


Figure 2.2 – Relationship between tube size and one year’s growth for *E. laminata* and *L. luymesii* (A) One year’s growth for all collected *E. laminata* plotted against the size of the tubeworm measured. The solid line is the best fit negative exponential equation $g=ae^{-bL}$ ($R^2 = 0.1302$), and the dashed lines show the 95% confidence interval around the equation. (B) Comparable measured growth data from the species *L. luymesii* and the negative exponential equation that best fit that dataset, reproduced from (E. E. Cordes, Bergquist, et al., 2007).

To estimate the mean age of the tubeworms in each population, the number of years required to reach the mean length of that population’s tubeworms’ lengths was estimated by recording what year the growth simulation exceeded this mean length. The same method was applied to estimate the age of the largest individuals collected from each population. To account for the fact that these *E. laminata* individuals may be the largest not because they are significantly older but because they grow faster than average, a second growth simulation for these sizes was run using an increased growth rate. These

maximum growth simulations used higher percentile values for a and b in the size-dependent annual growth rate equation (greater than the 50th percentile values used in the average simulation and based on the size of the population, percentiles given in Table 1), and tubeworms grew every year without exception. In each growth scenario (average growth to mean length, average growth to max length, max growth to max length), the number of years required to exceed the recorded length was averaged across 10,000 runs.

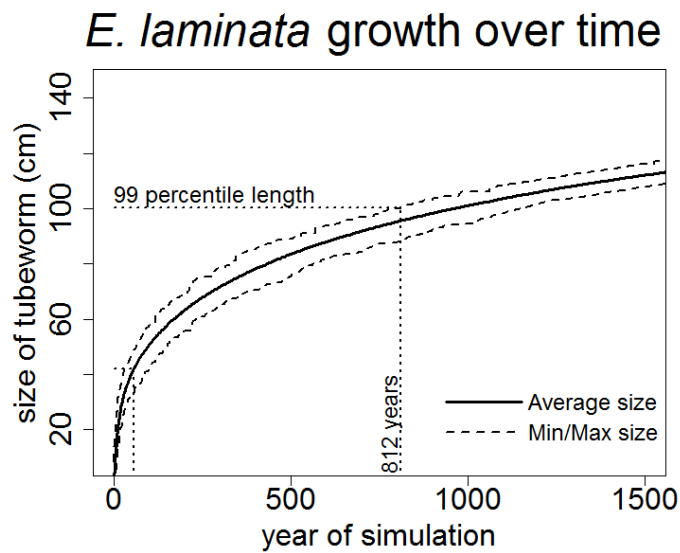


Figure 2.3 – Individual growth simulation results Growth was simulated for 1500 years for 10,000 individual tubeworms and the maximum, minimum, and averages sizes for each year were recorded. After 57 years, the average size of the simulated individuals was equal to the mean length of all collected *E. laminata* (42 cm), marked with vertical and horizontal dotted lines. It took 812 years for even the fastest growing tubeworms in the simulation to reach the 99th percentile length of all tubeworms collected (100 cm), shown with the larger vertical and horizontal dotted lines.

2.3.3 Population simulations

The average individual growth model was extended with mortality and recruitment rates to construct a population-wide simulation in order to estimate the ages of tubeworms in these collections while capturing more of the variability in their growth rates.

The rate of removal of individuals from the population was estimated by counting the number of empty tubes that were collected within the populations. Using *in situ* chitin degradation rates of *Riftia pachyptila* (a hydrothermal vent species of tubeworm) tube material and adjusting for the temperature difference between cold seeps and hydrothermal vents (Ravaux et al., 2003), it was estimated that the tubes can stand for three years in a seep environment after the death of the worm and still be solid enough (up to 50% degraded by microbial activity) to be collected and measured, allowing for the conversion of this count into an annual rate. The probability of a mortality event given a tubeworm's size was modeled by calculating the proportion of empty tubes collected across 5 cm size bins. The mortality rate for *E. laminata* was found to be extraordinarily low at 0.67% of the population dying annually, and this rate did not change with tubeworm length.

In order to successfully recruit to a seep, vestimentiferans require exposed hard substrate and hydrogen sulfide. Substrate surface area is rapidly occupied by the first recruits, and the low mortality rate of cold-seep vestimentiferans reduces the incidence of space being made available for a late recruit by the death of an individual already settled at that site. Additionally, hydrogen sulfide levels in the water column are depleted over

time, and thus recruitment ceases after a few decades (De Bergquist, Urcuyo, & Fisher, 2002; E. E. Cordes et al., 2003). This is evident in the complete absence of small tubeworms (<10cm) in any of the populations sampled for this study and challenges the application of recruitment models developed for other species. The density-dependent model $R = Gf$ published by Kohyama and Takada (1998) was adapted here for *E. laminata* (Kohyama & Takada, 1998). Instead of calculating recruitment rate from the smallest size classes, the maximum recruitment pulse was estimated from the most common size class. To calculate recruitment, the number of individuals in the most common 1 cm size class for each collected *E. laminata* population was correlated with the areal coverage of the aggregation in m^2 . The largest possible sampling area was $0.283 m^2$ (the size limit of the sampling device), and the smallest sampling area measured was $0.006 m^2$ due to the small ($n=5$) population of tubeworms. There was a significant linear relationship ($P < 0.0001$) with a slope of $76.36 \text{ ind } m^2$. The size class was assumed to represent one year's cohort ($R = 76.36 \text{ ind } m^2 \text{ year}^{-1}$), and sensitivity tests showed no significant effect on the estimated age of the simulated aggregation or the quality of the fit of the simulation to the collected data from varying this parameter between $7.64 \text{ ind } m^2 \text{ year}^{-1}$ to $152.7 \text{ ind } m^2 \text{ year}^{-1}$.

Each simulated tubeworm in the population grew at the rates defined by the average growth model. Individuals in the simulated population would be removed from the population if a uniformly-distributed random number between zero and one was less than the mortality rate $0.0067 \text{ ind } \text{year}^{-1}$. The population simulation continued to recruit the number of new individuals generated by a normally-distributed random number with

mean R until the population reached carrying capacity (defined as the total number of individuals collected in the reference population). Each year of the population simulation, the size distribution of the simulated tubeworm population was compared to the size distribution of the collected population using a log-likelihood test. The simulation year with the lowest log-likelihood test statistic was recorded as the estimated age of the population, and the age was then averaged across 10,000 simulation runs for each population.

2.4 Results

The *E. laminata* specimens measured displayed a similar trend to *L. luymesii* in decreasing annual growth with increasing size, although *E. laminata* tubeworms of comparable size grow less than half as fast (Figure 2.2). According to the average individual growth simulation, an *E. laminata* individual with an anterior length of 50 cm is predicted to be 116.1 (sd = 19.4) years of age, older than *L. luymesii* and *S. jonesii* individuals of the same size that have been estimated to be 21 and 96 years old respectively (E. E. Cordes, Bergquist, et al., 2007). At the fastest growth rates, corresponding to the 99th-percentile of measured rates, a 50 cm long *E. laminata* would be 19.8 (sd = 1.7) years of age. At greater lengths, the age disparity becomes larger with *E. laminata* estimated to reach 1 m anterior length after 1232 (sd = 85.6) years, 67.9 (sd = 2.3) years at maximum growth rates, compared to 68 years for *L. luymesii* and 605 years for *S. jonesii* to reach the same size. Although *L. luymesii* tubeworms frequently reach lengths longer than 1 m, 50 cm is a more ecologically relevant comparison for the smaller species *E. laminata* and *S. jonesii*. In the average growth simulations, the age at which

tubeworms could attain the mean length of each population ranged from 15 to 266 years from the smallest to the largest mean length (Table 2.1). The age estimates for the largest individuals from each population ranged from 77 to 15,834 years using the average growth model and from 17 to 1,059 years when the maximum growth model was applied (Table 2.1).

The range of growth rates measured from the banded *E. lamintata* individuals was 0.67 to 2.67 mm year⁻¹ with an average of 1.38 mm year⁻¹ over the 15 year period. Although the total length of the zip-tied individuals was not measured, these growth rates fall within the values predicted by the model for moderate to large tubeworms and suggests that the stained tubeworms' single year of growth was a representative sample of rates exhibited by *E. laminata* over their lifetime. At the average growth rate of 1.38 mm year⁻¹ from the 15-year banding data, it would take an individual 362 years to grow to 50 cm and 725 years to reach 1 m in length, both of which within the range of estimates from the other methods.

The averages for each collected population range from 21 years to over 9000 years (Table 2.2). In 10 of the 13 simulated populations, the mean length of tubeworms averaged across all simulation runs in the best-fit year was within 10 cm of the measured mean length for that collected population. Population-level simulations have the benefit of capturing more observed growth variation, but in four simulated populations the average log-likelihood comparisons between the modeled populations and the actual size-frequency histograms were significantly different ($p < 0.05$) in even the best-fit years. The nine simulated populations that were not significantly different from collected

Table 2.1
Individual simulation results

Population	Mean Length (cm)	Mean Age (yrs)	Largest Individual (cm)	Population size (and percentile)	Age of largest individual at mean growth (yrs)	Age of largest individual at max growth (yrs)
1	23.0	15 ± 0.03	44.2	158 (99)	77 ± 0.1	17 ± 0.02
2	33.2	34 ± 0.1	66.2	266 (99)	285 ± 0.4	31 ± 0.02
3	34.7	38 ± 0.1	69.0	30 (65)	328 ± 0.4	96 ± 0.07
4	39.6	55 ± 0.1	68.7	79 (89.5)	324 ± 0.4	60 ± 0.04
5	42.8	70 ± 0.1	50.2	5 (52.5)	115 ± 0.2	53 ± 0.06
6	44.0	76 ± 0.1	68.3	227 (99)	317 ± 0.4	33 ± 0.02
7	48.0	100 ± 0.2	80.0	203 (99)	545 ± 0.5	43 ± 0.02
8	51.8	127 ± 0.2	173.4	157 (99)	15834 ± 3.4	293 ± 0.03
9	52.6	135 ± 0.2	87.8	79 (89.5)	757 ± 0.6	107 ± 0.05
10	54.1	147 ± 0.2	100.4	118 (99)	1247 ± 0.9	69 ± 0.02
11	54.7	153 ± 0.2	66.8	14 (57)	294 ± 0.4	97 ± 0.08
12	60.1	207 ± 0.3	78.4	14 (57)	508 ± 0.5	150 ± 0.1
13	64.8	266 ± 0.3	148.8	52 (76)	7038 ± 71.0	1059 ± 0.2

Note: The mean length and largest individual measured from each population and the simulation year at which individual growth simulations reached these sizes (averaged across 10,000 simulation runs ± standard error) are reported. The Mean Age was estimated using only the average growth model whereas the age of the largest individual was simulated under both the average growth model and a model that assumed maximum growth rates. The maximum growth rate was simulated by above average model parameters adjusted according to the size of the population and corresponding percentile length the largest individual occupies.

Table 2.2
Population simulation results

Population	Measured from collected populations		Measured from simulated populations in best-fit year		Best-fit year
	Mean Length (cm)	Largest Individual (cm)	Simulated Mean Length (cm)	Simulated Largest Individual (cm)	Simulated Age (yrs)
1	23.0	44.2	22.5 ± 0.5	32.8 ± 1.2	21 ± 0.01*
2	33.2	66.2	30.5 ± 0.6	40.4 ± 1.2	35 ± 0.01
3	34.7	69.0	25.0 ± 1.1	32.9 ± 1.8	23 ± 0.02*
4	39.6	68.7	43.8 ± 3.3	69.8 ± 14.7	350 ± 2.7*
5	42.8	50.2	45.2 ± 1.9	48.4 ± 2.5	82 ± 0.1*
6	44.0	68.3	29.1 ± 21.6	39.0 ± 25.9	82 ± 0.6
7	48.0	80.0	45.0 ± 1.6	58.5 ± 2.2	129 ± 0.1
8	51.8	173.4	44.6 ± 2.6	58.6 ± 3.8	135 ± 0.3
9	52.6	87.8	52.0 ± 1.9	98.5 ± 12.1	9449 ± 59.9*
10	54.1	100.4	84.1 ± 7.1	153.5 ± 20.4	9311 ± 53.5*
11	54.7	66.8	51.5 ± 0.7	56.1 ± 1.5	127 ± 0.08*
12	60.1	78.4	59.7 ± 1.0	64.2 ± 1.7	205 ± 0.1*
13	64.8	148.8	41.4 ± 2.3	59.3 ± 5.5	179 ± 1.1*

Note: The best simulation years listed indicate the most likely age of the population (from the first recruited individual to time of collection) according to the best-fit year. Asterisks indicate that, on average, the simulated population distribution was not significantly different from the collected population distribution in the best-fit year. The largest individual and mean length of all individuals in the simulated population at the time of the best fit year were recorded. The mean length and largest individual measured from the collected populations are listed for comparison. All listed ages and sizes are averaged across 10,000 simulation runs with mean ± standard error reported for ages and mean ± standard deviation reported for simulated sizes.

populations are marked with asterisks in Table 2. The goodness-of-fit test between real and simulated data was most likely to indicate similar distributions when the reference population had a normal distribution and small range between the largest and smallest individual. The individual- and population-level approaches, despite their limitations, both indicate that the larger *E. laminata* individuals reach ages in excess of 250 years

2.5 Discussion

These findings all support the conclusion that *E. laminata* tubeworms are much older than similarly sized *L. luymesii* tubeworms. The explanation for this disparity is not immediately clear given the close phylogenetic relationship of these species and their ecological similarity. A full population simulation is more likely to capture the true growth rates of all the collected tubeworms whereas individual aging methods may be inaccurate if the largest tubeworms experienced anomalously fast growth rates.

Calculating the age of large tubeworms is also hampered by the asymptotic nature of the growth model, which introduces a high degree of error in the estimates of the age of the largest *E. laminata* individuals. The two oldest population simulation ages are more than 25 times larger than the next oldest estimate, suggesting that these results are outliers and not a reliable evaluation of *E. laminata*'s lifespan. Even removing these outliers, *E. laminata* individuals are reliably predicted to live in excess of 250 years, and may occasionally attain far greater ages if given a steady supply of hydrogen sulfide and oxygen in the absence of predation.

L. luymesii is found on the upper Louisiana slope between 300 and 950m deep whereas *E. laminata* occurs only on the lower slope below 1000m (Coward, Halanych, Schaeffer, & Fisher, 2014), and this difference in their depth ranges may potentially explain their lifespan disparity. Some studies have found decreasing rates of metabolism with increasing depth of occurrence in some deep sea species (Childress, Cowles, Favuzzi, & Mickel, 1990; Drazen & Seibel, 2007), and a lower resting metabolic rate can lead to a longer lifespan (Atanasov, 2005). Although the metabolic rate of *E. laminata* has not been measured directly, there was a significant relationship between depth and growth rate where tubeworms were more likely to grow less than the model predicted the deeper they were collected (between 1409 and 2746 m). This relationship only held for larger individuals, as the relationship was only significant when the high degree of variability from small individuals (<30cm) was removed from the dataset. Observed trends of decreased metabolism with depth are most likely due to the direct effect of temperature on metabolism, rather than depth per se (Childress et al., 1990). All *E. laminata* collection sites were between 4.2°C and 4.3°C, and the average temperature difference between these and *L. luymesii* sites is less than 4°C. According to the Metabolic Theory of Ecology, *E. laminata*'s lifespan would be only 1.34 times longer than *L. luymesii*'s if the difference were due to temperature alone (McClain et al., 2012).

The interactions between *E. laminata*'s metabolism, lifespan, and mortality can also be investigated through published allometric relationships. When calculating the predicted mortality using terms averaged across fish and invertebrates (McCoy & Gillooly, 2008), *E. laminata* has a mortality rate 15 times lower than the equation

predicts given the tubeworms' average dry mass and the ambient temperature of the seeps at which it was collected (avg. 4.2°C). Although hydrothermal vent and cold seep tubeworms may be subject to non-lethal plume-cropping (Dc Bergquist et al., 2007; E. E. Cordes, Becker, & Fisher, 2010), lethal predation of tubeworms has not been demonstrated (D. C. Bergquist et al., 2003). *E. laminata* does have a blood-sucking parasite in the polychaete *Protomystides* sp., and this small polychaete has also been found inside the empty tubes of dead tubeworms, but whether these small parasites can cause mortality at appreciable rates is unknown (Becker, Cordes, Macko, Lee, & Fisher, 2013). Thus *L. luymesii*, *S. jonesii*, and *E. laminata* all have similarly low mortality rates. This low rate of individual turnover places *E. laminata* in the category with *L. luymesii* and *S. jonesii* as anomalously long-lived deep-sea species according to the Metabolic Theory of Ecology (McClain et al., 2012). These calculations give increased importance to extrinsic mortality rate in increasing animals' lifespans.

At more than 250 years old, *E. laminata* achieves a lifespan that exceeds other longevity records such as 177-year-old Galapagos giant tortoises (the longest-lived land vertebrate), 211-year-old bowhead whales (the longest-lived mammal) (Deweerd, 2012). The marine clam *Arctica islandica* remains the oldest non-colonial animal known with an inferred age of 507 years (Ridgway & Richardson, 2011), but given the uncertainty associated with estimating the ages of the longest individuals, there may be large *E. laminata* tubeworms alive in nature that live even longer.

CHAPTER 3

FINE-SCALE HABITAT MAPPING OF THE INFLUENCE OF COLD SEEPS ON DEEP GULF OF MEXICO COMMUNITIES

3.1 Abstract

In the deep Gulf of Mexico, there are abundant methane seeps that punctuate the seafloor habitat. These seeps alter the local habitat when they release reducing chemicals into the water column and attract chemosymbiotic fauna to the community. The microbially-mediated reactions that occur throughout the lifespan of the seep also create authigenic carbonate rock. Background deep-sea animals such as corals rely on this hard substrate for their habitats but typically cannot tolerate the toxic sulfide and hydrocarbons released at active seep sites. This study examines the influence that seafloor seepage has on the distribution of seep-associated organisms (tubeworms, mussels, and bacterial mats) and background deep-sea taxa (scleractinian and non-scleractinian corals) using fine-scale AUV photo surveys. As expected, the presence of carbonate rocks was the most consistent predictor of coral distributions in addition to significantly predicting the presences of tubeworms, mussels, and bacterial mats. Another expected result was the association of scleractinian corals with higher than average oxygen levels. However, non-scleractinian corals were sometimes predicted by negative oxygen anomalies. Redox potential measurements were able to detect a significant effect of hydrogen sulfide levels on the distribution of tubeworms, demonstrating that this AUV survey design can identify seepage. This study adds evidence to the theory that seepage is an essential

environmental filter in niche-driven community assembly in the deep Gulf of Mexico, and from this dataset it appears that sulfide concentrations, dissolved oxygen levels, and substrate provision are more important seep influence variables than hydrocarbon concentrations.

3.2 Introduction

Whether community assembly is driven primarily by niche or neutral processes is an ongoing source of debate in ecology (Leibold et al., 2004; Urban et al., 2008). Neutral theory contends that random processes of speciation and extinction are primarily responsible for the biodiversity and community composition we observe today, as opposed to traditional ecological theories that assume organisms' distributions are shaped by their adaptations to the physical environment and niche processes (Hubbell, 2001). In the deep-sea, a recent study of octocoral communities, a highly diverse group of benthic invertebrates, found support for both niche and neutral drivers of species' distributions (A. M. Quattrini et al., 2017). The analysis showed species were filtered by depth. Besides the effects of pressure on organismal physiology, depth also co-varies with many other environmental variables that contribute to species turnover with depth (Angel, 2003; Somero, 1992). Temperature, dissolved oxygen levels, calcium carbonate saturation state, and photosynthetic input each change with depth and exert strong influences on coral distributions (Davies, Wisshak, Orr, & Murray Roberts, 2008; S.E. Georgian et al., 2016; Thistle, 2003; Yesson et al., 2012).

There are two additional environmental factors that are not determined by depth has also been found to shape cold-water coral distributions: the availability of hard

carbonate substrate and the presence of hydrocarbon seepage (Samuel E. Georgian et al., 2014; A. M. Quattrini et al., 2013, 2015). Hard substrata are considered necessary for the successful recruitment of coral larvae, and they are a limited commodity on the mostly soft sediment deep seafloor (J. M. Roberts et al., 2009). Most coral habitat suitability models, however, do not include this variable because it requires a higher resolution of bathymetric or photographic data that has not been sufficiently sampled for broad scale analyses (Davies et al., 2008; Yesson et al., 2012). A recent fine-scale niche model of the abundant scleractinian coral *Lophelia pertusa* that examined the environment down to 5 meter resolution did find that the presence of carbonate rocks was a predictor of this species' distribution in the Gulf of Mexico (Samuel E. Georgian et al., 2014).

These carbonate substrates of the deep Gulf of Mexico originated from hydrocarbon seeps. Microbes at these seeps increase the alkalinity of the seawater to allow carbonate to precipitate out of solution through the anaerobic oxidation of methane (Aharon & Fu, 2000; Joye et al., 2004). Because this region is home to hundreds of active seeps and widespread inactive authigenic carbonates ranging from a few hundred meters deep to over 2000m below the surface, seepage and carbonate rocks contribute significantly to the habitat heterogeneity of the deep Gulf of Mexico (C. Fisher, Roberts, Cordes, & Bernard, 2007). These hydrocarbon seeps are also temporally stable with the release of fluids potentially persisting up to a thousand years at a single site (E. E. Cordes et al., 2009; Ingram et al., 2010; H. H. Roberts & Aharon, 1994). Besides producing hard substrata, the bacteria at seeps that harness chemosynthesis for energy and carbon fixation also support diverse communities (E. E. Cordes et al., 2009). Methane seeps in

the Gulf of Mexico are colonized by foundation species including vestimentiferan tubeworms, bathymodiolin mussels, and vesicomylid clams, all of which rely on chemosynthetic bacterial symbionts for nutrition and create biogenic habitat for the seep community (D. C. Bergquist et al., 2003; E. E. Cordes, Cunha, et al., 2010).

While the value of carbonates created by past, now-inactive seeps to coral habitat is evident, the effect of active seeps on cold-water coral distributions is less well known. Seeps support high biomass relative to the surrounding deep benthos, and these habitats have previously been considered analogous to oases in a desert (Carney, 1994). Seepage occurs at discrete locations and supports assemblages of specialized, often endemic species that differ from background benthos and coral communities (E. E. Cordes et al., 2008, 2009; Kennicutt et al., 1992). The presence of seeps influences octocoral species distributions in the deep Gulf of Mexico by serving as attractant for the settlement of one species of non-scleractinian coral. *Callogorgia delta* has been found to diverge in its niche from congeners because it is more likely to be found in habitats closer to active seep sites (E. E. Cordes et al., 2009; A. M. Quattrini et al., 2013, 2017).

There is a new imperative to investigate the impact seeps have on the wider ecology and oceanographic processes of the deep sea (Lisa Ann Levin et al., 2016). In addition to contributing to environmental filtering in octocorals, these sites can export chemosynthetic productivity to the otherwise food-limited deep seafloor, provide habitat through authigenic carbonates as previously discussed, and alter local water chemistry (Lisa Ann Levin et al., 2016; Tunnicliffe et al., 2003). The increased biomass and productivity associated with chemosynthesis could be an ecological benefit to non-seep

species, but a stable isotope study of *L. pertusa* reef communities near seeps found that none of the coral-associated species derived nutrition from chemosynthesis (Becker, Cordes, Macko, & Fisher, 2009). Non-adapted species may be deterred from obtaining seep-produced organic carbon due to the toxicity of the hydrogen sulfide and hydrocarbons released at these sites (Evans, 1967). Additionally, the fluids released at seep sites are low in dissolved oxygen and locally depress oxygen levels in the water column, potentially to levels too low for coral habitat requirements (Davies et al., 2008; Tunnicliffe et al., 2003; Yesson et al., 2012).

To investigate the effects of these seep habitat variables on community assembly in the deep Gulf of Mexico, this study will map the distributions of seep chemosymbiotic megafauna, seep microbial mats, and scleractinian and non-scleractinian corals onto the environmental variables of dissolved oxygen, hydrocarbon concentrations, hydrogen sulfide concentrations, and carbonate substrate availability. Previous studies of community ecology in the Gulf of Mexico have found that these foundation taxa each host specialized communities that make them a reliable indicator of associated species' distributions (E. E. Cordes, Becker, Hourdez, et al., 2010; E. E. Cordes et al., 2009; Etnoyer et al., 2017). Additionally, these taxa have lifespans that persist from decades to centuries, making them a stable feature of the habitat (E. E. Cordes, Bergquist, et al., 2007; Roark et al., 2009). This study will map the distribution of these organisms using fine-scale, gridded AUV photo surveys at multiple sites along with concurrently collected water chemistry measurements to detect seepage through hydrocarbon concentrations, redox potential (a proxy for hydrogen sulfide concentrations), dissolved oxygen. The

photo survey will also indicate the presence of authigenic carbonates providing hard substrate. If this technique finds biotic responses to the environmental variables created by active and past seepage, it will support the proof of concept that this kind of AUV survey design can accurately detect seepage in the water column. Since seeps are already known to be a driver of community assembly in this region, this analysis may also help determine which environmental variables associated with seepage are directly responsible for this niche divergence and how far this influence extends locally from the seep.

3.3 Methods

3.3.1 AUV survey design and data collection

In April-May 2014, *AUV Sentry* was deployed off of the *R/V Atlantis* for a total of 13 separate dives at nine different sites across the northern Gulf of Mexico (Figure 3.1, Table 3.1). The average depths of the survey areas were between 400m and 600m except for GB903 and AT357 which were both found below 1000m (Table 3.1, Figure 3.2). During the photo survey portion of each dive, the vehicle moved back and forth on closely spaced tracks (referred to as “mowing the lawn”) according to a preset navigation plan (Figure 3.). *Sentry* took downward-facing photos once every 3.5 seconds at an altitude of 5-6m off the seafloor, capturing a total of 82,230 photos across all dives. These photos were taken less than 2m apart along the track, and tracks were spaced at least 5m apart from one another.

During the photo survey, *Sentry*'s sensors were simultaneously measuring the dissolved oxygen, hydrocarbon concentrations, and redox potential. Oxygen was recorded using an Anderaa optode model 4330. To examine the influence that oxygen

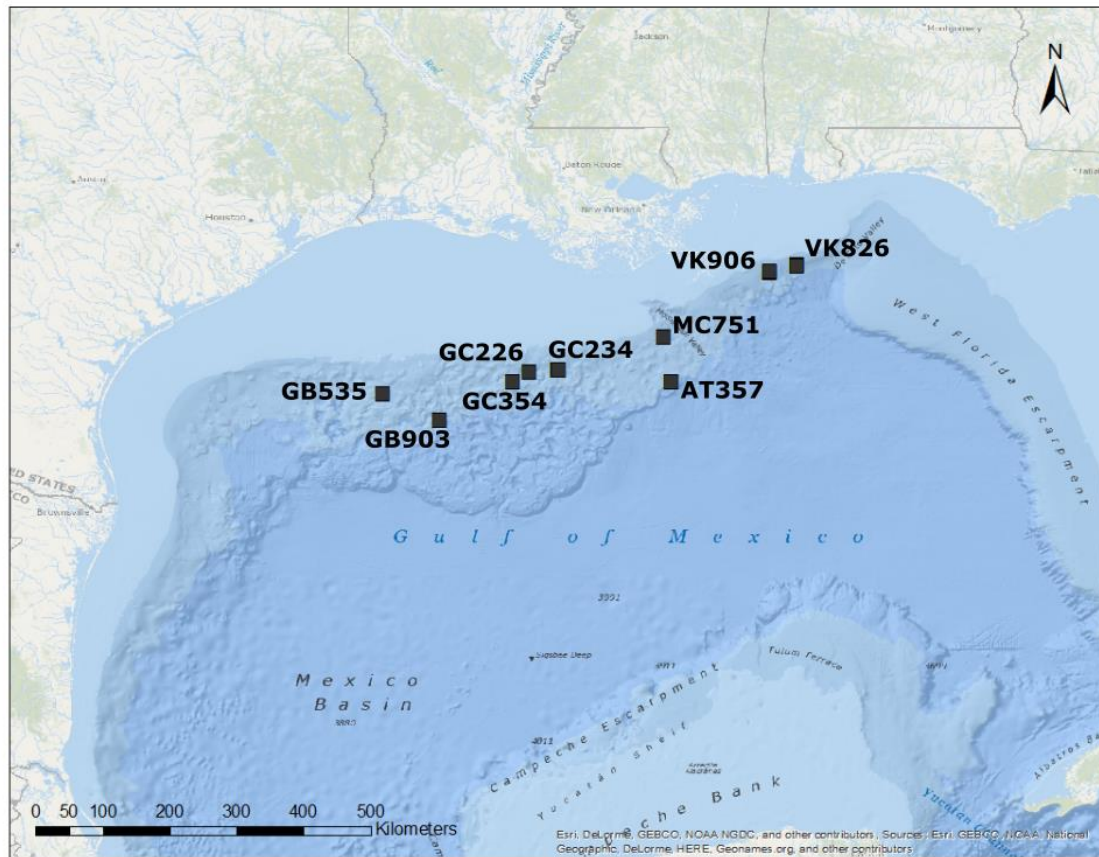


Figure 3.1. A map of the sites surveyed by Sentry in the Northern Gulf of Mexico.

Table 3.1
Details of Sentry survey locations

Site	Sentry Dives	Latitude	Longitude	Depth Range
GB535	238	27.43199	-93.5732	534-556m
GB903	239	27.08096	-92.8165	1040-1118m
GC354	240	27.59742	-91.8253	519-606m
GC226	242	27.72839	-91.61	489-519m
GC234	236, 237, 241	27.75074	-91.2228	462-559m
MC751	243	28.19425	-89.7988	427-436m
AT357	234, 235	27.58683	-89.7045	1038-1084m
VK906	232, 233	29.06766	-88.3771	380-489m
VK826	231	29.15716	-88.0148	449-605m

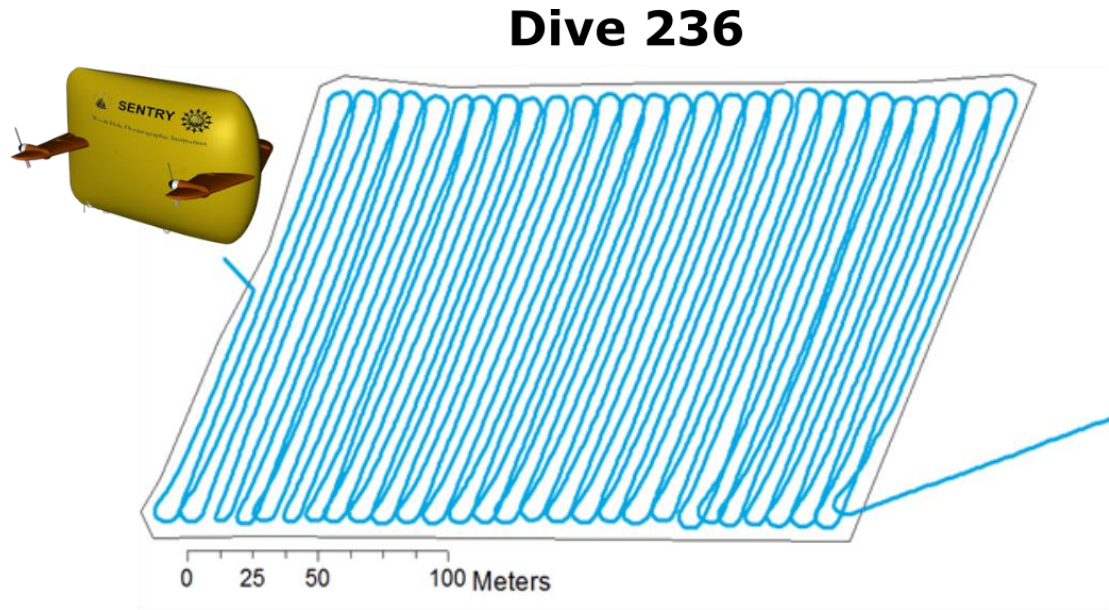


Figure 3.2. Map of Sentry's tracks during a single dive's photo survey

had on species' distributions independent of depth, local anomalies in dissolved oxygen levels were used as variables in the analysis instead of the measured absolute oxygen measurements. For each dive, a linear regressions between depth and dissolved oxygen were calculated from the bottom 100m of the water column measured during the dive. The residuals from this linear model were used as dissolved oxygen anomalies in later analyses and to create interpolated maps showing changes in oxygen levels across a site. The linear regressions were performed in R (R Core Team, 2015).

The water column measurements that most directly indicated seepage were hydrocarbon concentrations and redox potential. Hydrocarbons, including methane and longer chain hydrocarbons, were measured through fluorescence using a Chelsea Aquatraka Fluorometer, but this sensor was only installed on *Sentry* for dives 236 through 243. Measuring redox potential detects the presence of reducing or oxidizing

species and acted as a proxy for the presence of hydrogen sulfide at the seep sites. This water chemistry parameter was measured using Dr. Koichi Nakamura's electrochemical (Eh) sensor. Before the readings from this sensor were plotted and analyzed, the Eh measurements were differentiated to dEh/dt the presence of reducing species is detected when redox potential drops rapidly. A strong negative slope in dEh/dt indicates the presence of sulfide and a positive or horizontal slope indicates its absence.

3.3.2 Photo annotation and data analysis

For each individual photo, the presence or absence of seep foundation species (bacterial mats, tubeworms, mussels) and background foundation species (scleractinian corals and non-scleractinian corals) were noted (Figure 3.4). The seafloor habitat in each photo was also characterized by noting the presence of carbonate rocks or the absence of hard substrate amid the soft, muddy sediment (Figure 3.4). To visualize the distribution of these organisms relative to the chemical environment across the site, the point measurements from each water chemistry parameter were plotted and smoothed into an interpolated layer using inverse distance weighted interpolation in ArcGIS (ESRI, 2014).

The presence or absence of the five foundation taxa (tubeworms, mussels, bacterial mats, scleractinian corals, non-scleractinian corals) were modeled separately in response to the fixed effects dEh/dt , hydrocarbon concentrations, oxygen anomalies, and the presence of carbonate rocks using a generalized linear mixed model in R.

Additionally, the presence of bacterial mats were included as a fixed effect for all other foundation taxa's models. The GLMMs included the dive, the site, and a categorical depth variable (shallow <500m, mid >500m and <800m, deep >1000m) as random

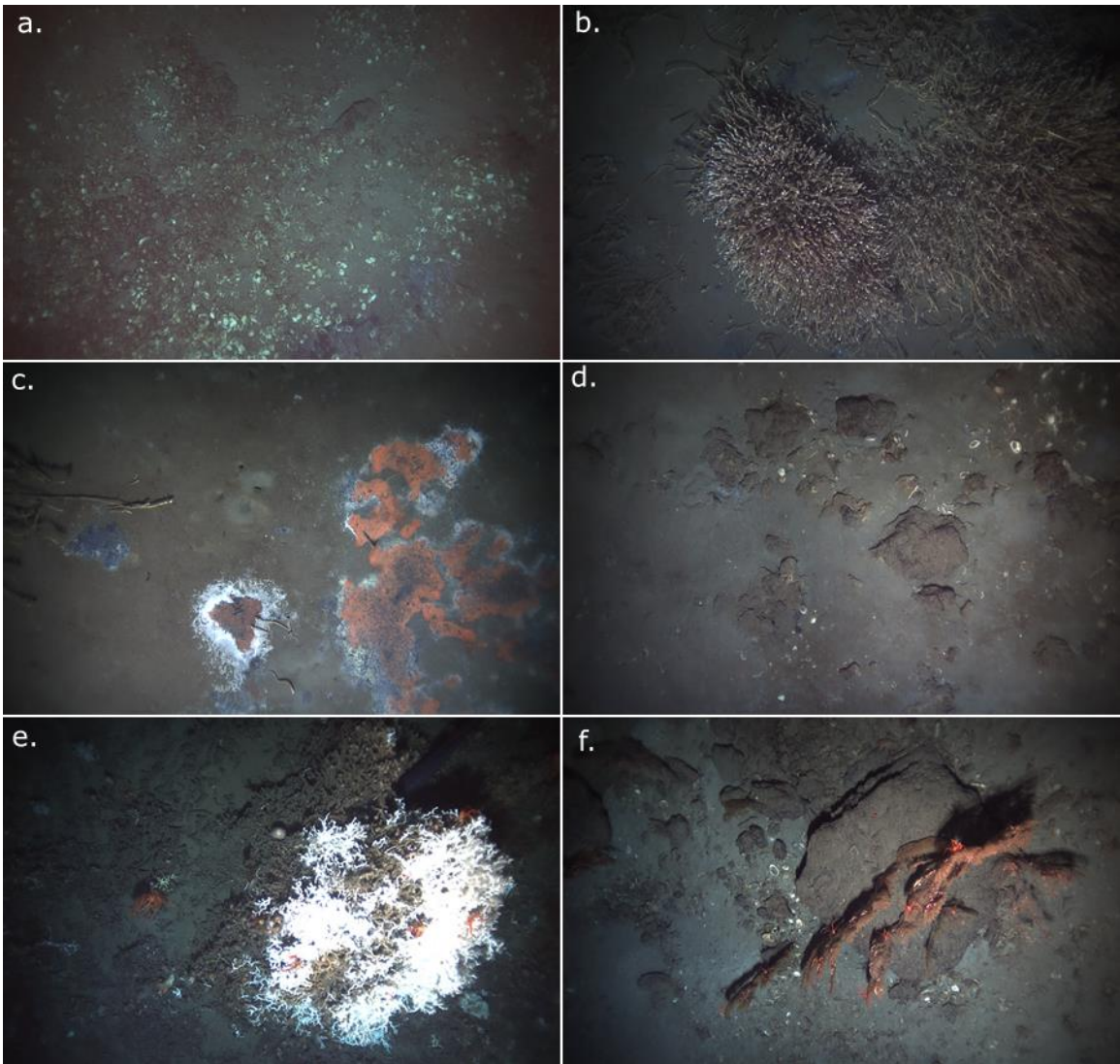


Figure 3.3. Examples of photo annotation categories. The six photos above each show an example of the six photo annotations used in this analysis. The seep foundation species of mussels, tubeworms, and bacterial mats are visible in photos a., b., and c. respectively. The presence of hard substrate in the form of carbonate rocks is noticeable in photos d and f. The two categories of corals, scleractinians and non-scleractinians, are shown in photos e. and f. respectively.

effects. The parameters of this model were estimated using Laplace approximations. To reduce spatial autocorrelation in the residuals as measured by Moran's I, observations were subsampled to a 10m by 10m grids within each site, condensing the dataset to a total of 7204 observations. The means of the hydrocarbon concentrations and dissolved oxygen anomalies were calculated within each grid cell along with the minimum dEh/dt value observed within the designated area. Because hydrocarbons were not measured on every dive, only the 4257 grid cells have hydrocarbon measurements are analyzed in the full GLMM that includes hydrocarbon as a fixed effect. GLMMs that use all 10m grid cells but do not include hydrocarbon concentration as a variable were additionally run for each foundation taxa.

3.4 Results

All sites had carbonate rocks available for settlement in addition to soft sediment habitats (Table 3.2). VK906 was the only site surveyed that had no visible seep fauna. All other sites had at least some bacterial mats (Table 3.2). GB535 was the only site that did not have any coral organisms within the photo survey region (Table 3.2).

Concentrations of hydrogen sulfide, as indicated by dEh/dt, successfully predicted the presence of tubeworms as expected. This measure of seepage had a large effect on the distribution of tubeworms, but was not a significant predictor in the other foundation taxas' responses (Table 3.3, Table 3.4). An example of this relationship is demonstrated in Figure 5. Dive 236 at site GC234 surveyed a dense tubeworm field in the eastern half of the site, and within the interpolated dEh/dt a clear, red spot in the southeastern corner

Table 3.2

Summary of the presence and absence of each photo category across each site.

Site	Carbonate rocks	Scleractinian Corals	Non-Scleractinians	Tubeworms	Mussels	Bacterial Mats
GB535	+	-	-	+	-	+
GB903	+	+	+	+	+	+
GC354	+	+	+	+	-	+
GC226	+	-	+	+	-	+
GC234	+	+	+	+	+	+
MC751	+	+	+	+		+
AT357	+	+	+	-	+	+
VK906	+	+	+	No seep organisms		
VK826	+	+	+	+		+
Total Observations	2249	746	1670	432	143	1386

Note: The total observations listed in the last row indicate how many grid cells out of the total 7204 that foundation taxa was present in.

indicates a strong redox potential signal and detectable levels of hydrogen sulfide above these tubeworms (Figure 3.5). Additional site maps are found in Appendix A.

The other direct measure of seepage, hydrocarbon concentrations, was also significant when modeling the distribution of a chemosymbiotic megafauna, but this measure was found to significantly predict the absence of mussels, converse to the relationship hypothesized for a seep species dependent on chemosynthesis (Table 3.4). The presence of bacterial mats was a predictor for the presence of both chemosymbiotic fauna (Table 3.4). Bacterial mats also predicted the absence of non-scleractinian corals (Table 3.3).

Areas of lower than average dissolved oxygen can also indicate seepage, but the relationship between taxonomic distributions and local oxygen anomalies were mixed between the GLMM with the full dataset and the GLMM that used only dives where hydrocarbon concentrations were measured (Table 3.3, Table 3.4). Several of the

Table 3.3

Summary of GLMM results for each foundation taxa using data from all dives.

Environmental Predictor		Scleractinian Corals	Non-Scleractinians	Tubeworms	Mussels	Bacterial Mats
dEh/dt	p-value	0.470	0.971	0.002	0.930	0.521
	estimate	4.359	-0.100	-13.260	-0.445	1.483
Oxygen	p-value	0.0161	0.362	0.053	0.803	<0.0001
	estimate	0.159	0.0562	0.105	0.0375	-0.274
Carbonate	p-value	<0.0001	<0.0001	<0.0001	<0.001	<0.001
	estimate	2.961	3.335	1.670	2.645	0.893
Bacterial Mats	p-value	0.600	<0.0001	<0.0001	0.284	
	estimate	0.0854	-0.464	3.851	0.201	

Table 3.4

Summary of GLMM results for each foundation taxa using data only from dives that measured hydrocarbon concentrations.

Environmental Predictor		Scleractinian Corals	Non-Scleractinians	Tubeworms	Mussels	Bacterial Mats
dEh/dt	p-value	0.639	0.621	0.004	0.961	0.739
	estimate	28.209	45.450	-13.224	3.077	1.519
Hydrocarbons	p-value	0.426	0.143	0.603	<0.0001	0.203
	estimate	-10.373	-7.313	-3.414	-301.2	-5.272
Oxygen	p-value	0.567	0.0003	0.0437	0.0168	0.232
	estimate	-0.318	-0.792	0.109	-1.501	0.0668
Carbonate	p-value	<0.0001	<0.0001	<0.0001	0.006	<0.001
	estimate	3.321	3.502	1.617	1.846	1.323
Bacterial Mats	p-value	0.939	0.395	<0.0001	0.004	
	estimate	0.0223	-0.129	3.810	1.427	

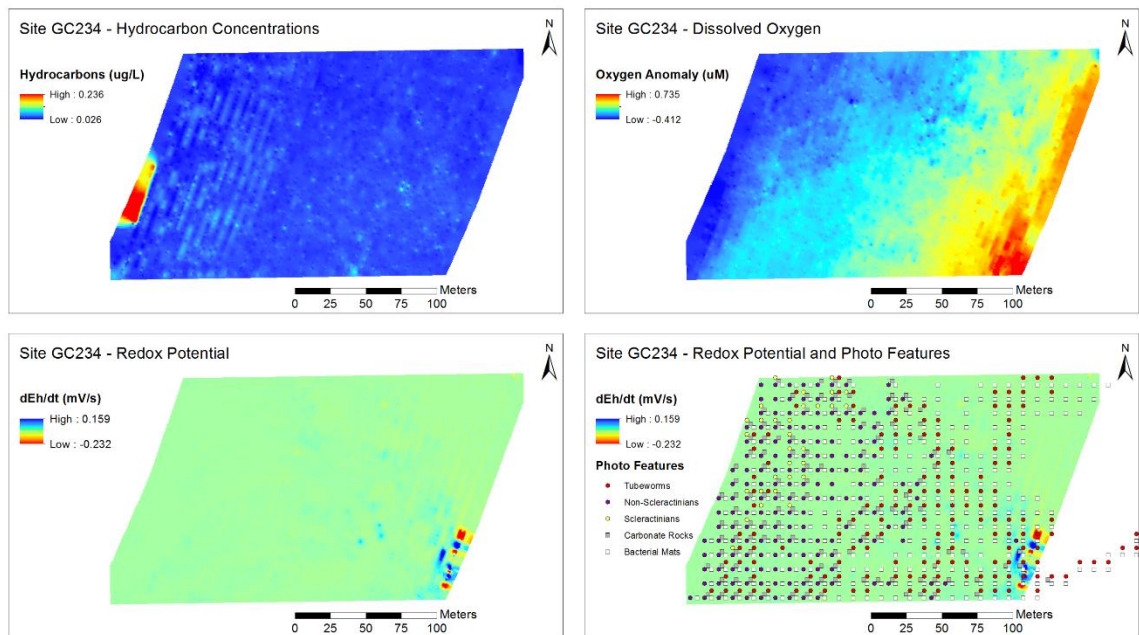


Figure 3.4. An example from Dive 236 at GC234 showing the habitat mapping process.

The first three maps show each of the three water chemistry layers interpolated over the survey site on their own. The fourth map displays the distribution of photo-visible features in within the 10m grid subsampling design over the interpolated later for dEh/dt.

foundation taxa had significant relationships with dissolved oxygen that agreed with hypotheses about seepage influence. The presences of bacterial mats and mussels were predicted by lower than average oxygen levels, indicating that their distributions are clustered around areas of active seepage (Table 3.3, Table 3.4). Tubeworms, on the other hand, were predicted by higher than average oxygen concentrations (Table 3.4). Scleractinian corals were also predicted by positive oxygen anomalies (Table 3.3), and

conversely, the presence of non-scleractinian corals was predicted by negative oxygen anomalies (Table 3.4).

The most consistent predictor of coral distributions was the presence of carbonate rocks (Table 3.3, Table 3.4). Hard substrate had highly significant p-values and a large effect size in predicting the presence of scleractinians and non-scleractinians regardless of whether the dataset included all dives. Tubeworm, mussel, and bacterial mat distributions were also positively associated with the distribution of carbonate rocks across all GLMMs. However, this is most likely caused by the tubeworms' microbial consortia actively producing the authigenic carbonates at an active seep that attracts mussels and bacteria due to other seepage factors.

3.5 Discussion

The presence of hydrogen sulfide in the water column, as measured by redox potential, was found to be a significant predictor of tubeworm distributions but had no measureable effect on any other foundation taxa. However, it is remarkable that a relationship with this measure was detected at all. At *Sentry*'s photo survey height, the sensors measuring water chemistry are at least five meters away from the seafloor to capture a broad view of the benthic community and to prevent the vehicle from running into obstacles. In previous studies of cold seep biogeochemistry in the Gulf of Mexico, researchers found that hydrogen sulfide concentrations are often below the limits of detection at tubeworm plume height in the water column (E. Cordes et al., 2005; Freytag et al., 2001). As seep community succession proceeds, microbial reactions create more authigenic carbonate and cause fluids to cease seeping from the seafloor (E. E. Cordes et

al., 2006; E. Cordes et al., 2005). Tubeworms are able to obtain sulfide through their posterior “root” extensions and tight sulfur recycling with a consortium of microbes, allowing them to continue thriving even when seep chemicals are no longer entering the water column (E. E. Cordes et al., 2003; Freytag et al., 2001). Therefore it is possible that sulfide concentrations would be determined to be an important environmental filter in a study that collected water chemistry measurements closer to the sediment surface. This analysis serves as a proof of concept that this survey method can detect seepage in the water column.

Methane and hydrocarbons, the other compounds released from the seafloor at seeps and utilized by bacteria for chemosynthesis, did not show a significant influence on community assembly in this study. This measure had no predictive relationship with corals, tubeworms, or bacterial mats, but it did have a significant and unexpected relationship with mussel distributions. Hydrocarbon concentrations strongly predicted the absence of mussels despite the fact that mussels are the only chemosymbiotic fauna included in this study whose bacteria can directly utilize methane (Duperron, 2010). This anomalous relationship, however, appears to be the result of a small sample size. Mussels were the least frequently observed foundation taxa in this study (Table 3.2), and the smaller sample size of the hydrocarbon measurement dataset included only 19 grid cells where mussels were present. Because hydrocarbons are buoyant and can rise higher in the water column than hydrogen sulfide, it is less likely that this study would have failed to detect a relationship between hydrocarbons and the other foundation taxa due to sampling sensitivity issues than was the case for hydrogen sulfide concentrations. This analysis

suggests that hydrocarbons released from methane seeps are not an essential contributor to the seep proximity environmental filter.

It was expected in this study that seep organisms would be associated with lower levels of dissolved oxygen due to the low oxygen content of seeping fluids (Tunnicliffe et al., 2003). However, oxygen anomalies had a mixed relationship with the distributions of seep taxa at the sites surveyed. While bacterial mats and mussels were sometimes found to be predicted by negative oxygen anomalies, tubeworms were predicted by higher than average dissolved oxygen levels. This may be due to the higher seep flow requirements of bacteria and mussels. These organisms extract methane and sulfide from the water column to fuel their chemosynthesis, but tubeworms can obtain sulfide through their roots and instead need to acquire oxygen through their plume in the water column (Duperron, 2010; Freytag et al., 2001). Coral distributions also showed differing relationships with dissolved oxygen levels. Scleractinian corals were predicted by the presence of positive oxygen anomalies, which is congruent with physiology experiments and habitat niche models that found corals' distributions are limited by their oxygen requirement (Davies et al., 2008; Lunden, McNicholl, Sears, Morrison, & Cordes, 2014; Yesson et al., 2012). Non-scleractinian corals, on the other hand, were predicted by lower than average dissolved oxygen concentrations. This negative relationship, however, was only observed when the smaller hydrocarbon dataset was analyzed (Table 3.4). When all grid cells were included in the GLMM, scleractinian corals had a positive but non-significant response to higher oxygen levels (Table 3.3). The non-scleractinians of the smaller dataset may have been biased towards seep-preferent *C. delta* individuals. It is

possible that *C. delta* is adapted to tolerate lower oxygen conditions than other corals to allow it to enter this new niche, and in this case oxygen may be a significant component of the seepage environmental filter.

The availability of hard substrate has often been found to be a significant part of cold-water coral niche models, and this study was no exception (Samuel E. Georgian et al., 2014; A. M. Quattrini et al., 2015). As expected, the fine scale of habitat analysis captured the influence of this highly localized, patchy feature. The results confirm that authigenic carbonate produced by past seepage in the Gulf of Mexico is essential for facilitating the settlement of coral larvae and the growth of scleractinian reefs and octocoral gardens (Lisa Ann Levin et al., 2016; J. M. Roberts et al., 2009).

Overall this study was able to detect a number of predictive relationships between environmental variables and biological distributions. These findings are additional evidence that niche driven processes play an important role in community assembly in the deep Gulf of Mexico and confirm that methane seeps act as an environmental filter on seep and coral species' distributions (A. M. Quattrini et al., 2017). Specifically, hydrogen sulfide concentrations, the provision of hard substrate, and dissolved oxygen levels are the most likely variables driving this niche divergence. Since a transition between seep and non-seep habitats can be detected at this spatial scale, this raises questions about the nature of the seep-background ecotone. Ecotones are areas of high diversity and potential speciation (Kark & van Rensburg, 2007; Risser, 1995). The adaptation of the octocoral *C. delta* to this near-seep habitat could illuminate the ways in which corals respond to environmental stressors (A. M. Quattrini et al., 2013). Cold-water corals are susceptible

to oil exposure and were most recently impacted by excess hydrocarbons during the Deepwater Horizon oil spill in the deep Gulf of Mexico in 2010 (C. R. Fisher et al., 2014). Although this massive oil spill and the dispersants applied at depth to mitigate the disaster damaged the animals, corals were not always negatively impacted by oil exposure in a laboratory setting (DeLeo, Ruiz-Ramos, Baums, & Cordes, 2016). This tolerance may have been acquired through the natural, low-level hydrocarbon exposure these corals experience due to their proximity to seepage in the Gulf of Mexico.

CHAPTER 4

COMMUNITY ECOLOGY OF METHANE SEEPS ALONG THE COSTA RICA MARGIN INCLUDING THE JACO SCAR HYDROTHERMAL SEEP

4.1 Abstract

The Costa Rica margin is home to many methane seeps that host diverse chemosynthetic communities. The seep sites in this region span a wide depth range from 1000-1800m and have a variety of chemosymbiotic foundation fauna including siboglinid tubeworms, bathymodiolin mussels, and vesicomid clams. The Jaco Scar site in this region is also the location of a hybrid hydrothermal seep community where hydrothermal vent and cold seep species coexist near a fluid flow source elevated above ambient temperature. This study examines the influence depth and regional proximity to other chemosynthetic habitats on community assembly at four seep sites along the Costa Rica Margin using community dissimilarity metrics and non-metric multidimensional scaling. This study also asks broader questions about the roles depth, habitat type, and biogeography play in community assembly for both seeps and vents worldwide. Within the Costa Rica Margin, only depth was found to be a significant driver behind community assembly across the sites sampled. Despite the unique assemblage at the Jaco Scar hydrothermal seep, this site was not found to be significantly different from other seep sites in the region, and temperature did not appear to be a determinant of community structure. Globally, depth was still an important influence on community composition at the family level along with the geographic location of the site and whether the habitat

was a seep or a vent. Geographic region explained the most variation in community composition globally both quantitatively and qualitatively, lending support to the hypothesis that factors common to both vents and seeps and biogeographic barriers play more of a role in community assembly than the differences between vents and seeps.

4.2 Introduction

The Costa Rica Margin is home to more than one hundred seep sites (Sahling et al., 2008b). Within the center segment of the margin, fluid seepage is primarily caused by seamounts on the Cocos Plate being subducted under the Caribbean Plate (Han, Suess, Sahling, & Wallmann, 2004; Hensen, Wallmann, Schmidt, Ranero, & Suess, 2004; Sahling et al., 2008b). Researchers have known for more than a decade that these methane seeps host chemosymbiotic megafauna including tubeworms, clams, and mussels (Bohrmann, Heeschen, Jung, Weinrebe, Baranov, Cailleau, Heath, Hühnerbach, et al., 2002). Although the carbonate rock-associated communities and a single tubeworm-associated community from this area have been previously described, the macrofaunal communities associated with other seep megafauna at these seeps have yet to be fully characterized (L. a. Levin et al., 2012; Lisa A Levin et al., 2015).

A factor that makes the Costa Rica Margin a unique setting for seep communities is its geographic proximity to other chemosynthetic communities: the nearest neighboring chemosynthetic habitats to this region are hydrothermal vents, not other seeps. The seeps are surrounded by the vents of the Northern East Pacific Rise (NEPR), the Southern East Pacific Rise (SEPR), the Galapagos Ridge, and the Guaymas Basin. The nearest seeps are those found along the margin of Peru approximately 1600km away. The nearest vents, on

the other hand, are found about 900km away on the Galapagos Ridge. The Costa Rica Margin seeps are also within 2000km of the seeps of the Florida Escarpment, but they only had a deep water connection until the Isthmus of Panama closed 3-5mya. Seeps and vents have been found to share more taxa when they are located within closer proximity to one another (Portail et al., 2015; Watanabe et al., 2010). The NEPR in particular is considered to be a center for larval export based on biogeography models and could potentially influence the community assembly and evolution of seep taxa at these Costa Rica Margin sites with its propagules (Bachraty et al., 2009).

The previously described tubeworm community was sampled at the hybrid “hydrothermal seep” site first discovered in 2009 (L. a. Levin et al., 2012). The key feature that makes this habitat novel is an anomalously warm (+1-3°C) and visibly shimmering flow of water from the base of an enormous vestimentiferan tubeworm aggregation. Fewer than 10% of all species known from hydrothermal vents and cold seeps are found across both habitat types, but this location within the Jaco Scar site was found to host vent and seep species together in an unprecedented intermediate assemblage that included species which have only ever been reported from vents before (L. a. Levin et al., 2012; Tunnicliffe et al., 2003). It was hypothesized that this site could serve as a critical biogeographic and evolutionary link between seeps and vents, but a recent network study of chemosynthetic habitat biogeography did not find Jaco Scar to be an essential node to the network based on bivalve and gastropod mollusk taxa (Kiel, 2016). Instead, sedimented vents were found to be a connection between seeps and vents moreso than whale falls or this hydrothermal seep (Kiel, 2016).

The purpose of this study is to first comprehensively describe the macrofaunal communities found at four different Costa Rica Margin seeps: Mound 12, Mount Parrita, Parrita Seep, and Jaco Scar. In the course of characterizing the faunal composition of each site, this study also investigated whether the hydrothermal seep at Jaco Scar influences community assembly at this site. By analyzing samples with community dissimilarity metrics, this study examined whether the communities collected at the three sites without hydrothermal seep influence are more similar to one another than they are to Jaco Scar. As an additional measure of the effect of the hydrothermal seep, the correlation between community composition and the temperature at each sample collection location will also be tested. This analysis also hopes to shed light on the global biogeography of chemosynthetic ecosystems by comparing the community structure of vents and seeps around the world.

4.3 Methods

4.3.1 Study site description

Mound 12 is the shallowest site sampled in this study (~1000m) and home to extensive mussel beds in the area of the site named “Mussel Beach” (Figure 4.1). Three co-occurring species of mussel: *Bathymodiolus earlougheri*, *B. nancyschneideri*, and *B. billschneideri* form dense aggregations in a large, craggy mounds of carbonate to give this area its namesake. The site is also home to a location nicknamed “Yetisburg” for its abundant populations of the yeti crab *Kiwa puravida*. Mound 12 offers an abundance of hard substrate habitat, and the morphology of the carbonate at this site tends to resemble

broken pavement. These slabs are especially prominent at the area nicknamed “Skate Park” where *Escarpia spicata* and *Lamellibrachia sp.* tubeworms form small aggregations in the cracks between carbonate rocks.

Mount Parrita also hosts rocky carbonate features, small mussel beds, and medium-sized tubeworm aggregations containing both *E. spicata* and *Lamellibrachia sp.* (Figure 4.1). The most conspicuous seep habitat feature at this site, however, is a widespread area of soft sediment dominated by *Archivesica gigas* clam beds. Mount Parrita was the only site in this study to have such a sizeable soft sediment area and abundant clam beds.

Only *Lamellibrachia sp.* was identified in the tubeworm community collections from Parrita Seep (Figure 4.1). The tubeworm aggregations at this site ranged in size from small populations where just a handful of tubeworms rose out of the cracks between carbonate pavement slabs to large bushes arranged vertically to anchor in all available hard substrate area left under an overhanging carbonate ledge. In addition to the varied physical habitat of multiple carbonate morphologies interspersed with soft sediment, Parrita Seep also hosted variation in biogenic habitat with mussels filling in crags next to tubeworms and vesicomid clams populating the mud between these rocky features.

Jaco Scar is the deepest site sampled for this study at around 1800m (Figure 4.1). The samples collected here span a broad 75m depth range due to the steep slope along which seepage occurs at this site. Abundant *E. spicata* and *Lamellibrachia sp.* populations are found along this vertical feature forming both continuous tubeworm fields as well as large spherical bushes with their aggregations. The largest tubeworm

bush at this site, nicknamed “The Volkswagen” because it was the approximate size of a VW Beetle automobile, was observed to have a fluctuating 1-3°C anomaly when the shimmering water was measured with a temperature probe and is the site of the hybrid hydrothermal seep community (L. a. Levin et al., 2012). Although tubeworms are the dominant foundation species at this site, Jaco Scar also features mussel and clam beds among its carbonate and soft sediment habitats respectively.

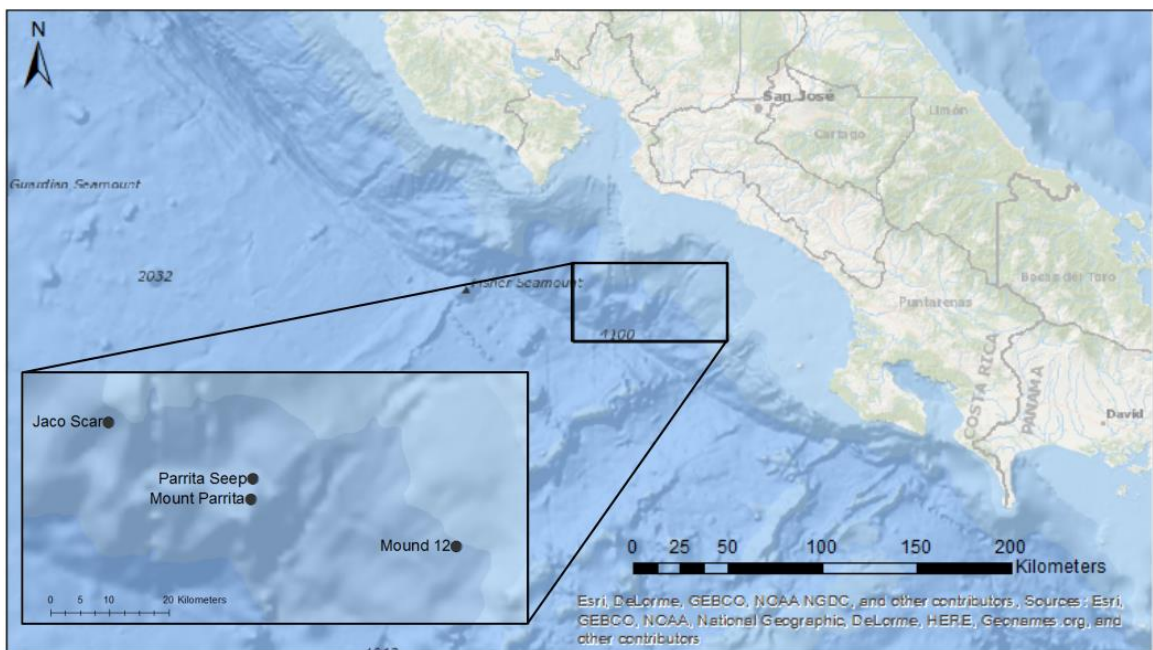


Figure 4.2. A map of the community collection sites along the Costa Rica Margin.

4.3.2 Community sample collection from the Costa Rica Margin and analysis

In February-March 2009 and May-June 2017, 18 community samples were collected with the *DSV Alvin* from four sites along the seamount subduction region of the Costa Rica margin (Figure 4.2, Table B1). The methane seep sites sampled were Mound 12, Mount Parrita, Parrita Seep, and Jaco Scar. Samples collected using the Bushmaster

Jr. tubeworm community sampling device (D. C. Bergquist et al., 2003) or mussel pots were processed quantitatively. All organisms captured in the devices' 63 μ m mesh and retained on a 1mm sieve were counted and identified to the lowest taxonomic level possible on board the ship. Ten total samples were processed in this manner with abundance data recorded for each species (Table 4.3, Table B2). The remaining eight community samples collected by either scoops or the submersible's manipulators could not be compared quantitatively and were processed qualitatively (Table 4.3, Table B3). Only the presence or absence of taxa retained on a 1mm sieve was recorded on board.

Table 4.3
Costa Rica Margin community sample locations

Site	Latitude	Longitude	Depth (m)	# Quantitative samples	# Qualitative Samples
Mound 12	8.923°N	84.312°W	995-997	5	2
Mount Parrita	9.001°N	84.623°W	1064-1405	1	1
Parrita Seep	9.032°N	84.621°W	1408	1	1
Jaco Scar	9.117°N	84.839°W	1742-1817	3	4

The differences between community samples were calculated using Bray-Curtis dissimilarity for the quantitative samples and Jaccard's index for the qualitative samples. Abundances in the quantitative analysis were first fourth-root transformed to down weight the effect of dominant species on community differences. Because Bushmaster collections target tubeworm-based communities and mussel pots and scoops target mussel-based communities, the foundation species (tubeworms and mussels) were excluded from the community datasets for both the quantitative and qualitative analyses to remove bias introduced by the differences in community sampling equipment (E. E.

Cordes, Carney, et al., 2007; E. E. Cordes, Becker, Hourdez, et al., 2010). The distances between community samples according to Bray-Curtis or Jaccard were visualized in NMDS plots using R's vegan package (Oksanen et al., 2016; R Core Team, 2015).

To detect the influence of site, habitat type, and sampling gear on community composition, the quantitative and qualitative samples were analyzed using a PERMANOVA in PRIMER (Anderson, Gorley, & Clarke, 2008; Clarke & Gorley, 2015). The PERMANOVA design tested site as a factor with four levels (Mound 12, Mount Parrita, Parrita Seep, and Jaco Scar) and a contrast representing the influence of the hydrothermal seep (Jaco Scar vs. the other three sites) along with a factor for sampling equipment. The effects of the depth and local temperature anomaly at the location of each sample collection were measured in addition to the previous factors by combining all five variables in a DistLM regression in PRIMER. The relationship between depth and temperature was calculated for each dive during which a community was sampled by fitting a linear regression in R using the data recorded by *Alvin*'s CTD during the vehicle's descent and ascent in the lowest 250m of the water column (R Core Team, 2015). To calculate a temperature anomaly value for each sample, the temperature recorded by *Alvin*'s CTD at the collection was compared to the temperature predicted from the depth of collection according to this linear relationship. Because *Alvin* CTD data was not available for dives 4511, 4513, and 4907, temperature anomalies could not be calculated for five of the community samples. Those samples that had temperature data were evaluated in a DistLM regression model that included all variables, and all samples

together were evaluated with another DistLM model that included only depth, habitat type (seep vs. hybrid), site, and sampling equipment.

4.3.3 Global comparison to published community collections

To compare the community composition of the Costa Rica sites to other vents and seeps around the world, additional community dissimilarity metrics were calculated from published community samples collected from different geographic regions (Table B4). Eight studies that also collected samples using mussel pots and the Bushmaster Jr. and processed the macrofaunal community with the same methods were compared to the Costa Rica Margin samples using abundance data. A total of 174 independent community samples taken from 16 individual sites across eight different regions in the Atlantic and Pacific oceans were analyzed together quantitatively (Figure 4.3). The maximum depth of the vent and seep samples was similar, but seep sites ranged in depth from 535m to 3466m whereas vent sites were limited to a much narrower depth range between 2122m and 3490m (Figure 4.5).

As expected, there was little overlap between vent and seep taxa at the species level in this combined dataset (Tunncliffe et al., 2003). Of the 333 species present in the quantitative collections, only 22 were shared (6.6% overlap) between vent and seep samples with 148 species found only at vents and 163 species found only at seeps. At the genus level, 37 of the total 245 genera were shared (15.1% overlap). At the family level, overlap reached 26.2% with 37 of the total 141 families shared between vents and seeps. To ensure shared taxa among the habitat types, collected abundance data was condensed to the family level for the analysis. Once again, foundation taxa (tubeworm family

Siboglinidae and mussel family Mytilidae) were removed from the analysis to reduce error from the bias introduced by the two quantitative sample types.

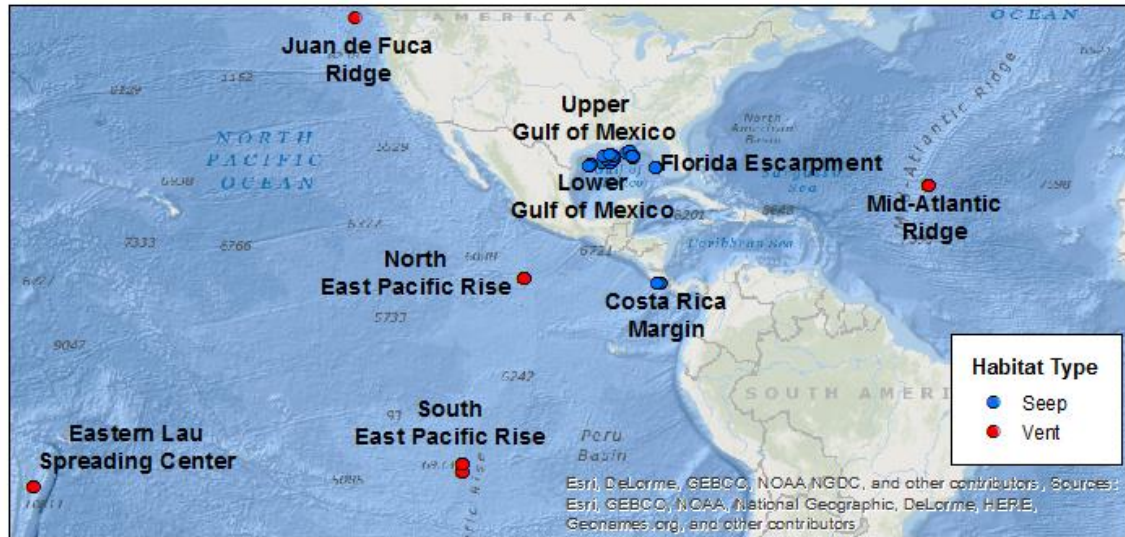


Figure 4.3. A map of all sites from which comparable family abundance data were collected and used in a quantitative global analysis of seep and vent communities.

To extend the community comparison to a broader geographic range, studies that used a variety of sampling methods were incorporated into a larger dataset used for a second global analysis based on taxonomic presence-absence data (Table B4). Community samples from 32 studies, including the eight quantitative studies previously evaluated for their abundance data, reported data from 448 individual collections from vents and seeps in every ocean on the planet (Figure 4.4). The seeps in this global comparison were collected from depths between 35m and 7380m, and again the vent samples were limited to a narrower depth range between 105m and 4150m (Figure 4.5).

Once again, data was consolidated to the family level of resolution to ensure a higher amount of overlap between the vent and seep communities. To standardize the taxonomic data across sampling methods, the analysis included only those families that were present in samples taken with the lowest resolution sampling method: video data. In total, 143 families were present in samples that relied only on video for taxonomic identification. 28 of these families were found only at vents, 47 only at seeps, and 88 were shared between the habitats (61.5% overlap).

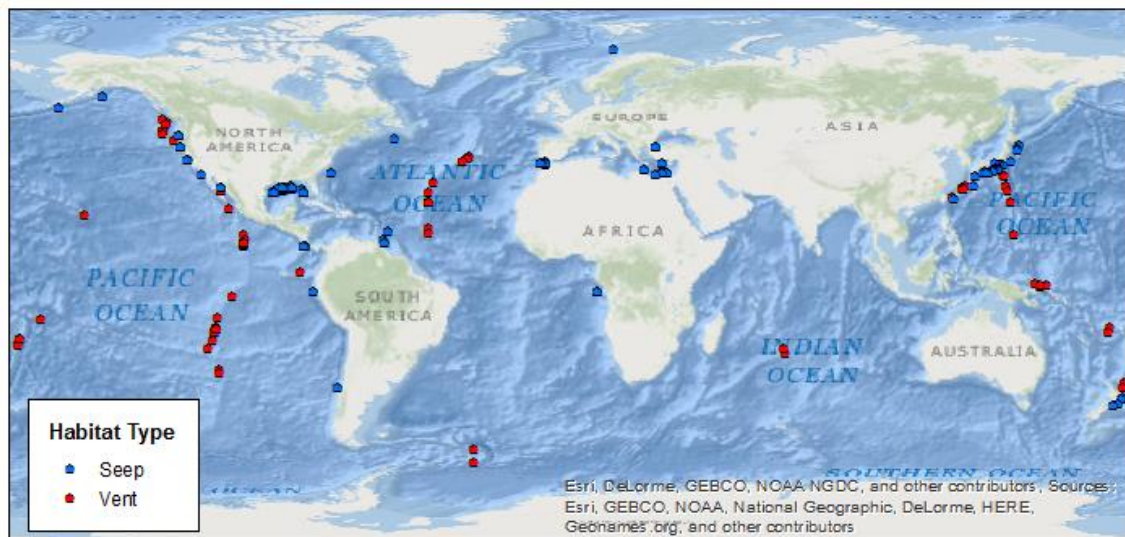


Figure 4.4. A map of all community samples included in the global analysis and compared using the presence-absence data of families visible in video analysis.

As with the Costa Rica Margin local analysis, abundance data were fourth-root transformed before calculating Bray-Curtis dissimilarity for NMDS plotting in R. The families visible in video data from those quantitative collections were also included in the

global qualitative analysis as presence-absence data, and distances were measured with the Jaccard index before plotting the samples on an NMDS.

The influence of geography and habitat type on community composition were tested with a PERMANOVA. The PERMANOVA design for the quantitative analysis included a factor of region with nine levels and a contrast for habitat type (all seep regions vs. all vent regions, Costa Rica Margin vs. all vent regions, Costa Rica Margin vs. all other seep regions) and a factor of sampling equipment with two levels (bushmaster and mussel pot). To investigate the effects of geographic region and habitat type after depth was accounted for, a DistLM regression was performed in PRIMER that included depth, habitat type (vent or seep), region, and sampling gear as variables in the model. The qualitative analysis used the same PERMANOVA and DistLM model design as the quantitative analysis. In addition, these analyses were also run with sedimented vents as another habitat factor level separate from hard substrate hydrothermal vents.

4.4 Results

4.4.1 Regional comparison among Costa Rica Margin sites

The communities at these three seep sites and Jaco Scar had a richness of 56 species in this dataset. Notably this included 15 different species of limpet, several of which occurred at high abundances of hundreds of individuals in a single community sample. In plotting the quantitative samples on an NMDS, depth appears to influence the observed pattern in community dissimilarity between sites (Figure 4.5). The samples collected from the shallowest seep (Mound 12) group together on the left half of the plot, and the rightmost portion of the plot contains two of the three samples from the deepest

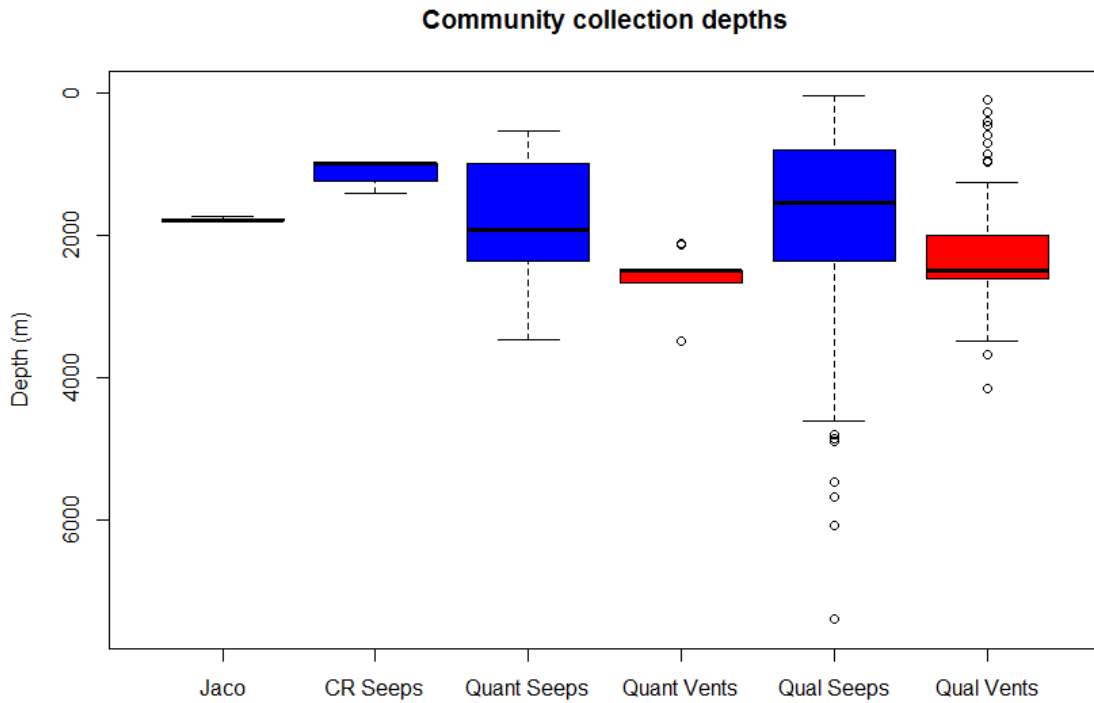


Figure 4.5. A boxplot displaying the range of depths from which communities were sampled for each analysis and habitat type.

seep (Jaco Scar). The intermediate depth samples from Parrita Seep and Mount Parrita fall in between these shallow and deep groupings. However, the DistLM regression that included all sites did not find depth to be a significant variable in determining community structure. Depth was significant in the marginal tests of the DistLM model that included temperature anomaly, but because this regression had only five samples with temperature data available for analysis the DistLM was unable to run the full model in addition to the marginal tests. The variables for site, habitat type, and sampling equipment were not found to be significant either in the DistLM. The PERMANOVA test reiterated these

results, where site, sampling equipment, or the site contrast between Jaco Scar and the other three sites were not significant factors in structuring communities.

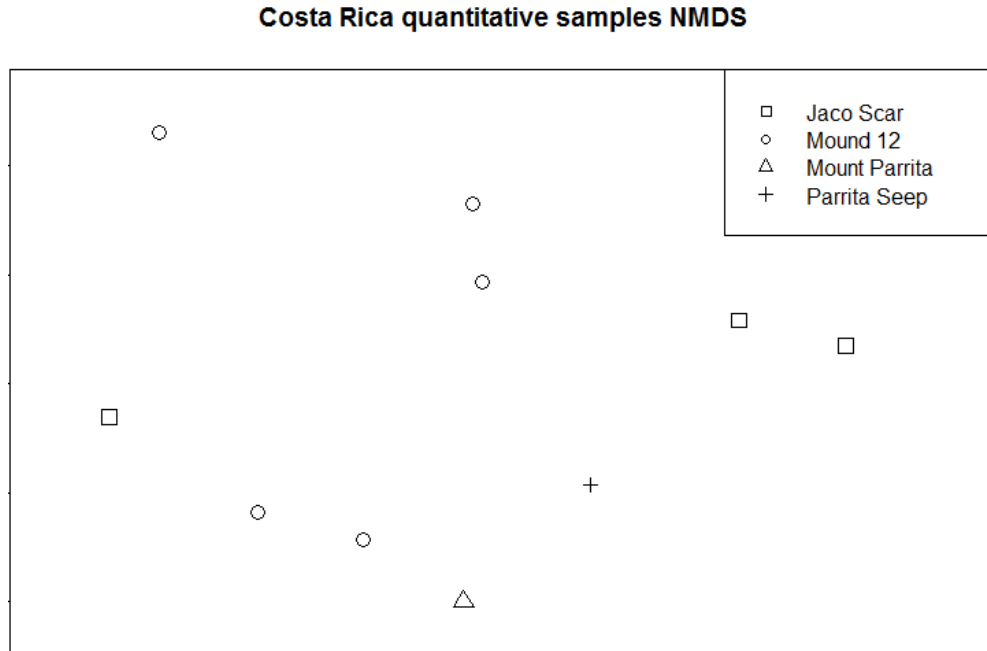


Figure 4.6. NMDS of Costa Rica quantitative community samples using distances calculated with the Bray-Curtis dissimilarity index. (Stress = 0.0705)

When all Costa Rica Margin samples were analyzed qualitatively, a similar pattern was observed in the NMDS with shallow Mound 12 samples grouping towards the left portion of the plot and all but one of the deep Jaco Scar samples clustering towards the right (Figure 4.6). The DistLM analyses that included all sites or just those with temperature data both confirmed that depth was a significant variable in determining community structure ($p < 0.05$). The depth of collection accounted for 11.3% of the sample variation when all sites were included and 13.7% of the variation when only samples that had corresponding temperature were included. After depth was accounted

for first in the sequential regression, no other variables were significant. The PERMANOVA test confirmed that neither site, either by itself or with the Jaco Scar vs. the other three seeps contrast, nor sampling equipment were significant factors for explaining the differences between communities.

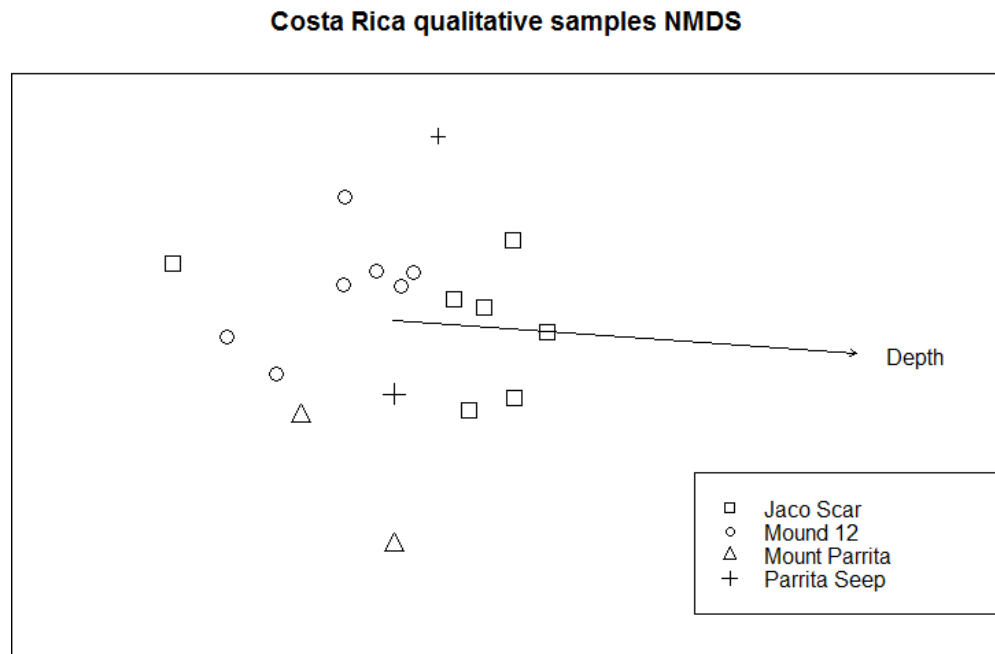


Figure 4.7. NMDS of Costa Rica qualitative community samples overlaid with a vector representing the correlation between depth and community dissimilarity as fit by R's envfit function. Distances calculated with Jaccard. (Stress = 0.1333)

4.4.2 Global quantitative analysis

When the Costa Rica Margin quantitative samples were compared to quantitative seep and vent samples globally, a pattern of community dissimilarity influenced by depth emerges again. The shallowest sites, seeps in the Upper Gulf of Mexico (GoM), are all found in the lower left portion of the NMDS plot on the opposite side from the

hydrothermal vent samples which are all collected from a narrow, much deeper depth range (Figure 4.7). The vents sampled for this analysis are closest in depth range to the seeps from the Florida Escarpment, and this similarity is reflected in the NMDS as these deep seeps are the nearest region to the vent regions (Figure 4.8). The narrow depth range from which vents were sampled quantitatively most likely also explains why the hydrothermal vents cluster together more tightly than the widespread seep regions. Besides depth, the nine different geographic regions from which these seeps and vents were sampled are another evident influence on the community similarity between samples as evidenced by the 95% confidence interval ellipses drawn to represent each level of this factor (Figure 4.8).

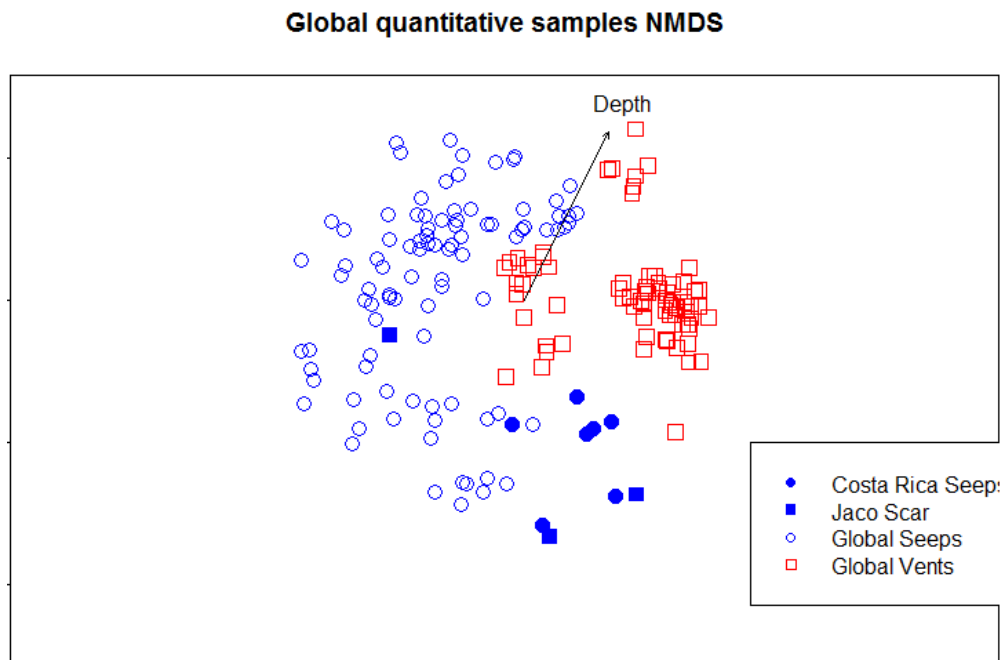


Figure 4.8. NMDS plot of Bray-Curtis distances between all global quantitative samples overlaid with a vector representing the correlation of depth with community ordination as fit by R's envfit function. (Stress = 0.1961)

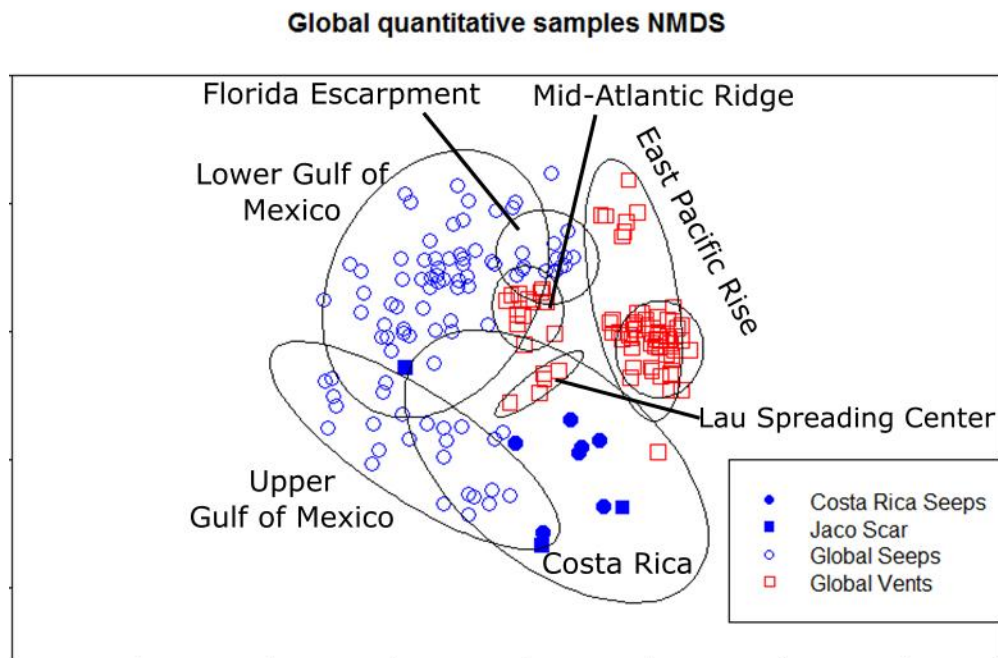


Figure 4.9: The same NMDS plot of Bray-Curtis distances between all global quantitative samples as Figure 4.7 also overlaid with 95% confidence interval ellipses for each geographic region. (Stress = 0.1961)

The DistLM results confirmed that this relationship between community composition and depth was significant ($p < 0.01$). All variables included in the DistLM regression were significant ($p < 0.01$). Region was significant even after accounting for depth and habitat type and explained the most variation in community samples. A regression model that included region with depth and habitat type explained 51.3% of the variation in community composition which was almost twice the R^2 value of the model based on depth and habitat type alone. When added as a fourth variable to this model, the equipment used to collect samples was significant despite the exclusion of foundation species, but this regression captured only 5.0% more variation than the three term

DistLM. The PERMANOVA test confirmed that region was a significant factor for determining community differences, and all habitat-based contrasts tested (vents vs. seeps, Costa Rica Margin vs vents, and Costa Rica Margin vs. other seeps) were also significant.

According to similarity percentage (SIMPER) tests, many of the taxonomic differences driving this distinction by habitat type were families that were either observed only at vents or much more abundant at vents. The crustacean taxa, uristid amphipods and copepods, were found exclusively at vents in the Southern and Northern East Pacific Rise. Vents in the quantitative analysis were also distinguished by higher abundances of lepetodrilid limpets and ampharetid worms. All vents had higher abundances of ampharetids than Costa Rica seeps, and the Mid-Atlantic Ridge was the only vent region that did not have higher abundances of lepetodrilids than Costa Rica.

Although the seeps of the Costa Rica Margin had generally lower abundances of lepetodrilid limpets than vents, the presence of this family at these sites distinguished it from other seeps as these gastropods were not present at any of the other three seep regions. The seeps of the upper and lower Gulf of Mexico were also lacking actiniarian anemones, which were abundant at the Costa Rica seeps. Although the Costa Rica Margin is found within the same depth range as the Lower Gulf of Mexico, the Costa Rica sites had far lower abundances of ophiuroids than the deep Gulf of Mexico and Florida Escarpment sites. The Upper Gulf of Mexico seeps completely lack brittle stars, and this taxa likely contributes to the higher overlap of Costa Rica with these shallower seeps. Another taxon in low abundance at Costa Rica was alvinocarid shrimp, which

were found in high abundance at all other seep regions in the quantitative analysis. Similar to the vent communities, the Florida Escarpment communities were the only seeps to have high abundances of ampharetids.

4.4.3 Global qualitative analysis

At this geographic breadth of analysis at the family level, patterns among the many community samples are no longer clear in the NMDS plot of Jaccard index values (Figure 4.9). One similarity to the global quantitative analysis is that vents are once again clustering slightly closer to one another than the widespread seep samples cluster to other seep samples. Although the vents sampled for the qualitative analysis constitute a wider depth range, they are still limited to a narrower range than the depth of seep sites, making it likely again that depth is responsible for shaping this pattern in the plot.

The DistLM regression analysis confirmed again that Depth is a significant variable in structuring community composition. The other variables included in the model (habitat type, geographic region, and sampling equipment) were also all significant in sequential regression. The geographic PERMANOVA testing also confirmed that geographic region and habitat type (seep or vent) were significant factors for community composition globally. Geographic region explained the most variation in community samples again, even more so than in the global quantitative analysis. A regression based on depth and habitat type explained just 4.9% of the variation in community composition, but when region was included, this three variable model captured 45.0% of all observed variation. Surprisingly, depth was the variable that added the lowest R^2 to the model and

Global qualitative samples NMDS

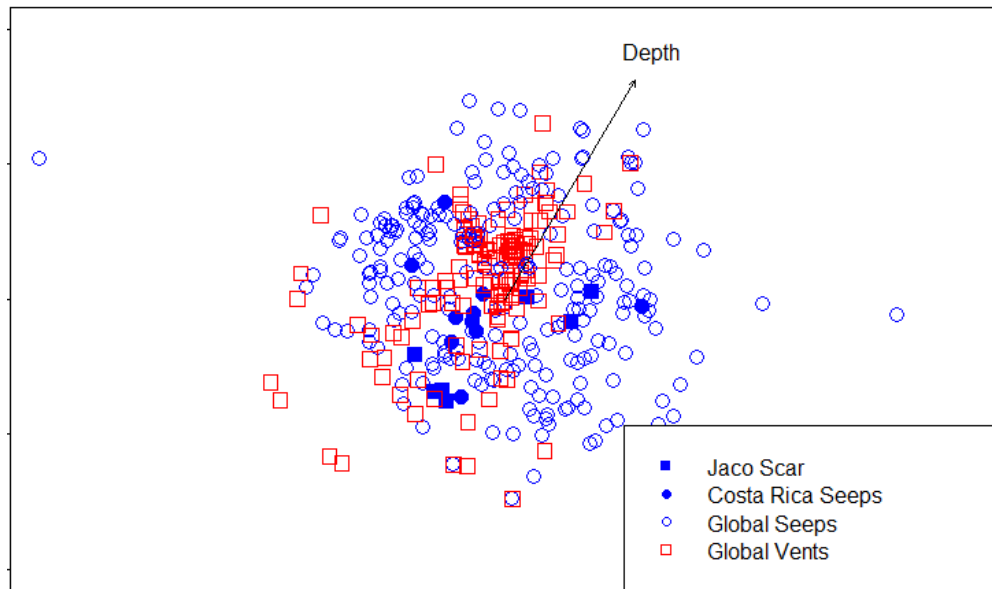


Figure 4.10. NMDS plot of Jaccard distances between all global qualitative samples overlaid with a vector representing the correlation of depth with community ordination as fit by R's envfit function. (Stress = 0.1902)

explained only 1.8% of the variation in community structure across all samples.

PERMANOVA results confirmed that both region and habitat type were significant factors in determining community structure. Including sedimented vents as a third level in the habitat factor did not change the DistLM regression and PERMANOVA test results. A pairwise PERMANOVA found that vents and seeps and seeps and sedimented vents were significantly different from one another, but sedimented vent communities were not significantly different from the communities sampled at hard substrate vents.

As with the quantitative analysis, SIMPER tests between habitat types showed Ampharetidae and Lepetodrilidae were more common across vent community samples

than seeps. Ampharetid worms were again found at vent sites than at Costa Rica Margin seeps, but samples from Costa Rica were on average more likely to contain lepetodrilid limpets than vent samples when the analyzed at this level. Additionally, hesionid worms were more common in vent samples than at seeps globally or Costa Rica seeps. The presence of polynoid worms at the Costa Rica seeps had an intermediate occurrence rate between seeps samples, where they were rarest, and vent samples, where they were most likely to be members of the community. Serpulid worms were not among the top contributors to the differences between vents and seeps, but this family was more likely to be collected from the Costa Rica Margin than from either vents or seeps globally.

4.5 Discussion

The Costa Rica Margin is home to a remarkable diversity of seep habitats. The physical habitat at these sites includes a range of authigenic carbonate morphologies to provide hard substrate for tubeworms and mussels along with areas of soft sediment where bacterial mats and vesicomyid clams dominate the communities. This diversity of seep foundation species was previously known, but this study represents the first survey of the associated macrofaunal community from Mound 12, Mount Parrita, and Parrita Seep (Bohrmann, Heeschen, Jung, Weinrebe, Baranov, Cailleau, Heath, Hühnerbach, et al., 2002). The wide depth range these sites span within a relatively small geographic distance also contributes to the diversity of seep-associated species in this area.

A previous study in this region proposed that the hydrothermal seep found at Jaco Scar could serve as an important evolutionary and biogeographic link between vents and seeps, as evidenced by its unique intermediate environmental conditions and mixed

community (L. a. Levin et al., 2012). It is most likely that this novel community containing both vent and seep species is shaped by the high rate of fluid flux containing elevated sulfide and methane concentrations flowing out of the base of the Volkswagen tubeworm bush (L. a. Levin et al., 2012; Portail et al., 2015). The current study, however, did not find that this local fluid flow feature has much influence on the surrounding Jaco Scar communities. Samples from the Jaco Scar site were not significantly different from the other Costa Rica seep sites when analyzed quantitatively or qualitatively. Additionally, there was no significant relationship between the temperature anomaly of each sample and community composition. A recently biogeographic network analysis of vents, seeps, and organic falls globally also did not find the Jaco Scar hydrothermal seep to be a noteworthy link between vents and seeps (Kiel, 2016).

Instead, this analysis found that depth was the most important influence on community assembly for the Costa Rica Margin seeps. The turnover of species with depth is a common contributor to community dissimilarity in the deep sea generally and at deep-sea chemosynthetic sites in particular (Angel, 2003; E. E. Cordes, Carney, et al., 2007; Karine Olu et al., 2010). Depth remained a significant variable in determining community structure when global vent and seep communities were analyzed quantitatively and qualitatively in this study. Seeps and vents were also significantly different from one another when compared globally at the family level. The geographic region of each community, however, explained the most variation in community composition across all quantitative and qualitative samples in this study.

Consistent with recent work that has found that vents and seeps share more taxa in common when biogeographic barriers are removed, region was the most essential factor in community structure in this analysis (Baco et al., 2010; Portail et al., 2015; Watanabe et al., 2010). When vents and seeps are in close proximity to one another, one study has found that the foundation species, substrate type, and flow rate were all better predictors of community composition at the family level than whether the habitat was a seep or a vent (Portail et al., 2015). The harsh chemicals and higher temperatures of vent fluids were not as great a barrier to fauna colonization as previously predicted. This suggests that biogeographic barriers may play a more important role in community assembly at higher taxonomic levels than adaptations to vent and seep environmental conditions.

This study also found that although the warm fluid flow from the Jaco Scar hydrothermal seep did not have an appreciable effect on the surrounding communities, there were still several similarities between hydrothermal vents and Costa Rica Margin seeps overall. The Costa Rica sites had an intermediate rate of occurrence of the family Polynoidae between vents and seeps. These scaleworms are common predators at vents and less frequently found at seeps. This may suggest that Costa Rica Margin food webs are able to sustain higher order consumers in a vent-like food web (Turnipseed, Jenkins, & Dover, 2004). A more in-depth analysis of the consumer relationships using stable isotopes would be required to examine more precisely how much the food web structure resembles other seeps and vents. The Costa Rica seeps also had higher abundances of lepetodrilid limpets than other seeps, a family that is most common at vents (Johnson, Warén, & Vrijenhoek, 2008; Portail et al., 2015). The high abundance of these limpets

and other families shared with vents is most likely due to the proximity of the Costa Rica Margin to the East Pacific Rise. Located in the oldest ocean basin at the fastest spreading center, the NEPR and SEPR have the highest recorded species richness of any hydrothermal vent province (Bachraty et al., 2009). The region has been proposed as a major source of dispersal for vent taxa is likely sending propagules to the Costa Rica Margin (Bachraty et al., 2009). Population genetics studies of the species shared between Costa Rica and the East Pacific Rise in addition to phylogeography would be necessary to confirm this dispersal pathway.

CHAPTER 5

CONCLUSIONS

In this dissertation, I investigated the influences of environmental conditions on chemosynthetic populations and communities. This project took a unique multi-scale perspective to answer this question and examine how the effects of chemosynthetic habitats on biology change across different spatial and ecological scales.

At the broadest scale, I found that the community composition of seeps and vents at the family level driven by the universal factors of biogeography and dispersal limitation more than it is shaped by chemosynthetic habitat-specific features. This result was surprising given the highly distinct physical environments of seeps and vents and their historical dichotomy in the research, but my conclusion is in line with recent studies that are finding more in common between these two habitats. Other researchers have also found that geographic proximity can bridge the higher-level taxonomic differences between seeps and vents despite their different abiotic habitat conditions (Kiel, 2016; Portail et al., 2015). The close biogeographic links between eastern Pacific vents and the Costa Rica Margin are likely responsible for the similarities I observed between these seep communities and typical vent community structure at the family level. Within the region, however, depth was the only demonstrated driver of community composition, and there was no detectable influence of the unique hydrothermal seep feature on the other seep communities at Jaco Scar or the other three seep sites sampled along the margin. Depth was also found to significantly shape the community composition of other vents

and seeps globally, a finding consistent with the rates of species turnover observed across other deep-sea habitats with depth (Angel, 2003).

When I examined the abiotic influences of seeps on community structure at a smaller spatial scale within sites in the Gulf of Mexico, I found evidence for seep-driven community assembly. My study adds to the extant body of evidence that seeps serve as an environmental filter for seep and non-seep community assembly in this region (A. M. Quattrini et al., 2017). Furthermore, my analysis clarifies that hydrogen sulfide concentrations have a detectable effect on seep community assembly, and the local depressions of dissolved oxygen levels at seeps appear to influence the distributions of both seep and non-seep coral taxa. The release of hydrocarbons at these sites, a necessary fuel for chemosynthesis but a potential toxin for non-adapted background species, had no significant effect on the distributions of foundation taxa and does not seem to be an essential component of the seep proximity environmental filter. As has been found with other studies, the presence of carbonate rocks were required for coral settlement and serve as a connection between past, inactive seeps and present-day non-seep communities (J. M. Roberts et al., 2009).

When I zoomed in to analyze a single species' population dynamics within these seeps in the Gulf of Mexico, the effect of the seep environment on this animal's evolution was evident. I showed that the stability of deep cold seeps in this region allow the tubeworm species *Escarpia laminata* to reach ages over 300 years old. Both individual-based models and population-wide simulations that used *in situ* growth and mortality data supported this estimate. The stable environment relaxes the need for the tubeworms to

develop mechanisms for withstanding disturbance, and the lack of lethal predation on this species further reduces external mortality threats (Williams, 1957). Instead selective pressure on *E. laminata* and its fellow seep vestimentiferans in the Gulf of Mexico pushes these species towards longer and longer lifespans, allowing them to exceed ages predicted by universal metabolic scaling laws (McClain et al., 2012).

The work of this dissertation has tested relationships between environmental factors and species' responses at deep-sea chemosynthetic ecosystems. Within the Gulf of Mexico, niche processes are supported as important ecological and evolutionary drivers. The temporal stability of the widespread seepage in this region has allowed vestimentiferan tubeworms to reach record-breaking lifespans and shaped the species composition of seep and coral communities. In the Costa Rica Margin, an expected ecological relationship was observed between species turnover and depth, but the temperature anomaly and elevated flow of one unique feature at Jaco Scar was found to have a very limited, localized influence on community assembly. These ecological interactions between environment variables and species' distributions remained significant in predicting community composition when a global dataset of chemosynthetic habitats was analyzed. They became dwarfed, however, by the influence of neutral dispersal limitation and biogeographic barriers at this broadest geographic scale.

BIBLIOGRAPHY

- Aharon, P., & Fu, B. (2000). Microbial sulfate reduction rates and sulfur and oxygen isotope fractionations at oil and gas seeps in deepwater Gulf of Mexico. *Geochimica et Cosmochimica Acta*, 64(2), 233–246. Retrieved from <http://www.sciencedirect.com/science/article/pii/S0016703799002926>
- Aharon, P., Roberts, H. H., & Snelling, R. (1992). Submarine venting of brines in the deep Gulf of Mexico: observations and geochemistry. *Geology*, 20(6), 483–486. doi:10.1130/0091-7613(1992)020<0483:SVOBIT>2.3.CO;2
- Anderson, M. J., Gorley, R. N., & Clarke, K. R. (2008). PERMANOVA+ for PRIMER: Guide to Software and Statistical Methods. In *Plymouth, UK* (pp. 1–214).
- Andrews, A., Cordes, E., & Mahoney, M. (2002). Age, growth and radiometric age validation of a deep-sea, habitat-forming gorgonian (*Primnoa resedaeformis*) from the Gulf of Alaska. *Hydrobiologia*, (471), 101–110. Retrieved from <http://www.springerlink.com/index/3TBECDAL2T4NNJQF.pdf>
- Angel, M. V. (2003). The pelagic environment of the open ocean. In P. A. Tyler (Ed.), *Ecosystems of the world: The Deep Ocean* (pp. 39–80). Amsterdam: Elsevier.
- Atanasov, A. T. (2005). The linear allometric relationship between total metabolic energy per life span and body mass of poikilothermic animals. *BioSystems*, 82(2), 137–142. doi:10.1016/j.biosystems.2005.06.006
- Austad, S. N. (1993). Retarded senescence in an insular population of Virginia opossums (*Didelphis virginiana*). *Journal of Zoology*, 229(4), 695–708. doi:10.1111/j.1469-7998.1993.tb02665.x
- Bachraty, C., Legendre, P., & Desbruyères, D. (2009). Biogeographic relationships among deep-sea hydrothermal vent faunas at global scale. *Deep Sea Research Part I: Oceanographic Research Papers*, 56(8), 1371–1378. doi:10.1016/j.dsr.2009.01.009
- Baco, A. R., Rowden, A. A., Levin, L. A., Smith, C. R., & Bowden, D. A. (2010). Initial characterization of cold seep faunal communities on the New Zealand Hikurangi margin. *Marine Geology*, 272(1–4), 251–259. doi:10.1016/j.margeo.2009.06.015
- Beaulieu, S. E., Baker, E. T., German, C. R., & Maffei, A. (2013). An authoritative global database for active submarine hydrothermal vent fields. *Geochemistry, Geophysics, Geosystems*, 14(11), 4892–4905. doi:10.1002/2013GC004998
- Becker, E. L., Cordes, E. E., Macko, S. a., & Fisher, C. R. (2009). Importance of seep primary production to *Lophelia pertusa* and associated fauna in the Gulf of Mexico.

Deep Sea Research Part I: Oceanographic Research Papers, 56(5), 786–800.
doi:10.1016/j.dsr.2008.12.006

- Becker, E. L., Cordes, E. E., Macko, S. a., Lee, R. W., & Fisher, C. R. (2013). Using Stable Isotope Compositions of Animal Tissues to Infer Trophic Interactions in Gulf of Mexico Lower Slope Seep Communities. *PLoS ONE*, 8(12), e74459. doi:10.1371/journal.pone.0074459
- Bergquist, D. C., Ward, T., Cordes, E. E., McNelis, T., Howlett, S., Kosoff, R., ... Fisher, C. R. (2003). Community structure of vestimentiferan-generated habitat islands from Gulf of Mexico cold seeps. *Journal of Experimental Marine Biology and Ecology*, 289(2), 197–222. doi:10.1016/S0022-0981(03)00046-7
- Bergquist, D., Eckner, J., Urcuyo, I., Cordes, E., Hourdez, S., Macko, S., & Fisher, C. (2007). Using stable isotopes and quantitative community characteristics to determine a local hydrothermal vent food web. *Marine Ecology Progress Series*, 330(1), 49–65. doi:10.3354/meps330049
- Bergquist, D., Urcuyo, I., & Fisher, C. (2002). Establishment and persistence of seep vestimentiferan aggregations on the upper Louisiana slope of the Gulf of Mexico. *Marine Ecology Progress Series*, 241, 89–98. doi:10.3354/meps241089
- Bergquist, D., Williams, F., & Fisher, C. (2000). Longevity record for deep-sea invertebrate. *Nature*, 403, 499–500. Retrieved from <http://www.nature.com/nature/journal/v403/n6769/full/403499a0.html>
- Boetius, A., Ravenschlag, K., & Schubert, C. (2000). A marine microbial consortium apparently mediating anaerobic oxidation of methane. *Nature*, 407(October), 623–626. Retrieved from <http://www.nature.com/nature/journal/v407/n6804/abs/407623a0.html>
- Bohrmann, G., Heeschen, K., Jung, C., Weinrebe, W., Baranov, B., Cailleau, B., ... Trummer, I. (2002). Widespread fluid expulsion along the seafloor of the Costa Rica convergent margin. *Terra Nova*, 14(2), 69–79. doi:10.1046/j.1365-3121.2002.00400.x
- Bohrmann, G., Heeschen, K., Jung, C., Weinrebe, W., Baranov, B., Cailleau, B., ... Trummer, I. (2002). Widespread fluid expulsion along the seafloor of the Costa Rica convergent margin. *Terra Nova*, 14(2), 69–79. doi:10.1046/j.1365-3121.2002.00400.x
- Bright, M., & Lallier, F. H. (2010). The biology of vestimentiferan tubeworms. *Oceanography and Marine Biology: ...*, 48(July 2009), 213–266. Retrieved from <http://www.sb-roscoff.fr/Ecchis/pdf/10-Bright-OMBAR.pdf>
- Brown, A., & Thatje, S. (2014). Explaining bathymetric diversity patterns in marine

- benthic invertebrates and demersal fishes: physiological contributions to adaptation of life at depth. *Biological Reviews of the Cambridge Philosophical Society*, 89(2), 406–26. doi:10.1111/brv.12061
- Buesseler, K. O., Lamborg, C. H., Boyd, P. W., Lam, P. J., Trull, T. W., Bidigare, R. R., ... Wilson, S. (2007). Revisiting Carbon Flux Through the Ocean ' s Twilight Zone. *Science*, 316(April), 567–570. doi:10.1126/science.1137959
- Cailliet, G. ., Andrews, a. ., Burton, E. ., Watters, D. ., Kline, D. ., & Ferry-Graham, L. . (2001). Age determination and validation studies of marine fishes: do deep-dwellers live longer? *Experimental Gerontology*, 36(4–6), 739–764. doi:10.1016/S0531-5565(00)00239-4
- Carney, R. S. (1994). Consideration of the oasis analogy for chemosynthetic communities at Gulf of Mexico hydrocarbon vents. *Geo-Marine Letters*, 14(2–3), 149–159. doi:10.1007/BF01203726
- Cavanaugh, C. M., Gardiner, S. L., Jones, M. L., Jannasch, H. W., & Waterbury, J. B. (1981). Prokaryotic Cells in the Hydrothermal Vent Tube Worm Riftia pachyptila Jones: Possible Chemoautotrophic Symbionts. *Science*, 213(4505), 340–342. doi:10.1126/science.213.4505.340
- Childress, J. J., Cowles, D. L., Favuzzi, J. A., & Mickel, T. J. (1990). Metabolic rates of benthic deep-sea decapod crustaceans decline with increasing depth primarily due to the decline in temperature. *Deep Sea Research Part A. Oceanographic Research Papers*, 37(6), 929–949. doi:10.1016/0198-0149(90)90104-4
- Clarke, K. R., & Gorley, R. N. (2015). PRIMER v7: User Manual/Tutorial. Plymouth: PRIMER-E Ltd.
- Cordes, E. E., Arthur, M. a, Shea, K., Arvidson, R. S., & Fisher, C. R. (2005). Modeling the mutualistic interactions between tubeworms and microbial consortia. *PLoS Biology*, 3(3), e77. doi:10.1371/journal.pbio.0030077
- Cordes, E. E., Becker, E. L., & Fisher, C. R. (2010). Temporal shift in nutrient input to cold-seep food webs revealed by stable-isotope signatures of associated communities. *Limnology and Oceanography*, 55(6), 2537–2548. doi:10.4319/lo.2010.55.6.2537
- Cordes, E. E., Becker, E. L., Hourdez, S., & Fisher, C. R. (2010). Influence of foundation species, depth, and location on diversity and community composition at Gulf of Mexico lower-slope cold seeps. *Deep Sea Research Part II: Topical Studies in Oceanography*, 57(21–23), 1870–1881. doi:10.1016/j.dsr2.2010.05.010
- Cordes, E. E., Bergquist, D. C., & Fisher, C. R. (2009). Macro-Ecology of Gulf of Mexico Cold Seeps. *Annual Review of Marine Science*, 1(1), 143–168.

doi:10.1146/annurev.marine.010908.163912

- Cordes, E. E., Bergquist, D. C., Predmore, B. L., Jones, C., Deines, P., Telesnicki, G., & Fisher, C. R. (2006). Alternate unstable states: Convergent paths of succession in hydrocarbon-seep tubeworm-associated communities. *Journal of Experimental Marine Biology and Ecology*, 339(2), 159–176. doi:10.1016/j.jembe.2006.07.017
- Cordes, E. E., Bergquist, D. C., Redding, M. L., & Fisher, C. R. (2007). Patterns of growth in cold-seep vestimentiferans including *Seepiophila jonesi*: a second species of long-lived tubeworm. *Marine Ecology*, 28(1), 160–168. doi:10.1111/j.1439-0485.2006.00112.x
- Cordes, E. E., Bergquist, D. C., Shea, K., & Fisher, C. R. (2003). Hydrogen sulphide demand of long-lived vestimentiferan tube worm aggregations modifies the chemical environment at deep-sea hydrocarbon seeps. *Ecology Letters*, 6(3), 212–219. doi:10.1046/j.1461-0248.2003.00415.x
- Cordes, E. E., Carney, S. L., Hourdez, S., Carney, R. S., Brooks, J. M., & Fisher, C. R. (2007). Cold seeps of the deep Gulf of Mexico: Community structure and biogeographic comparisons to Atlantic equatorial belt seep communities. *Deep Sea Research Part I: Oceanographic Research Papers*, 54(4), 637–653. doi:10.1016/j.dsr.2007.01.001
- Cordes, E. E., Cunha, M. R., Galéron, J., Mora, C., Olu-Le Roy, K., Sibuet, M., ... Levin, L. a. (2010). The influence of geological, geochemical, and biogenic habitat heterogeneity on seep biodiversity. *Marine Ecology*, 31(1), 51–65. doi:10.1111/j.1439-0485.2009.00334.x
- Cordes, E. E., McGinley, M. P., Podowski, E. L., Becker, E. L., Lessard-Pilon, S., Viada, S. T., & Fisher, C. R. (2008). Coral communities of the deep Gulf of Mexico. *Deep Sea Research Part I: Oceanographic Research Papers*, 55(6), 777–787. doi:10.1016/j.dsr.2008.03.005
- Cordes, E., Hourdez, S., Predmore, B., Redding, M., & Fisher, C. (2005). Succession of hydrocarbon seep communities associated with the long-lived foundation species *Lamellibrachia luymesii*. *Marine Ecology Progress Series*, 305, 17–29. doi:10.3354/meps305017
- Cowart, D. A., Halanych, K. M., Schaeffer, S. W., & Fisher, C. R. (2014). Depth-dependent gene flow in Gulf of Mexico cold seep *Lamellibrachia* tubeworms (Annelida, Siboglinidae). *Hydrobiologia*, 736, 139–154. doi:10.1007/s10750-014-1900-y
- Dattagupta, S., Miles, L. L., Barnabei, M. S., & Fisher, C. R. (2006). The hydrocarbon seep tubeworm *Lamellibrachia luymesii* primarily eliminates sulfate and hydrogen ions across its roots to conserve energy and ensure sulfide supply. *The Journal of*

Experimental Biology, 209, 3795–3805. doi:10.1242/jeb.02413

- Davies, A. J., Wisshak, M., Orr, J. C., & Murray Roberts, J. (2008). Predicting suitable habitat for the cold-water coral *Lophelia pertusa* (Scleractinia). *Deep-Sea Research Part I: Oceanographic Research Papers*, 55(8), 1048–1062. doi:10.1016/j.dsr.2008.04.010
- DeLeo, D. M., Ruiz-Ramos, D. V., Baums, I. B., & Cordes, E. E. (2016). Response of deep-water corals to oil and chemical dispersant exposure. *Deep-Sea Research Part II: Topical Studies in Oceanography*, 129, 137–147. doi:10.1016/j.dsr2.2015.02.028
- Desbruyères, D., Biscoito, M., Caprais, J.-C., Colaço, A., Comtet, T., Crassous, P., ... Vangriesheim, A. (2001). Variations in deep-sea hydrothermal vent communities on the Mid-Atlantic Ridge near the Azores plateau. *Deep Sea Research Part I: Oceanographic Research Papers*, 48(5), 1325–1346. doi:10.1016/S0967-0637(00)00083-2
- Desbruyères, D., Segonzac, M., & Bright, M. (2006). *Handbook of deep-sea hydrothermal vent fauna*. Land Oberösterreich, Biologiezentrum der Oberösterreichische Landesmuseen.
- Deweerd, S. (2012). Comparative biology: Looking for a master switch. *Nature*, 492(7427), S10–S11. doi:10.1038/492S10a
- Drazen, J. C., & Seibel, B. A. (2007). Depth-related trends in metabolism of benthic and benthopelagic deep-sea fishes. *Limnology and Oceanography*, 52(5), 2306–2316. doi:10.4319/lo.2007.52.5.2306
- Dubilier, N., Bergin, C., & Lott, C. (2008). Symbiotic diversity in marine animals: the art of harnessing chemosynthesis. *Nature Reviews. Microbiology*, 6(10), 725–40. doi:10.1038/nrmicro1992
- Duperron, S. (2010). The diversity of deep-sea mussels and their bacterial symbioses. In S. Kiel (Ed.), *The Vent and Seep Biota* (pp. 137–168). Springer Netherlands, Dordrecht.
- ESRI. (2014). ArcGIS Desktop: Release 10.3. Redlands CA.
- Etnoyer, P. J., Wagner, D., Fowle, H. A., Poti, M., Kinlan, B., Georgian, S. E., & Cordes, E. E. (2017). Models of habitat suitability, size, and age-class structure for the deep-sea black coral *Leiopathes glaberrima* in the Gulf of Mexico. *Deep Sea Research Part II: Topical Studies in Oceanography*, (xxxx), 0–1. doi:https://doi.org/10.1016/j.dsr2.2017.10.008
- Evans, C. (1967). The toxicity of hydrogen sulphide and other sulphides. *Experimental Physiology*, LII(3), 231–248. Retrieved from

<http://ep.physoc.org/content/52/3/231.short>

- Fisher, C. R. (1990). Chemoautotrophic and methanotrophic symbioses in marine invertebrates. *Reviews in Aquatic Sciences*, 2(3–4), 399–436.
- Fisher, C. R., Hsing, P.-Y., Kaiser, C. L., Yoerger, D. R., Roberts, H. H., Shedd, W. W., ... Brooks, J. M. (2014). Footprint of Deepwater Horizon blowout impact to deep-water coral communities. *Proceedings of the National Academy of Sciences*, 111(32), 11744–11749. doi:10.1073/pnas.1403492111
- Fisher, C., Roberts, H., Cordes, E., & Bernard, B. (2007). Cold Seeps and Associated Communities of the Gulf of Mexico. *Oceanography*, 20(4), 118–129. doi:10.5670/oceanog.2007.12
- Freiwald, A., Wilson, J. B., & Henrich, R. (1999). Grounding pleistocene icebergs shape recent deep-water coral reefs. *Sedimentary Geology*, 125(1–2), 1–8. doi:10.1016/S0037-0738(98)00142-0
- Freytag, J. K., Girguis, P. R., Bergquist, D. C., Andras, J. P., Childress, J. J., & Fisher, C. R. (2001). A paradox resolved: sulfide acquisition by roots of seep tubeworms sustains net chemoautotrophy. *Proceedings of the National Academy of Sciences of the United States of America*, 98(23), 13408–13. doi:10.1073/pnas.231589498
- Gage, J. D. (2003). Food inputs, utilization, carbon flow and energetics. In P. A. Tyler (Ed.), *Ecosystems of the world: The Deep-Sea* (pp. 313–380). Amsterdam: Elsevier.
- Gebruk, A., Krylova, E., Lein, A., Vinogradov, G., Anderson, E., Pimenov, N., ... Crane, K. (2003). Methane seep community of the Håkon Mosby mud volcano (the Norwegian Sea): composition and trophic aspects. *Sarsia: North Atlantic Marine Science*, 88(6), 394–403. doi:10.1080/00364820310003190
- Georgian, S. E., Deleo, D., Durkin, A., Gomez, C. E., Kurman, M., Lunden, J. J., & Cordes, E. E. (2016). Oceanographic patterns and carbonate chemistry in the vicinity of cold-water coral reefs in the Gulf of Mexico: Implications for resilience in a changing ocean. *Limnology and Oceanography*, 61(2). doi:10.1002/lno.10242
- Georgian, S. E., Shedd, W., & Cordes, E. E. (2014). High-resolution ecological niche modelling of the cold-water coral *Lophelia pertusa* in the Gulf of Mexico. *Marine Ecology Progress Series*, 506, 145–161. doi:10.3354/meps10816
- Govenar, B., Le Bris, N., Gollner, S., Glanville, J., Aperghis, A. B., Hourdez, S., & Fisher, C. R. (2005). Epifaunal community structure associated with Riftia pachytila aggregations in chemically different hydrothermal vent habitats. *Marine Ecology Progress Series*, 305(Chase 2003), 67–77. doi:10.3354/meps305067
- Guinan, J., Brown, C., Dolan, M. F. J., & Grehan, A. J. (2009). Ecological niche

- modelling of the distribution of cold-water coral habitat using underwater remote sensing data. *Ecological Informatics*, 4(2), 83–92. doi:10.1016/j.ecoinf.2009.01.004
- Han, X., Suess, E., Sahling, H., & Wallmann, K. (2004). Fluid venting activity on the Costa Rica margin: New results from authigenic carbonates. *International Journal of Earth Sciences*, 93(4), 596–611. doi:10.1007/s00531-004-0402-y
- Helly, J. J., & Levin, L. A. (2004). Global distribution of naturally occurring marine hypoxia on continental margins. *Deep-Sea Research Part I: Oceanographic Research Papers*, 51(9), 1159–1168. doi:10.1016/j.dsr.2004.03.009
- Hensen, C., Wallmann, K., Schmidt, M., Ranero, C. R., & Suess, E. (2004). Fluid expulsion related to mud extrusion off Costa Rica - A window to the subducting slab. *Geology*, 32(3), 201–204. doi:10.1130/G20119.1
- Hubbell, S. P. (2001). *The Unified Neutral Theory of Biodiversity and Biogeography*. Princeton University Press.
- Ingram, W. C., Meyers, S. R., Brunner, C. A., & Martens, C. S. (2010). Late Pleistocene – Holocene sedimentation surrounding an active sea floor gas-hydrate and cold-seep field on the Northern Gulf of Mexico Slope. *Marine Geology*, 278(1–4), 43–53. doi:10.1016/j.margeo.2010.09.002
- Johnson, S. B., Warén, A., & Vrijenhoek, R. C. (2008). DNA Barcoding of Lepetodrilus Limpets Reveals Cryptic Species. *Journal of Shellfish Research*, 27(1), 43–51. doi:10.2983/0730-8000(2008)27[43:DBOLLR]2.0.CO;2
- Joye, S. B., Boetius, A., Orcutt, B. N., Montoya, J. P., Schulz, H. N., Erickson, M. J., & Lugo, S. K. (2004). The anaerobic oxidation of methane and sulfate reduction in sediments from Gulf of Mexico cold seeps. *Chemical Geology*, 205(3–4), 219–238. doi:10.1016/j.chemgeo.2003.12.019
- Kark, S., & van Rensburg, B. J. (2007). Ecotones: Marginal or Central Areas of Transition? *Israel Journal of Ecology and Evolution*, 52(1), 29–53. doi:10.1560/IJEE.52.1.29
- Kennicutt, M. C., McDonald, T. J., Comet, P. A., Denoux, G. J., & Brooks, J. M. (1992). The origins of petroleum in the northern Gulf of Mexico. *Geochimica et Cosmochimica Acta*, 56(3), 1259–1280. doi:10.1016/0016-7037(92)90061-M
- Kiel, S. (Ed.). (2010). *The Vent and Seep Biota. Topics in Geobiology*. Dordrecht: Springer Netherlands, Dordrecht. doi:10.1007/978-90-481-9572-5
- Kiel, S. (2016). A biogeographic network reveals evolutionary links between deep-sea hydrothermal vent and methane seep faunas. *Proceedings of the Royal Society B Biological Sciences*, 283(1844), 1–9. doi:10.1098/rspb.2016.2337

- Kirkwood, T. B., & Austad, S. N. (2000). Why do we age? *Nature*, 408(6809), 233–238. doi:10.1038/35041682
- Kohyama, T., & Takada, T. (1998). Recruitment rates in forest plots: Gf estimates using growth rates and size distributions. *Journal of Ecology*, 86(4), 633–639. Retrieved from <http://onlinelibrary.wiley.com/doi/10.1046/j.1365-2745.1998.00286.x/full>
- Leibold, M. a., Holyoak, M., Mouquet, N., Amarasekare, P., Chase, J. M., Hoopes, M. F., ... Gonzalez, A. (2004). The metacommunity concept: a framework for multi-scale community ecology. *Ecology Letters*, 7(7), 601–613. doi:10.1111/j.1461-0248.2004.00608.x
- Levin, L. A., Baco, A. R., Bowden, D., Colaço, A., Cordes, E., Cunha, M. R., ... Watling, L. (2016). Hydrothermal Vents and Methane Seeps: Rethinking the Sphere of Influence. *Frontiers in Marine Science*, 3(May), 72. doi:10.3389/fmars.2016.00072
- Levin, L. A., James, D. W., Martin, C. M., Rathburn, A. E., Harris, L. H., & Michener, R. H. (2000). Do methane seeps support distinct macrofaunal assemblages? Observations on community structure and nutrition from the northern California slope and shelf. *Marine Ecology Progress Series*, 208(March), 21–39. doi:10.3354/meps208021
- Levin, L. A., & Mendoza, G. F. (2007). Community structure and nutrition of deep methane-seep macrobenthos from the North Pacific (Aleutian) Margin and the Gulf of Mexico (Florida Escarpment). *Marine Ecology*, 28(1), 131–151. doi:10.1111/j.1439-0485.2006.00131.x
- Levin, L. A., Mendoza, G. F., Grupe, B. M., Gonzalez, J. P., Jellison, B., Rouse, G., ... Waren, A. (2015). Biodiversity on the Rocks: Macrofauna Inhabiting Authigenic Carbonate at Costa Rica Methane Seeps. *PloS One*, 10(7), e0131080. doi:10.1371/journal.pone.0131080
- Levin, L. a., Orphan, V. J., Rouse, G. W., Rathburn, A. E., Ussler, W., Cook, G. S., ... Strickrott, B. (2012). A hydrothermal seep on the Costa Rica margin: middle ground in a continuum of reducing ecosystems. *Proceedings of the Royal Society B: Biological Sciences*, 279(1738), 2580–2588. doi:10.1098/rspb.2012.0205
- Lonsdale, P. (1977). Clustering of suspension-feeding macrobenthos near abyssal hydrothermal vents at oceanic spreading centers. *Deep Sea Research*, 24(9), 857–863. doi:10.1016/0146-6291(77)90478-7
- Lunden, J. J., McNicholl, C. G., Sears, C. R., Morrison, C. L., & Cordes, E. (2014). Acute survivorship of the deep-sea coral *Lophelia pertusa* from the Gulf of Mexico under acidification, warming, and deoxygenation. *Frontiers in Marine Science*, 1(December), 74. doi:10.3389/fmars.2014.00078

- Lutz, R. A., Shank, T. M., Fornari, D. J., Haymon, R. M., Lilley, M. D., Von Damm, K. L., & Desbruyeres, D. (1994). Rapid growth at deep-sea vents. *Nature*, *371*(6499), 663–664. doi:10.1038/371663a0
- McClain, C. R., Allen, a. P., Tittensor, D. P., & Rex, M. a. (2012). Energetics of life on the deep seafloor. *Proceedings of the National Academy of Sciences*, *109*(38), 15366–15371. doi:10.1073/pnas.1208976109
- McClain, C. R., & Hardy, S. M. (2010). The dynamics of biogeographic ranges in the deep sea. *Proceedings of the Royal Society B: Biological Sciences*, *277*(1700), 3533–3546. doi:10.1098/rspb.2010.1057
- McCoy, M. W., & Gillooly, J. F. (2008). Predicting natural mortality rates of plants and animals. *Ecology Letters*, *11*(7), 710–716. doi:10.1111/j.1461-0248.2008.01190.x
- Mienis, F., Duineveld, G. C. A., Davies, A. J., Ross, S. W., Seim, H., Bane, J., & van Weering, T. C. E. (2012). The influence of near-bed hydrodynamic conditions on cold-water corals in the Viosca Knoll area, Gulf of Mexico. *Deep-Sea Research Part I: Oceanographic Research Papers*, *60*, 32–45. doi:10.1016/j.dsr.2011.10.007
- Oksanen, J., Blanchet, F. G., Kindt, R., Legendre, P., Minchin, P. R., O’Hara, R. B., ... Wagner, H. (2016). *vegan: Community Ecology Package*. Retrieved from <https://cran.r-project.org/package=vegan>
- Olu-Le Roy, K., Sibuet, M., Fiala-Médioni, A., Gofas, S., Salas, C., Mariotti, A., ... Woodside, J. (2004). Cold seep communities in the deep eastern Mediterranean Sea: composition, symbiosis and spatial distribution on mud volcanoes. *Deep Sea Research Part I: Oceanographic Research Papers*, *51*(12), 1915–1936. doi:10.1016/j.dsr.2004.07.004
- Olu, K., Caprais, J. C., Galéron, J., Causse, R., von Cosel, R., Budzinski, H., ... Sibuet, M. (2009). Influence of seep emission on the non-symbiont-bearing fauna and vagrant species at an active giant pockmark in the Gulf of Guinea (Congo–Angola margin). *Deep Sea Research Part II: Topical Studies in Oceanography*, *56*(23), 2380–2393. doi:10.1016/j.dsr2.2009.04.017
- Olu, K., Cordes, E. E., Fisher, C. R., Brooks, J. M., Sibuet, M., & Desbruyères, D. (2010). Biogeography and potential exchanges among the atlantic Equatorial belt cold-seep faunas. *PLoS One*, *5*(8), e11967. doi:10.1371/journal.pone.0011967
- Olu, K., Duperret, A., Sibuet, M., Foucher, J. P., & Fiala-Médioni, A. (1996). Structure and distribution of cold seep communities along the Peruvian active margin: Relationship to geological and fluid patterns. *Marine Ecology Progress Series*, *132*(1–3), 109–125. doi:10.3354/meps132109
- Paull, C. K., Hecker, B., Commeau, R., Freeman-Lynde, R. P., Neumann, C., Corso, W.

- P., ... Curray, J. (1984). Biological communities at the Florida escarpment resemble hydrothermal vent taxa. *Science (New York, N.Y.)*, 226(4677), 965–7. doi:10.1126/science.226.4677.965
- Paull, C. K., Jull, A. J. T., Toolin, L. J., & Linick, T. (1985). Stable isotope evidence for chemosynthesis in an abyssal seep community. *Nature*, 317(6039), 709–711. doi:10.1038/317709a0
- Pinheiro, L. ., Ivanov, M. ., Sautkin, A., Akhmanov, G., Magalhães, V. ., Volkonskaya, A., ... Cunha, M. . (2003). Mud volcanism in the Gulf of Cadiz: results from the TTR-10 cruise. *Marine Geology*, 195(1–4), 131–151. doi:10.1016/S0025-3227(02)00685-0
- Podowski, E. L., Moore, T. S., Zelnio, K. A., Luther, G. W., & Fisher, C. R. (2009). Distribution of diffuse flow megafauna in two sites on the Eastern Lau Spreading Center, Tonga. *Deep Sea Research Part I: Oceanographic Research Papers*, 56(11), 2041–2056. doi:10.1016/j.dsr.2009.07.002
- Portail, M., Olu, K., Escobar-Briones, E., Caprais, J. C., Menot, L., Waeles, M., ... Sarrazin, J. (2015). Comparative study of vent and seep macrofaunal communities in the Guaymas Basin. *Biogeosciences*, 12(18), 5455–5479. doi:10.5194/bg-12-5455-2015
- Quattrini, A. M. A. M., Baums, I. B. I. B., Shank, T. M., Morrison, C. L., & Cordes, E. E. E. E. (2015). Testing the depth-differentiation hypothesis in a deepwater octocoral. *Proceedings of the Royal Society B*, 282(1807), 20150008. doi:10.1098/rspb.2015.0008
- Quattrini, A. M., Georgian, S. E., Byrnes, L., Stevens, A., Falco, R., & Cordes, E. E. (2013). Niche divergence by deep-sea octocorals in the genus *Callogorgia* across the continental slope of the Gulf of Mexico. *Molecular Ecology*, 22(15), 4123–40. doi:10.1111/mec.12370
- Quattrini, A. M., Gómez, C. E., & Cordes, E. E. (2017). Environmental filtering and neutral processes shape octocoral community assembly in the deep sea. *Oecologia*, 183(1), 221–236. doi:10.1007/s00442-016-3765-4
- Quattrini, A. M., Nizinski, M. S., Chaytor, J. D., Demopoulos, A. W. J., Roark, E. B., France, S. C., ... Shank, T. M. (2015). Exploration of the canyon-incised continental margin of the northeastern United States reveals dynamic habitats and diverse communities. *PLoS ONE*, 10(10), 1–32. doi:10.1371/journal.pone.0139904
- R Core Team. (2015). R: A Language and Environment for Statistical Computing. Vienna, Austria: R Foundation for Statistical Computing. Retrieved from <http://www.r-project.org/>

- Radice, V. Z., Quattrini, A. M., Wareham, V. E., Edinger, E. N., & Cordes, E. E. (2016). Vertical water mass structure in the North Atlantic influences the bathymetric distribution of species in the deep-sea coral genus *Paramuricea*. *Deep-Sea Research Part I: Oceanographic Research Papers*, *116*, 253–263. doi:10.1016/j.dsr.2016.08.014
- Ramirez-Llodra, E., Brandt, a., Danovaro, R., De Mol, B., Escobar, E., German, C. R., ... Vecchione, M. (2010). Deep, diverse and definitely different: unique attributes of the world's largest ecosystem. *Biogeosciences*, *7*(9), 2851–2899. doi:10.5194/bg-7-2851-2010
- Ravaux, J., Zbinden, M., Voss-Foucart, M. F., Compère, P., Goffinet, G., & Gaill, F. (2003). Comparative degradation rates of chitinous exoskeletons from deep-sea environments. *Marine Biology*, *143*(2), 405–412. doi:10.1007/s00227-003-1086-8
- Rex, M. a., & Etter, R. J. (2010). *Deep-Sea Biodiversity: Pattern and Scale. Zoology* (Vol. 61). doi:10.1525/bio.2011.61.4.17
- Ridgway, I. D., & Richardson, C. a. (2011). *Arctica islandica*: The longest lived non colonial animal known to science. *Reviews in Fish Biology and Fisheries*, *21*(3), 297–310. doi:10.1007/s11160-010-9171-9
- Risser, P. G. (1995). The status of the science examining ecotones. *BioScience*, *45*(5), 318–325. doi:10.2307/1312492
- Ritt, B., Pierre, C., Gauthier, O., Wenzhofer, F., Boetius, A., & Sarrazin, J. (2011). Diversity and distribution of cold-seep fauna associated with different geological and environmental settings at mud volcanoes and pockmarks of the Nile Deep-Sea Fan. *Marine Biology*, *158*(6), 1187–1210. doi:10.1007/s00227-011-1679-6
- Ritt, B., Sarrazin, J., Caprais, J. C., Noz?l, P., Gauthier, O., Pierre, C., ... Desbruyeres, D. (2010). First insights into the structure and environmental setting of cold-seep communities in the Marmara Sea. *Deep-Sea Research Part I: Oceanographic Research Papers*, *57*(9), 1120–1136. doi:10.1016/j.dsr.2010.05.011
- Roark, E. B., Guilderson, T. P., Dunbar, R. B., Fallon, S. J., & Mucciarone, D. a. (2009). Extreme longevity in proteinaceous deep-sea corals. *Proceedings of the National Academy of Sciences of the United States of America*, *106*(13), 5204–5208. doi:10.1073/pnas.0810875106
- Roberts, H. H., & Aharon, P. (1994). Hydrocarbon-derived carbonate buildups of the northern Gulf of Mexico continental slope: A review of submersible investigations. *Geo-Marine Letters*, *14*(2–3), 135–148. doi:10.1007/BF01203725
- Roberts, J. M., Wheeler, A. J., Freiwald, A., Cairns, S., & Brooke, S. (2009). *Cold water corals: the Biology and Geology of Deep-sea Coral Habitats*.

doi:10.5670/oceanog.2010.105.COPYRIGHT

- Robison, B., Seibel, B., & Drazen, J. (2014). Deep-Sea Octopus (*Graneledone boreopacifica*) Conducts the Longest-Known Egg-Brooding Period of Any Animal. *PLoS ONE*, *9*(7), e103437. doi:10.1371/journal.pone.0103437
- Rogers, A. D., Tyler, P. A., Connelly, D. P., Copley, J. T., James, R., Larter, R. D., ... Zwirgmaier, K. (2012). The discovery of new deep-sea hydrothermal vent communities in the southern ocean and implications for biogeography. *PLoS Biology*, *10*(1), e1001234. doi:10.1371/journal.pbio.1001234
- Sahling, H., Masson, D. G., Ranero, C. R., Hühnerbach, V., Weinrebe, W., Klauke, I., ... Suess, E. (2008a). Fluid seepage at the continental margin offshore Costa Rica and southern Nicaragua. *Geochemistry, Geophysics, Geosystems*, *9*(5). doi:10.1029/2008GC001978
- Sahling, H., Masson, D. G., Ranero, C. R., Hühnerbach, V., Weinrebe, W., Klauke, I., ... Suess, E. (2008b). Fluid seepage at the continental margin offshore Costa Rica and southern Nicaragua. *Geochemistry, Geophysics, Geosystems*, *9*(5), n/a-n/a. doi:10.1029/2008GC001978
- Sahling, H., Rickert, D., Lee, R. W., Linke, P., & Suess, E. (2002). Macrofaunal community structure and sulfide flux at gas hydrate deposits from the Cascadia convergent margin, NE Pacific. *Marine Ecology Progress Series*, *231*, 121–138. doi:10.3354/meps231121
- SAS Institute Inc. (n.d.). JMP®, Version 11. Cary, NC.
- Sellanes, J., Quiroga, E., & Neira, C. (2008). Megafauna community structure and trophic relationships at the recently discovered Concepcion Methane Seep Area , Chile , 36 S. *ICESjms*, 1102–1111. doi:10.1093/icesjms/fsn099
- Sibuet, M., & Olu, K. (1998). Biogeography, biodiversity and fluid dependence of deep-sea cold-seep communities at active and passive margins. *Deep-Sea Research Part II: Topical Studies in Oceanography*, *45*(1–3), 517–567. doi:10.1016/S0967-0645(97)00074-X
- Somero, G. N. (1992). Adaptations to High Hydrostatic Pressure. *Annu. Rev. Physiol.*, *54*(1), 557–577. doi:10.1146/annurev.ph.54.030192.003013
- Somero, G. N. (1995). Proteins and Temperature, 43–68. doi:doi:10.1146/annurev.ph.57.030195.000355
- Taylor, J. D., & Glover, E. A. (2010). Chemosymbiotic Bivalves. In S. Kiel (Ed.), *The Vent and Seep Biota* (pp. 107–136). Springer Netherlands, Dordrecht.

- Thistle, D. (2003). The deep-sea floor: an overview. In *Ecosystems of the deep oceans* (pp. 5–39).
- Tunnicliffe, V., Juniper, S. K., & Sibuet, M. (2003). Reducing environments of the deep-sea floor. In P. A. Tyler (Ed.), *Ecosystems of the Deep Oceans* (pp. 81–110). Elsevier.
- Turnipseed, M., Jenkins, C. D., & Dover, C. L. (2004). Community structure in Florida Escarpment seep and Snake Pit (Mid-Atlantic Ridge) vent mussel beds. *Marine Biology*, *145*(1), 121–132. doi:10.1007/s00227-004-1304-z
- Urban, M. C., Leibold, M. a, Amarasekare, P., De Meester, L., Gomulkiewicz, R., Hochberg, M. E., ... Wade, M. J. (2008). The evolutionary ecology of metacommunities. *Trends in Ecology & Evolution*, *23*(6), 311–7. doi:10.1016/j.tree.2008.02.007
- Van Dover, C. L. (2000). *The Ecology of Deep-Sea Hydrothermal Vents*. Princeton, NJ: Princeton University Press.
- Van Dover, C. L. (2002). Community structure of mussel beds at deep-sea hydrothermal vents. *Marine Ecology Progress Series*, *230*, 137–158. doi:10.3354/meps230137
- Van Dover, C. L. (2003). Variation in community structure within hydrothermal vent mussel beds of the East Pacific Rise. *Marine Ecology Progress Series*, *253*, 55–66. doi:10.3354/meps253055
- Watanabe, H., Fujikura, K., Kojima, S., Miyazaki, J.-I., & Fujiwara, Y. (2010). Japan: Vents and Seeps in Close Proximity. In S. Kiel (Ed.), *The Vent and Seep Biota* (pp. 379–401). Springer Netherlands. doi:10.1007/978-90-481-9572-5_12
- Webber, A. P., Roberts, S., Murton, B. J., & Hodgkinson, M. R. S. (2015). Geology, sulfide geochemistry and supercritical venting at the Beebe Hydrothermal Vent Field, Cayman Trough. *Geochemistry Geophysics Geosystems*, *18*(1–2), 1541–1576. doi:10.1002/2014GC005684.Key
- Williams, G. C. (1957). Pleiotropy, Natural Selection, and the Evolution of Senescence. *Evolution*, *11*(4), 398–411.
- Yesson, C., Taylor, M. L., Tittensor, D. P., Davies, A. J., Guinotte, J., Baco, A., ... Rogers, A. D. (2012). Global habitat suitability of cold-water octocorals. *Journal of Biogeography*, *39*(7), 1278–1292. doi:10.1111/j.1365-2699.2011.02681.x

APPENDIX A

ADDITIONAL GULF OF MEXICO HABITAT MAPS

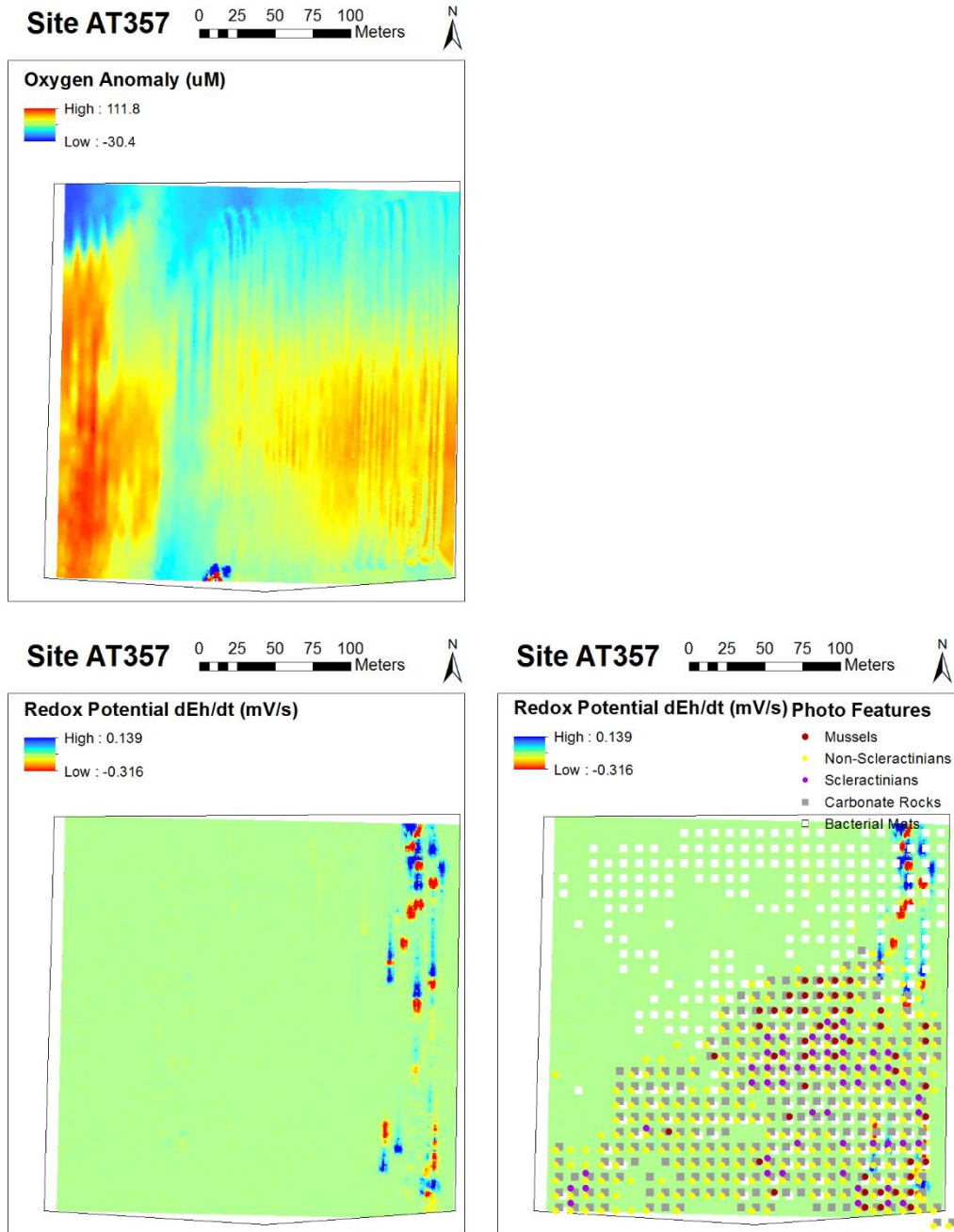


Figure A1. Three maps of Site AT357 showing the dissolved oxygen anomalies, redox potential, and taxa distributions across the site.

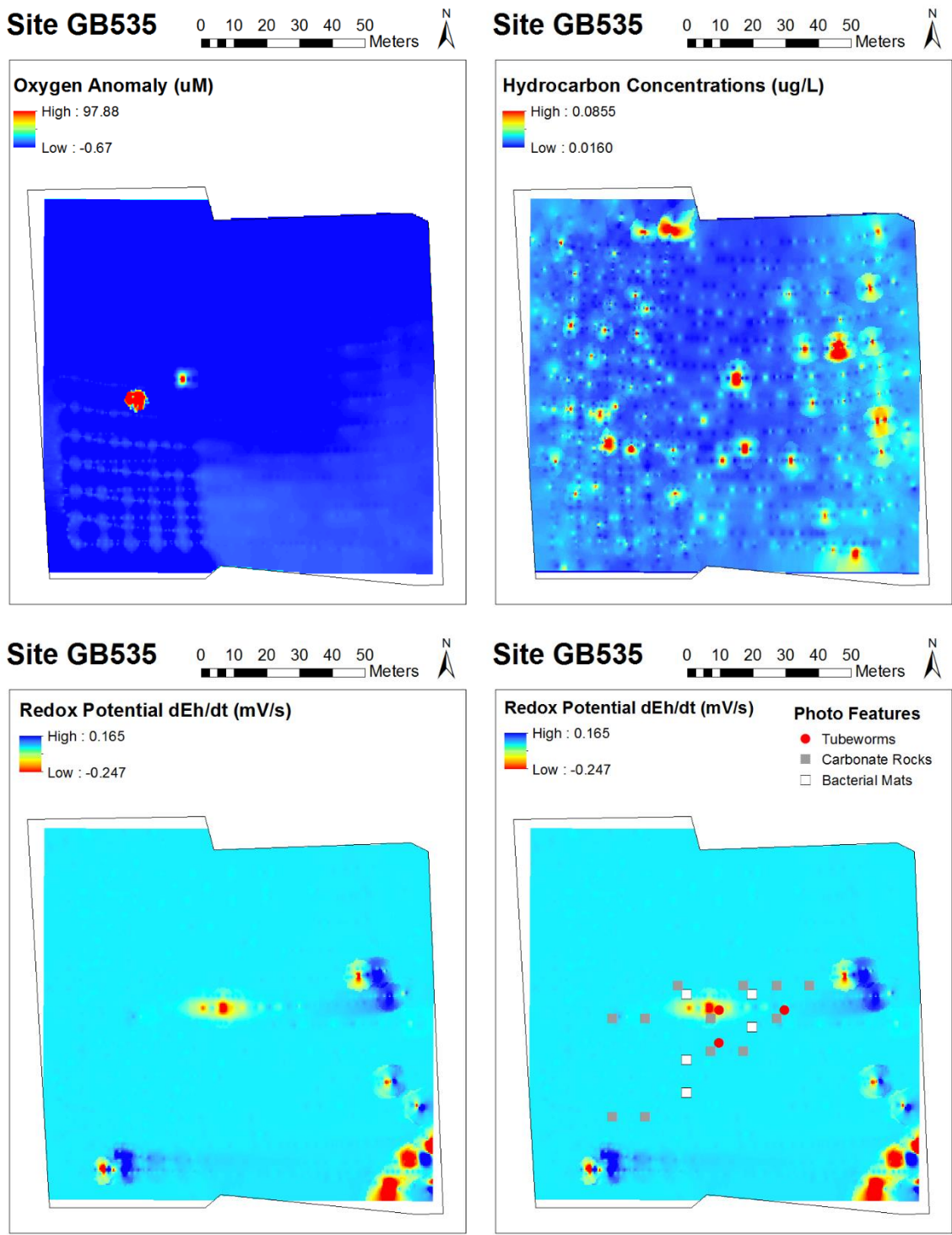


Figure A2. Four maps of Site GB535 showing the dissolved oxygen anomalies, hydrocarbon concentrations, redox potential, and taxa distributions across the site.

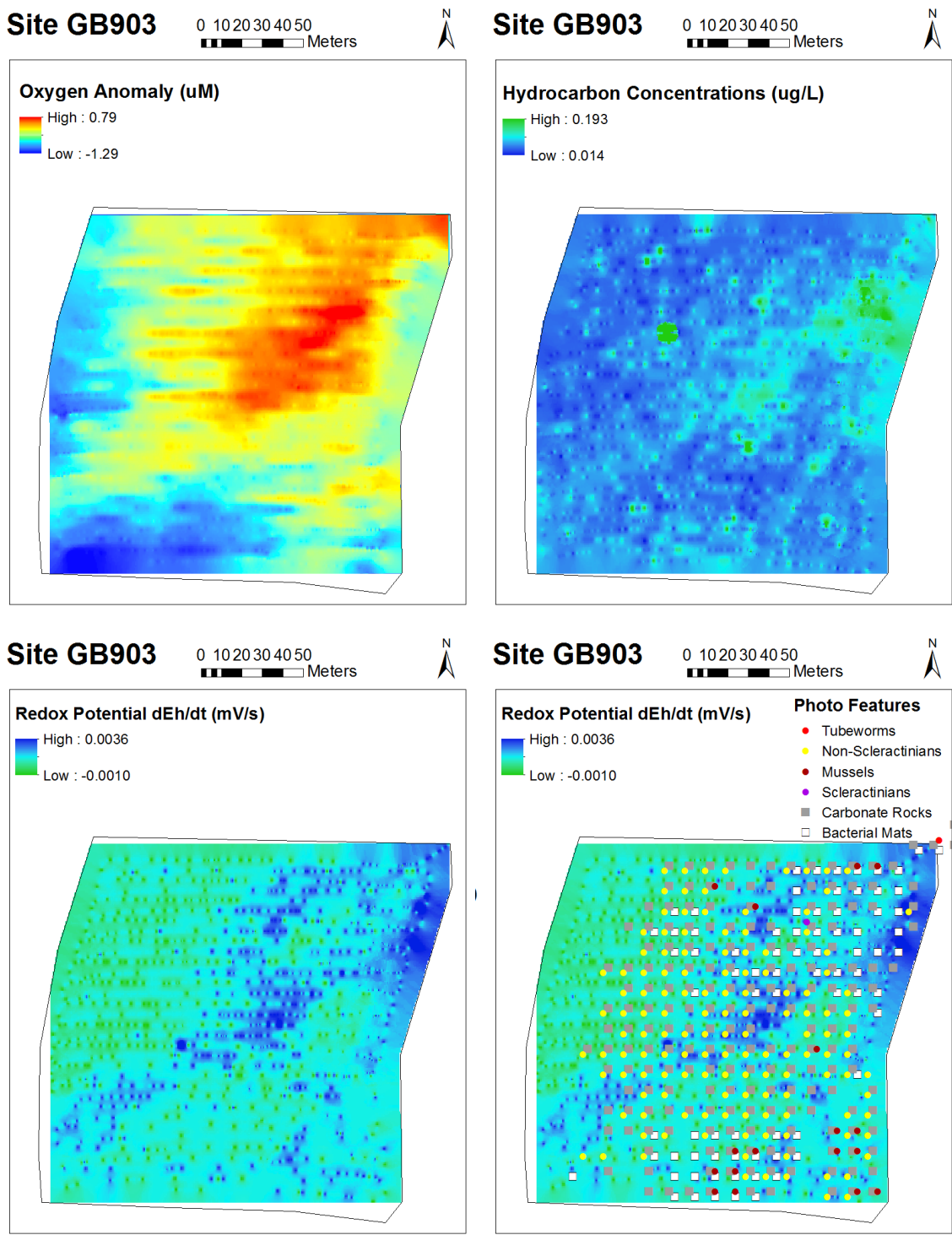


Figure A3. Four maps of Site GB903 showing the dissolved oxygen anomalies, hydrocarbon concentrations, redox potential, and taxa distributions across the site.

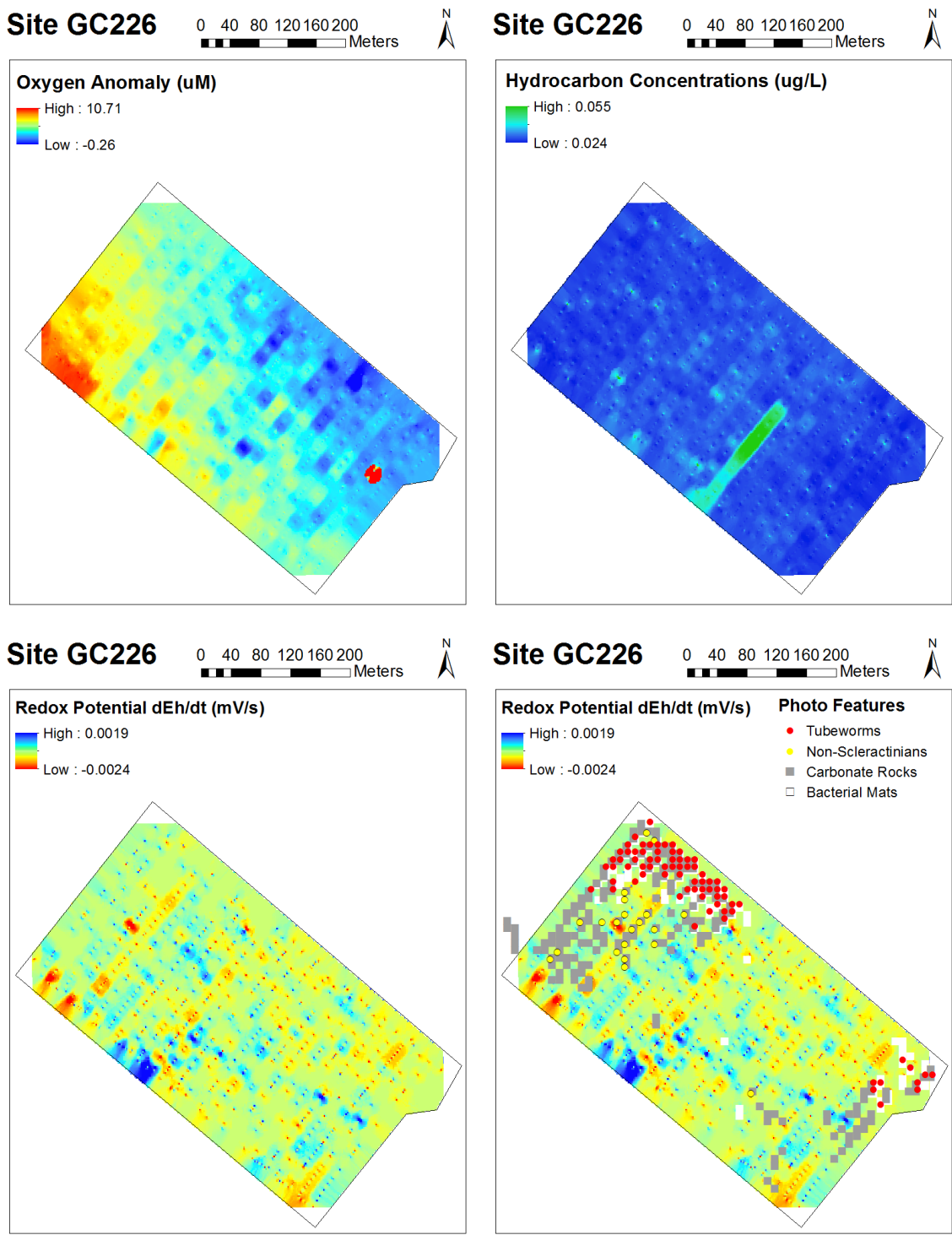


Figure A4. Four maps of Site GC226 showing the dissolved oxygen anomalies, hydrocarbon concentrations, redox potential, and taxa distributions across the site.

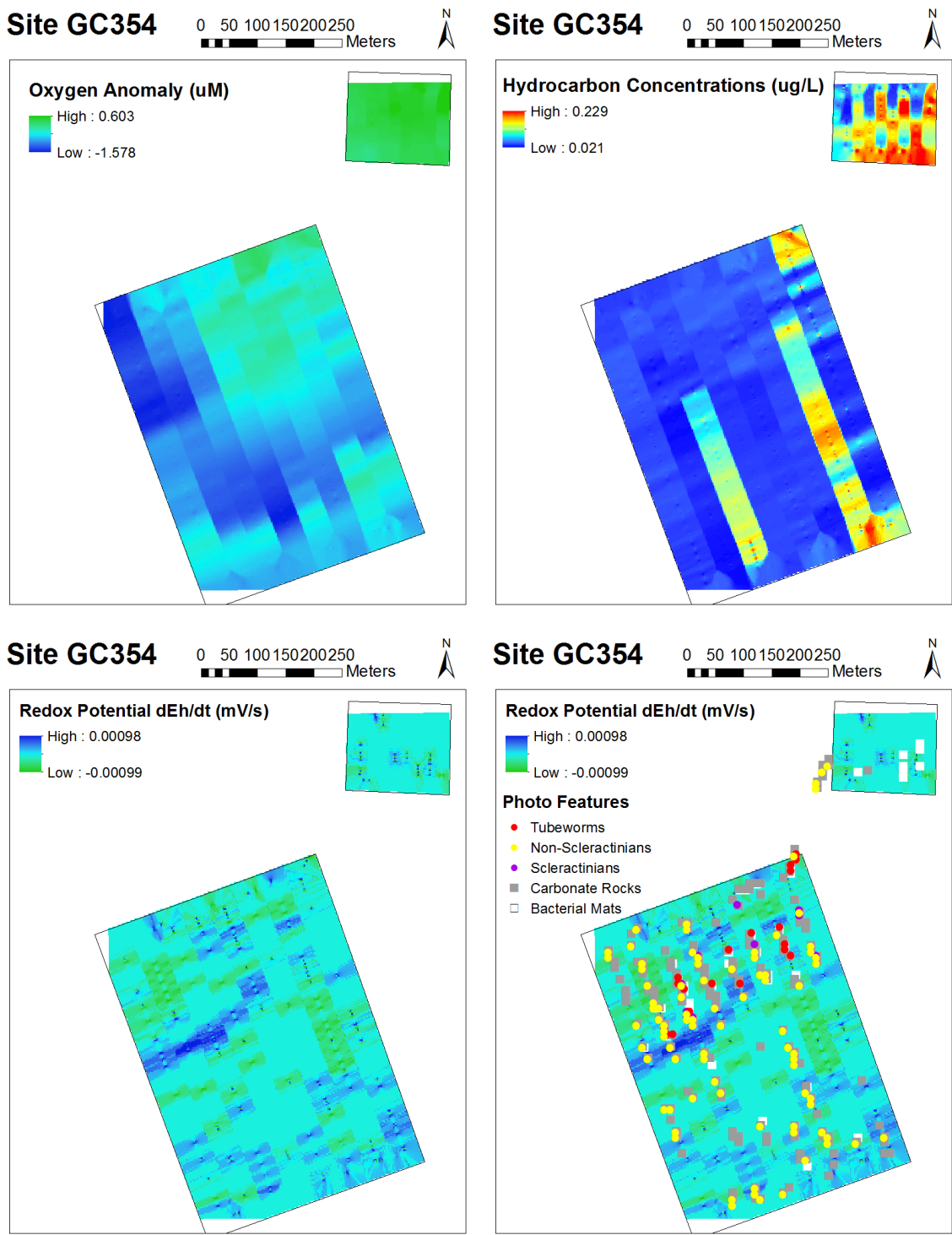


Figure A5. Four maps of Site GC354 showing the dissolved oxygen anomalies, hydrocarbon concentrations, redox potential, and taxa distributions across the site.

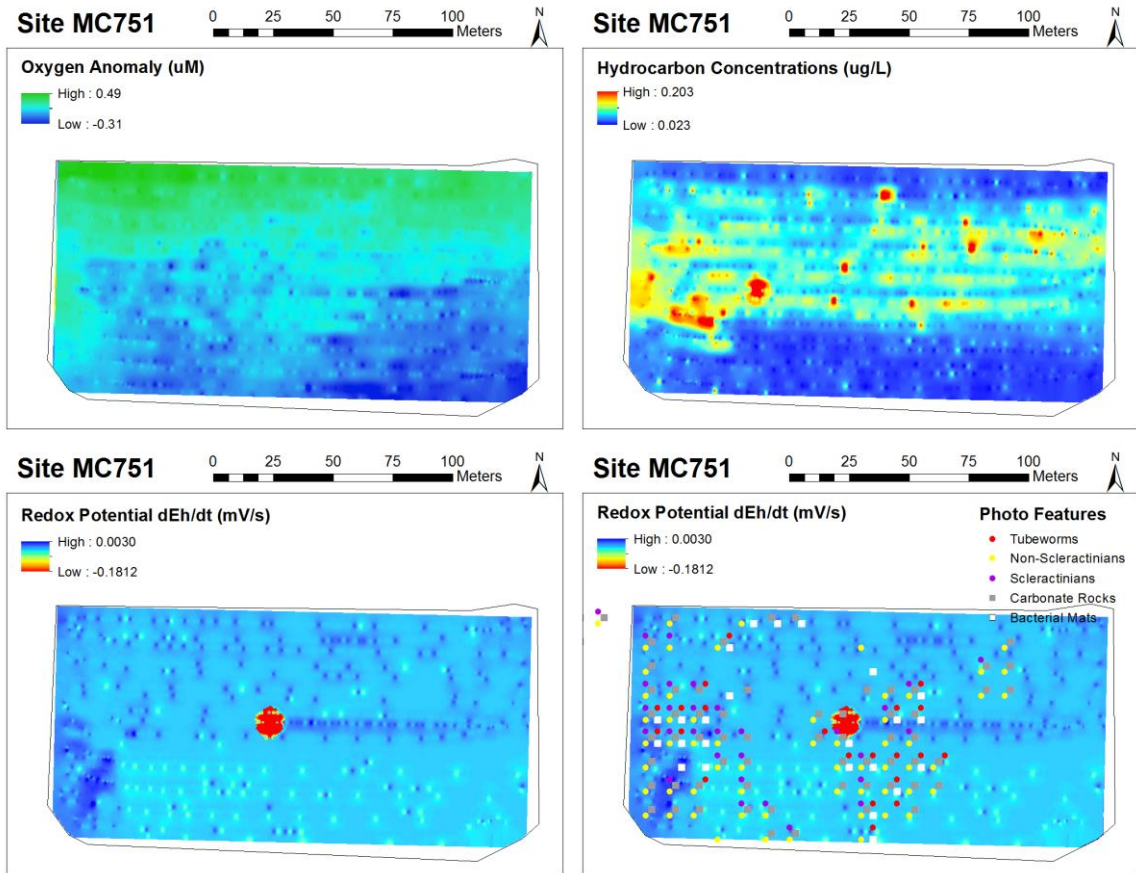


Figure A6. Four maps of Site MC751 showing the dissolved oxygen anomalies, hydrocarbon concentrations, redox potential, and taxa distributions across the site.

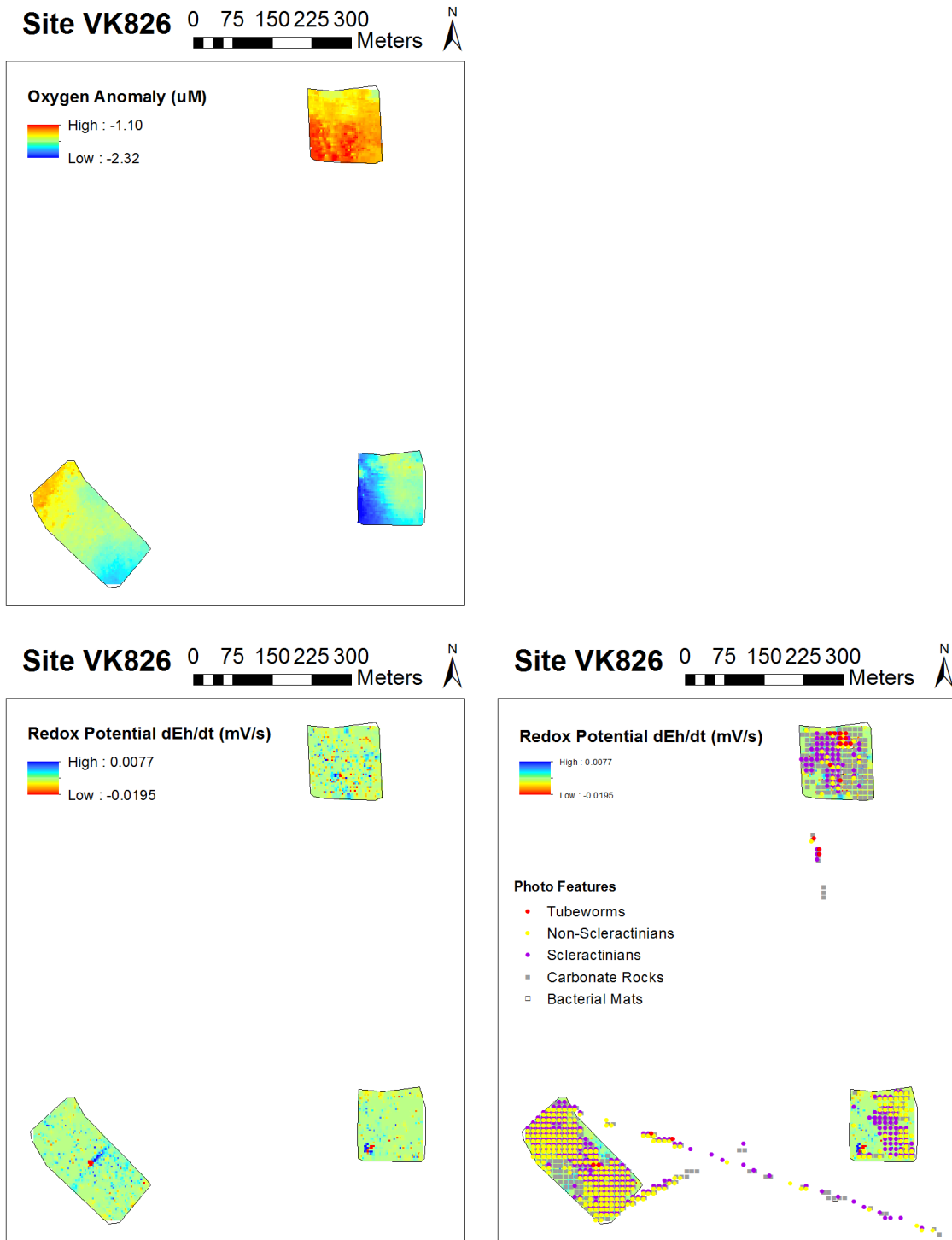


Figure A7. Three maps of Site VK826 showing the dissolved oxygen anomalies, redox potential, and taxa distributions across the site.

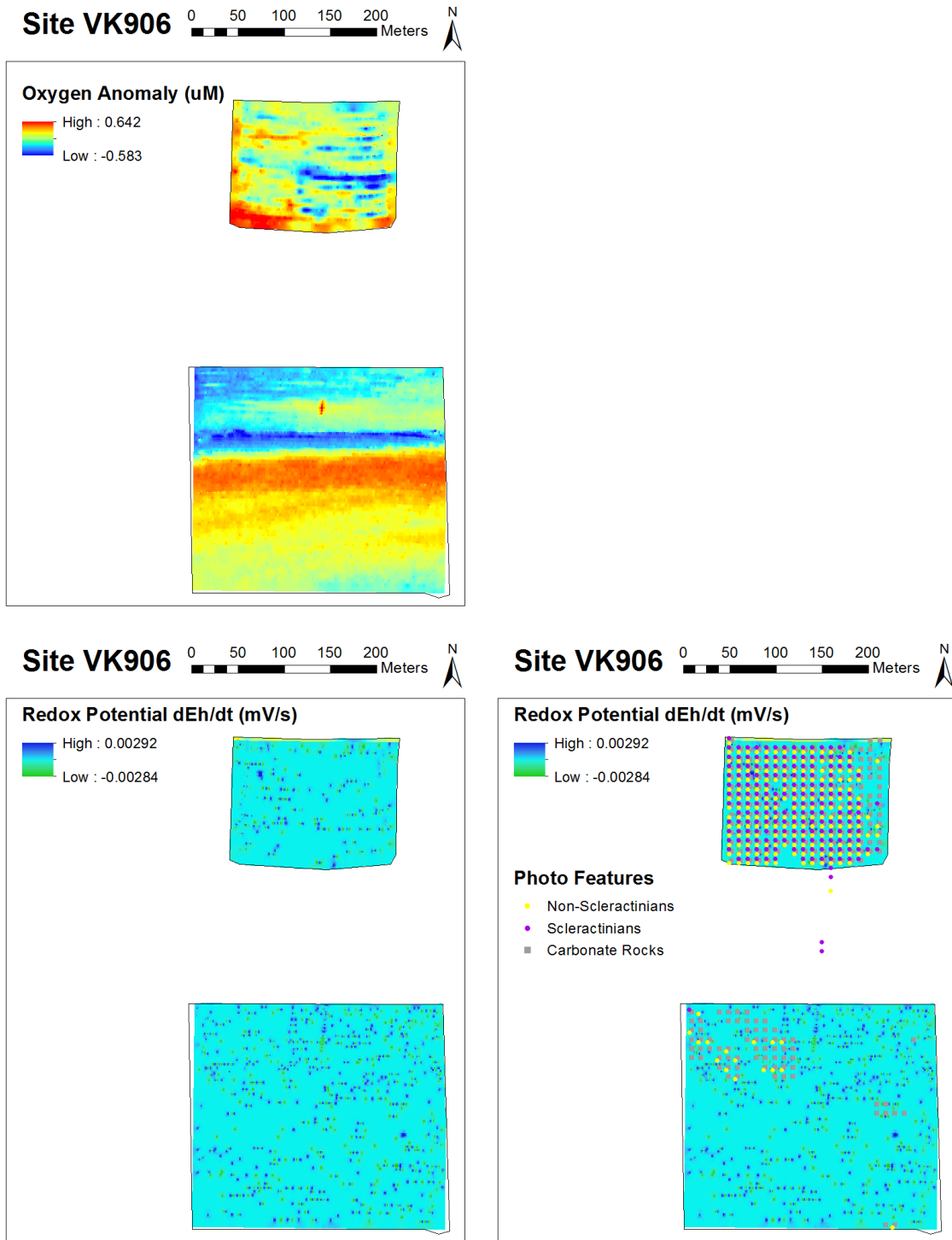


Figure A8. Three maps of Site VK906 showing the dissolved oxygen anomalies, redox potential, and taxa distributions across the site.

APPENDIX B

COSTA RICA MARGIN COMMUNITY ANALYSIS DATA

Table B1

Costa Rica Margin community sample collection information

Sample	Site	Sample Type	Sample Location	Depth (m)	Temperature (°C)	Temperature Anomaly (°C)
CR4503	Mound 12	Bushmaster	8.930, -84.312	1001.1	4.735	-0.0190
CR4508	Mount Parrita	Bushmaster	9.032, -84.622	1418.8	3.302	-0.0350
CR4511T	Mound 12	Mussel Scoop	8.931, -84.312	995	NA	NA
CR4511S	Mound 12	Mussel Scoop	8.931, -84.312	995	NA	NA
CR4513	Jaco Scar	Bushmaster	9.118, -84.839	1817	NA	NA
CR4907BM	Mound 12	Bushmaster	8.930, -84.312	996	NA	NA
CR4907MP	Mound 12	Mussel Pot	8.931, -84.313	998	NA	NA
CR4914BM	Jaco Scar	Bushmaster	9.118, -84.841	1751.2	2.582	-0.0115
CR4916BM	Jaco Scar	Bushmaster	9.118, -84.841	1737.5	2.652	-0.0269
CR4924BM	Parrita Seep	Bushmaster	9.032, -84.622	1408.4	3.410	0.1481
CR4912	Jaco Scar	Grab	9.117, -84.840	1797.5	2.532	0.0033
CR4914MS	Jaco Scar	Mussel Scoop	9.117, -84.840	1795	2.519	-0.0232
CR4915G1	Jaco Scar	Grab	9.117, -84.840	1797.9	2.445	-0.0502
CR4915G2	Jaco Scar	Grab	9.117, -84.840	1797.9	2.445	-0.0502
CR4917	Mound 12	Grab	8.930, -84.312	995.3	4.783	-0.0593
CR4922	Mound 12	Mussel Scoop	8.930, -84.312	996.8	4.738	-0.0408
CR4923	Mount Parrita	Clam Scoop	8.968, -84.635	1063.7	4.337	-0.0960
CR4924G	Parrita Seep	Grab	9.032, -84.621	1403.9	3.439	0.1621

Table B2

Costa Rica Margin community sample species abundance data

Phylum	Family	Species	CR4503	CR4508	CR4511T	CR4511S	CR4513	CR4907BM	CR4907MP	CR4914BM	CR4916BM	CR4924BM	
Annelida	Amphinomidae	<i>Archinome levinae</i>	0	0	0	0	0	0	0	3	4	0	
	Ampharetidae	<i>Amphisamytha fauchaldi</i>	0	0	0	3	0	0	0	0	0	0	
	Hesionidae	<i>Neogyptis</i> sp.nov.	1	0	0	0	0	0	0	0	0	0	
	Polynoidae		<i>Branchinotogluma</i> sp.1	0	0	0	2	0	0	0	0	0	0
			<i>Branchipolynoe</i> sp.2	0	0	0	48	0	0	18	0	0	0
			Unid.	10	1	0	0	0	0	0	0	0	0
	Sabellidae		<i>Fabrisabella</i> sp.	3	0	0	0	0	0	0	0	0	0
			Unid.	0	0	0	0	0	0	0	39	26	0
	Serpulidae		<i>Laminatubus</i> sp.nov.	0	0	0	1	0	0	0	0	0	0
			Unid.	0	50	0	0	0	18	0	5	22	0
	Spionidae		<i>Lindaspio</i> sp.	0	0	1	0	0	0	0	0	0	0
	Terebellidae		<i>Eupolymnia heterobranchia</i>	4	2	1	0	0	0	0	0	0	0
			<i>Neoamphitrite</i>	0	0	0	0	0	0	0	0	13	0
	Capitellidae		Unid.	0	1	0	0	0	0	0	0	0	0
	Phyllodocidae		<i>Galapagomystides</i> sp.	79	137	0	0	0	0	0	0	7	2
Nereididae		Unid.	0	1	0	0	0	0	0	0	0	0	
		Unid. polychaete	0	0	0	0	11	0	0	0	0	0	
Arthropoda	Alvinocarididae	<i>Alvinocaris</i> sp.nov.	0	0	2	1	16	0	0	0	0	0	
	Ampeliscidae	Unid.	1	0	0	0	0	0	0	0	0	0	

Table B2 (continued)

Phylum	Family	Species	CR4503	CR4508	CR4511T	CR4511S	CR4513	CR4907BM	CR4907MP	CR4914BM	CR4916BM	CR4924BM	
Arthropoda (continued)	Gammaridae	Unid.	1	0	0	0	0	0	0	0	0	0	
	Kiwaidae	<i>Kiwa puravida</i>	0	0	0	3	0	0	1	0	0	0	
	Amphipoda	Unid.	0	210	0	0	0	0	0	0	1	0	
	Cirripedia	Unid.	0	4	0	0	0	0	0	0	0	0	
	Munidopsidae	<i>Munidopsis "orange eyes"</i>	0	0	0	0	0	0	0	0	1	2	0
		<i>Munidopsis "white eyes"</i>	0	0	0	0	0	0	0	0	1	1	0
	Colossendeidae	<i>Colossendeis</i> sp.	0	0	0	0	0	0	0	0	2	0	0
Lithodidae	Unid.	0	0	0	0	0	0	0	0	0	1	0	
Bryozoa	Unidentified	Unid.	0	0	0	0	0	0	0	0	0	0	
Chordata	Zoarcidae	Unid.	0	0	0	0	0	0	0	0	1	0	
Cnidaria	Actiniaria	Unid.	0	1	127	146	73	2	1	53	21	0	
	Hydrozoa	Unid.	0	36	0	0	0	0	0	12	0	0	
Echinodermata	Ophiuridae	<i>Ophiura</i> sp.	1	0	0	0	1	0	0	0	0	0	
		Unid.	0	0	0	0	0	0	0	0	0	1	
Mollusca	Cerithopsidae	<i>Cerithopsis</i> sp.	1	0	0	0	0	0	0	0	0	0	
	Lepetidae	<i>Iothia</i> sp.	0	0	0	0	0	0	0	0	0	2	
	Lepetodrilidae	<i>Lepetodrilus pustulosis</i>	0	7	0	0	0	0	0	0	0	0	
		<i>Lepetodrilus ovalis</i>	106	79	245	0	5	0	0	0	0	0	
		<i>Lepetodrilus</i> sp.2	0	0	91	0	0	0	0	0	0	0	
<i>Lepetodrilus guaymasensis</i>		0	0	0	0	0	11	286	0	0	0		

Table B2 (continued)

Phylum	Family	Species	CR4503	CR4508	CR4511T	CR4511S	CR4513	CR4907BM	CR4907MP	CR4914BM	CR4916BM	CR4924BM	
Mollusca (continued)	Lepetodrilidae	<i>Lepetodrilus</i> "tall"	0	0	0	0	0	0	0	97	0	0	
	Lepetopsidae	<i>Neolepetopsis</i> sp.1	0	1	0	0	0	0	0	0	0	0	4
		<i>Neolepetopsis</i> sp.2	93	4	89	0	0	0	0	0	0	0	0
		<i>Neolepetopsis</i> sp.3	1	0	0	0	0	0	0	0	0	0	0
	Neolepetopsidae	<i>Paralepetopsis</i> sp.	1	0	5	0	0	55	344	0	0	0	
	Lucinidae	Unid.	7	0	0	0	0	0	0	0	0	0	
	Mytilidae	<i>Bathymodiolus earlougheri</i>	0	0	0	0	0	2	0	0	0	0	0
		<i>Bathymodiolus nancyschneideri</i>	0	0	0	0	0	0	0	0	0	0	0
	Orbitestellidae	<i>Lurifax</i> sp.	10	1	4	0	0	0	0	0	0	0	0
	Provannidae	<i>Provanna</i> sp.	1	0	11	0	0	19	0	0	0	0	0
		<i>Provanna laevis</i>	0	0	0	0	0	0	11	0	0	0	0
	Pyramidellidae	<i>Eulimella</i> sp.	0	0	0	0	0	0	0	0	0	0	1
	Pyropeltidae	<i>Pyropelta</i> sp.1	1	0	0	0	0	8	46	0	0	0	11
		Unid.	1	0	0	0	0	0	0	0	0	0	0
		Unid.	0	0	2	0	0	0	0	0	0	0	0
	Skeneidae	<i>Fucaria</i> sp.	1	1	0	0	0	0	0	0	0	0	0
	Raphitomidae	<i>Phymorhynchus</i> sp.	0	1	0	0	0	0	0	0	2	0	1
	Cataegidae	<i>Kanoia</i> sp.	0	0	0	0	0	2	2	14	22	0	0
	Pectinodontidae	<i>Bathyacmaea</i> sp.	0	0	0	0	0	2	1	0	38	1	0
	Limpets	Unid.	0	0	0	0	0	0	0	0	82	5	0

Table B2 (continued)

Phylum	Family	Species	CR4503	CR4508	CR4511T	CR4511S	CR4513	CR4907BM	CR4907MP	CR4914BM	CR4916BM	CR4924BM	
Mollusca (continued)	Aplacophora	Unid.	0	2	0	0	0	0	0	0	0	0	
	Gastropoda	Unid.	0	0	0	9	1	0	0	0	0	0	
	Nudibranchia	<i>Nudibranchia</i> sp.	0	1	0	0	0	0	0	0	0	0	0
		<i>Nudibranchia tritonia</i>	0	1	0	0	0	0	0	0	0	0	0
Nemertea	Unidentified	Unid.	0	0	0	0	0	0	0	1	0	0	

Table B3

Costa Rica Margin community sample species presence-absence data

Phylum	Family	Species	CR4503	CR4508	CR4511T	CR4511S	CR4513	CR4907BM	CR4907MP	CR4914BM	CR4916BM	CR4924BM	CR4912	CR4914MS	CR4915G1	CR4915G2	CR4917	CR4922	CR4923	CR4924G	
Annelida	Amphinomidae	<i>Archinome levinae</i>	0	0	0	0	0	0	0	1	1	0	0	1	0	0	0	0	0	0	
	Ampharetidae	<i>Amphisamytha fauchaldi</i>	0	0	0	1	0	0	0	0	0	0	1	1	0	1	0	0	0	0	
	Chrysopetalidae	<i>Shinkai fontefridae</i>	0	0	0	0	0	0	0	0	0	0	0	0	0	0	0	0	0	1	0
	Cirratulidae	<i>Cirratulus</i> sp.	0	0	0	0	0	0	0	0	0	0	0	0	0	0	0	0	0	1	0
	Dorvilleidae	<i>Parougia sulleyi</i>	0	0	0	0	0	0	0	0	0	0	0	0	0	0	0	0	1	0	0
	Maldanidae	Unid.	0	0	0	0	0	0	0	0	0	0	0	0	0	0	0	0	0	1	0
	Siboglinidae	<i>Lamellibrachia barhami</i>	1	1	0	0	1	0	0	0	1	1	1	1	0	1	1	1	0	0	0
		<i>Escarpia spicata</i>	1	1	0	0	1	0	0	0	1	1	0	0	0	1	0	1	0	0	0
	Hesionidae	<i>Neogyptis</i> sp.nov.	1	0	0	0	0	0	0	0	0	0	0	0	0	0	0	0	0	0	0
		<i>Gyptis</i> sp.	0	0	0	0	0	0	0	0	0	0	0	0	0	0	1	0	0	0	0
	Polynoidae	<i>Branchinotogluma</i> sp.1	0	0	0	1	0	0	0	0	0	0	0	0	0	1	1	0	0	0	1
		<i>Branchipolynoe</i> sp.2	0	0	0	1	0	0	1	0	0	0	0	0	0	0	0	1	0	0	0
		Unid.	1	1	0	0	0	0	0	0	0	0	0	0	0	0	0	0	0	0	0
	Sabellidae	<i>Fabrisabella</i> sp.	1	0	0	0	0	0	0	0	0	0	0	0	0	0	0	0	0	0	0
		Unid.	0	0	0	0	0	0	0	0	1	1	0	0	1	1	0	0	0	0	0
	Serpulidae	<i>Laminatubus</i> sp.nov.	0	0	0	1	0	0	0	0	0	0	0	0	0	0	0	0	0	0	0
		Unid.	0	1	0	0	0	0	1	0	1	1	0	0	0	1	1	1	1	0	0

Table B3 (continued)

Phylum	Family	Species	CR4503	CR4508	CR4511T	CR4511S	CR4513	CR4907BM	CR4907MP	CR4914BM	CR4916BM	CR4924BM	CR4912	CR4914MS	CR4915G1	CR4915G2	CR4917	CR4922	CR4923	CR4924G	
Annelida (continued)	Spionidae	<i>Lindaspio</i> sp.	0	0	1	0	0	0	0	0	0	0	0	0	0	0	0	0	0	0	
		Unid.	0	0	0	0	0	0	0	0	0	0	0	0	0	0	0	1	0	0	0
	Terebellidae	<i>Eupolymnia heterobranchia</i>	1	1	1	0	0	0	0	0	0	0	0	0	0	0	0	0	0	0	0
		<i>Eupolymnia</i> sp.	0	0	0	0	0	0	0	0	0	0	0	0	0	1	0	1	0	0	0
		<i>Neoamphitrite</i> sp.	0	0	0	0	0	0	0	0	0	1	0	0	0	1	1	1	1	0	0
	Capitellidae	Unid.	0	1	0	0	0	0	0	0	0	0	0	0	0	0	0	0	0	0	0
	Phyllodocidae	<i>Galapagomystides</i> sp.	1	1	0	0	0	0	0	0	1	1	1	0	0	1	1	0	0	0	0
	Polychaeta	Unid.	0	0	0	0	0	0	0	0	0	0	0	1	0	0	0	0	0	0	0
	Nereididae	<i>Nereis</i> sp.	0	0	0	0	0	0	0	0	0	0	0	0	0	0	0	0	1	0	0
		Unid.	0	1	0	0	0	0	0	0	0	0	0	0	0	0	0	0	1	0	0
Unidentified	Unid.	0	0	0	0	1	0	0	0	0	0	0	0	0	0	0	0	0	0	0	
Arthropoda	Alvinocarididae	<i>Alvinocaris</i> sp.nov.	0	0	1	1	1	0	0	0	0	0	0	0	0	0	0	0	0	0	
	Ampeliscidae	Unid.	1	0	0	0	0	0	0	0	0	0	0	0	0	0	0	0	0	0	
	Gammaridae	Unid.	1	0	0	0	0	0	0	0	0	0	0	0	0	0	0	0	0	0	
	Kiwaidae	<i>Kiwa puravida</i>	0	0	0	1	0	0	1	0	0	0	0	0	0	0	1	1	0	0	
	Amphipoda	Unid.	0	1	0	0	0	0	0	0	1	0	0	0	0	0	0	0	0	0	
	Cirripedia	Unid.	0	1	0	0	0	0	0	0	0	0	0	0	0	0	0	0	0	0	
	Munidopsidae	<i>Munidopsis</i> "orange eyes"	0	0	0	0	0	0	0	0	1	1	0	0	0	1	0	0	0	0	0

Table B3 (continued)

Phylum	Family	Species	CR4503	CR4508	CR4511T	CR4511S	CR4513	CR4907BM	CR4907MP	CR4914BM	CR4916BM	CR4924BM	CR4912	CR4914MS	CR4915G1	CR4915G2	CR4917	CR4922	CR4923	CR4924G
Arthropoda (continued)	Munidopsidae	<i>Munidopsis</i> "white eyes"	0	0	0	0	0	0	0	1	1	0	0	0	0	0	0	0	0	0
	Colossendeidae	<i>Colossendeis</i> sp.	0	0	0	0	0	0	0	1	0	0	0	0	0	0	0	0	0	0
	Lithodidae	Unid.	0	0	0	0	0	0	0	0	1	0	0	0	0	0	0	0	0	0
Bryozoa	Unidentified	Unid.	0	0	0	0	0	0	0	0	0	0	0	0	0	0	0	0	0	0
Chordata	Zoarcidae	Unid.	0	0	0	0	0	0	0	0	1	0	0	0	0	0	0	0	0	0
Cnidaria	Actinaria	Unid.	0	1	1	1	1	1	1	1	1	0	1	1	1	1	0	0	0	0
	Hydrozoa	Unid.	0	1	0	0	0	0	0	1	0	0	0	0	1	0	0	0	0	0
Echinodermata	Ophiuridae	<i>Ophiura</i> sp.	1	0	0	0	1	0	0	0	0	0	0	0	0	0	0	0	0	0
		Unid.	0	0	0	0	0	0	0	0	0	0	1	0	0	0	0	0	0	0
Mollusca	Cerithopsidae	<i>Cerithopsis</i> sp.	1	0	0	0	0	0	0	0	0	0	0	0	0	0	0	0	0	0
	Lepetidae	<i>Iothia</i> sp.	0	0	0	0	0	0	0	0	0	1	0	0	1	0	0	0	0	0
	Lepetodrilidae	<i>Lepetodrilus pustulosus</i>	0	1	0	0	0	0	0	0	0	0	0	0	0	0	0	0	0	0
		<i>Lepetodrilus ovalis</i>	1	1	1	0	1	0	0	0	0	0	0	0	0	0	0	0	0	0
		<i>Lepetodrilus</i> sp.2	0	0	1	0	0	0	0	0	0	0	0	0	0	0	0	0	0	0
		<i>Lepetodrilus guaymasensis</i>	0	0	0	0	0	1	1	0	0	0	0	0	0	0	1	0	1	0
		<i>Lepetodrilus</i> "tall"	0	0	0	0	0	0	0	0	1	0	0	1	1	0	1	0	0	0
		<i>Lepetodrilus</i> sp.	0	0	0	0	0	0	0	0	0	0	0	0	0	0	0	1	0	0
Lepetopsidae	<i>Neolepetopsis</i> sp.1	0	1	0	0	0	0	0	0	0	0	0	0	0	0	0	0	0	0	

Table B3 (continued)

Phylum	Family	Species	CR4503	CR4508	CR4511T	CR4511S	CR4513	CR4907BM	CR4907MP	CR4914BM	CR4916BM	CR4924BM	CR4912	CR4914MS	CR4915G1	CR4915G2	CR4917	CR4922	CR4923	CR4924G	
Mollusca (continued)	Lepetopsidae	<i>Neolepetopsis</i> sp.2	1	1	1	0	0	0	0	0	0	0	0	0	0	0	0	0	0	0	
		<i>Neolepetopsis</i> sp.3	1	0	0	0	0	0	0	0	0	0	0	0	0	0	0	0	0	0	0
		<i>Neolepetopsis</i> sp.	0	0	0	0	0	0	0	0	0	0	1	0	0	1	1	0	0	0	0
	Neolepetopsidae	<i>Paralepetopsis</i> sp.	1	0	1	0	0	1	1	0	0	0	0	0	0	0	0	1	1	0	0
	Lucinidae	Unid.	1	0	0	0	0	0	0	0	0	0	0	0	0	0	0	0	0	0	0
	Nuculanidae	<i>Nuculana</i> sp.	0	0	0	0	0	0	0	0	0	0	0	0	0	0	0	0	0	1	0
	Orbitestellidae	<i>Lurifax</i> sp.	1	1	1	0	0	0	0	0	0	0	0	0	0	0	0	0	0	0	0
	Provannidae	<i>Provanna</i> sp.	1	0	1	0	0	1	0	0	0	0	0	0	0	0	0	0	0	0	0
		<i>Provanna laevis</i>	0	0	0	0	0	0	1	0	0	0	0	0	0	0	0	1	1	0	0
		<i>Provanna</i> "spiny"	0	0	0	0	0	0	0	0	0	0	0	0	1	0	0	0	0	0	0
	Pyramidellidae	<i>Eulimella</i> sp.	0	0	0	0	0	0	0	0	0	0	1	0	0	0	0	0	0	1	0
	Pyropeltidae	<i>Pyropelta</i> sp.1	1	0	0	0	0	1	1	0	0	0	1	0	0	0	0	0	0	0	0
		Unid.	1	0	0	0	0	0	0	0	0	0	0	0	0	0	0	0	0	0	0
		Unid.	0	0	1	0	0	0	0	0	0	0	0	0	0	0	0	0	0	0	0
	Skeneidae	<i>Fucaria</i> sp.	1	1	0	0	0	0	0	0	0	0	0	0	0	0	0	0	0	1	0
	Raphitomidae	<i>Phymorhynchus</i> sp.	0	1	0	0	0	0	0	0	1	0	1	0	0	0	0	0	0	0	0
	Cataegidae	<i>Kanoia</i> sp.	0	0	0	0	0	1	1	1	1	1	0	0	0	1	1	1	1	0	0
	Pectinodontidae	<i>Bathyacmaea</i> sp.	0	0	0	0	0	0	1	0	1	1	1	0	1	0	1	1	1	0	0
		<i>Bathyacmaea</i> "tall"	0	0	0	0	0	0	0	0	0	0	0	0	0	1	0	0	0	0	0

Table B3 (continued)

Phylum	Family	Species	CR4503	CR4508	CR4511T	CR4511S	CR4513	CR4907BM	CR4907MP	CR4914BM	CR4916BM	CR4924BM	CR4912	CR4914MS	CR4915G1	CR4915G2	CR4917	CR4922	CR4923	CR4924G	
Mollusca (continued)	Hyalogyrinidae	<i>Hyalogyrina</i> sp.	0	0	0	0	0	0	0	0	0	0	0	0	0	0	0	1	1	0	
	Limpets	Unid.	0	0	0	0	0	0	0	0	1	1	0	0	0	0	0	0	0	1	0
	Aplacophora	Unid.	0	1	0	0	0	0	0	0	0	0	0	0	0	0	0	0	0	0	0
	Gastropoda	Unid.	0	0	0	1	1	0	0	0	0	0	0	0	0	0	0	0	0	0	0
	Nudibranchia	<i>Nudibranchia</i> sp.	0	1	0	0	0	0	0	0	0	0	0	0	0	0	0	0	0	0	0
		<i>Nudibranchia tritonia</i>	0	1	0	0	0	0	0	0	0	0	0	0	0	0	0	0	0	0	0
	Vesicomylidae	<i>Archivesica gigas</i>	0	0	0	0	0	0	0	0	0	0	0	0	1	0	0	0	0	1	0
	Mytilidae	<i>Bathymodiolus earlougheri</i>	0	0	0	0	0	0	1	1	0	0	0	0	0	0	0	1	1	0	0
<i>Bathymodiolus nancyschneideri</i>		0	0	0	0	0	0	0	1	0	0	0	0	0	0	0	0	1	0	0	
Nemertea	Unidentified	Unid.	0	0	0	0	0	0	0	1	0	0	0	0	1	0	0	0	0	1	

Table B4

Sites included in global family-level community analysis

Site	Habitat	Region	Sample Type	Depth (m)	# Samples	Reference
11°N	Vent	Northern East-Pacific Rise	Presence-Absence	2580	1	(Bachraty, Legendre, & Desbruyères, 2009)
13°N	Vent	Northern East-Pacific Rise	Presence-Absence	2615	1	(Bachraty et al., 2009)
14°S	Vent	Southern East-Pacific Rise	Presence-Absence	2635	1	(Bachraty et al., 2009)
17°24S	Vent	Southern East-Pacific Rise	Presence-Absence	2590	1	(Bachraty et al., 2009)
17°34S	Vent	Southern East-Pacific Rise	Presence-Absence	2600	1	(Bachraty et al., 2009)
17°S	Vent	Southern East-Pacific Rise	Presence-Absence	2680	1	(Bachraty et al., 2009)
18°S	Vent	Southern East-Pacific Rise	Presence-Absence	2680	1	(Bachraty et al., 2009)
21°N	Vent	Northern East-Pacific Rise	Presence-Absence	2600	1	(Bachraty et al., 2009)
21°S	Vent	Southern East-Pacific Rise	Presence-Absence	2900	1	(Bachraty et al., 2009)
23°S	Vent	Southern East-Pacific Rise	Presence-Absence	2600	1	(Bachraty et al., 2009)
31°S	Vent	Southern East-Pacific Rise	Presence-Absence	2360	1	(Bachraty et al., 2009)
7°S	Vent	Southern East-Pacific Rise	Presence-Absence	2600	1	(Bachraty et al., 2009)
9°N	Vent	Northern East-Pacific Rise	Presence-Absence	2585	1	(Bachraty et al., 2009)

Table B4 (continued)

Site	Habitat	Region	Sample Type	Depth (m)	# Samples	Reference
ABE vent field	Vent	Eastern Lau Spreading Center	Abundance	2140	5	(Podowski, Moore, Zelnio, Luther, & Fisher, 2009)
Alaminos Canyon	Seep	Lower Gulf of Mexico	Abundance	2208-2223	4	(Cordes et al., 2007)
Alaminos Canyon	Seep	Lower Gulf of Mexico	Presence-Absence	2200	1	(Sibuet & Olu, 1998)
Aleutian Trench	Seep	Alaska	Presence-Absence	3200-5900	1	(Sibuet & Olu, 1998)
Anaximander Mountains	Seep	Mediterranean	Presence-Absence	1850	3	(Olu-Le Roy et al., 2004)
Animal Farm	Vent	Southern East Pacific Rise	Abundance	2675	7	(Van Dover, 2002)
Ashadze 1	Vent	Mid-Atlantic Ridge	Presence-Absence	4150	1	(Bachraty et al., 2009)
Ashizuri Knoll	Seep	Nankai Trough	Presence-Absence	600	1	(Watanabe, Fujikura, Kojima, Miyazaki, & Fujiwara, 2010)
Atwater Valley	Seep	Lower Gulf of Mexico	Abundance	1893	1	(Cordes et al., 2007)
Axial Volcano	Vent	Juan de Fuca	Presence-Absence	1525	1	(Bachraty et al., 2009)
Axial Volcano Ashes Vent Field	Vent	Juan de Fuca	Presence-Absence	1540	1	(Bachraty et al., 2009)
Axial Volcano Coaxial Seamount	Vent	Juan de Fuca	Presence-Absence	1580	1	(Bachraty et al., 2009)
Barbados North	Seep	Barbados Accretionary Prism	Presence-Absence	4700-5000	1	(Sibuet & Olu, 1998)
Barbados South	Seep	Barbados Accretionary Prism	Presence-Absence	1000-2000	1	(Sibuet & Olu, 1998)

Table B4 (continued)

Site	Habitat	Region	Sample Type	Depth (m)	# Samples	Reference
Barbados Trench	Seep	Barbados Accretionary Prism	Presence-Absence	4850	1	(Cordes et al., 2007)
Biovent	Vent	Northern East Pacific Rise	Abundance	2494	7	(Van Dover, 2003)
Blake Ridge	Seep	Blake Ridge	Presence-Absence	2150	1	(Cordes et al., 2007)
Bonjardim mud volcano	Seep	Gulf of Cadiz	Presence-Absence	3059-3150	4	(Pinheiro et al., 2003)
Broken Spur	Vent	Mid-Atlantic Ridge	Presence-Absence	3100	1	(Bachraty et al., 2009)
Brothers Seamount	Vent	Kermadec Arc	Presence-Absence	1500	1	(Bachraty et al., 2009)
Bush Hill	Seep	Upper Gulf of Mexico	Abundance	540	4	(D. C. Bergquist et al., 2003)
California shelf	Seep	California Margin	Presence-Absence	35-50	3	(L. A. Levin et al., 2000)
California slope	Seep	California Margin	Presence-Absence	515	6	(L. A. Levin et al., 2000)
Carlos Ribeiro mud volcano	Seep	Gulf of Cadiz	Presence-Absence	2200	2	(Pinheiro et al., 2003)
Chile Trench	Seep	Chile Margin	Presence-Absence	1400	1	(Sibuet & Olu, 1998)
Cleft Segment	Vent	Juan de Fuca	Presence-Absence	2200	1	(Bachraty et al., 2009)
Coaxial Segment	Vent	Juan de Fuca	Presence-Absence	2055	1	(Bachraty et al., 2009)
Concepción	Seep	Chilean Margin	Presence-Absence	814	1	(Sellanes, Quiroga, & Neira, 2008)

Table B4 (continued)

Site	Habitat	Region	Sample Type	Depth (m)	# Samples	Reference
Costa Rica Prism	Seep	Mid-American Trench	Presence-Absence	3500	1	(Sibuet & Olu, 1998)
Dai-ichi Kashima Seamount	Seep	Japan Trench	Presence-Absence	5640-5695	1	(Watanabe et al., 2010)
Dai-ichi Kumano Knoll	Seep	Nankai Trough	Presence-Absence	1900	1	(Watanabe et al., 2010)
Dai-ichi Minami-Muroto Knoll	Seep	Nankai Trough	Presence-Absence	3540-3620	1	(Watanabe et al., 2010)
Dai-ni Atsumi Knoll	Seep	Nankai Trough	Presence-Absence	1042-1100	1	(Watanabe et al., 2010)
Dai-ni Tenryu Knoll	Seep	Nankai Trough	Presence-Absence	500-900	1	(Watanabe et al., 2010)
Dai-roku Kumano Knoll	Seep	Nankai Trough	Presence-Absence	2000	1	(Watanabe et al., 2010)
Dai-san Tenryu Canyon	Seep	Nankai Trough	Presence-Absence	3700-3800	1	(Watanabe et al., 2010)
Dai-yon Kumano Knoll	Seep	Nankai Trough	Presence-Absence	2000	1	(Watanabe et al., 2010)
Desmos Cauldron	Vent	Manus Back-Arc Basin	Presence-Absence	2000	1	(Bachraty et al., 2009)
East Scotia Ridge	Vent	Southern Ocean	Presence-Absence	2400-2600	2	(Rogers et al., 2012)
East Wall	Vent	Northern East Pacific Rise	Abundance	2499	8	(Van Dover, 2003)
Eastern Mediterranean	Seep	Mediterranean	Presence-Absence	1700-2000	1	(Sibuet & Olu, 1998)
Edison Seamount	Vent	Tabar-Feni Volcanic Fore Arc	Presence-Absence	1450	1	(Bachraty et al., 2009)

Table B4 (continued)

Site	Habitat	Region	Sample Type	Depth (m)	# Samples	Reference
Edmond Vent Field	Vent	Central Indian Ridge	Presence-Absence	3300	1	(Bachraty et al., 2009)
El Pilar	Seep	Barbados Accretionary Prism	Presence-Absence	1300	1	(Cordes et al., 2007)
Endeavour Segment	Vent	Juan de Fuca Ridge	Abundance	2122	1	(D. Bergquist et al., 2007)
Endeavour Segment	Vent	Juan de Fuca	Presence-Absence	2210	1	(Bachraty et al., 2009)
Escanaba Trough	Vent	Gorda Ridge	Presence-Absence	3280	1	(Bachraty et al., 2009)
Florida Escarpment	Seep	Florida Escarpment	Abundance	3286-3291	16	(Cordes et al., 2007; Turnipseed, Jenkins, & Dover, 2004)
Florida Escarpment	Seep	Florida Escarpment	Presence-Absence	3234-3500	2	(Lisa A. Levin & Mendoza, 2007; Sibuet & Olu, 1998)
Galapagos Spreading Center	Vent	Galapagos Ridge	Presence-Absence	2560	1	(Bachraty et al., 2009)
German Flats	Vent	Southern East-Pacific Rise	Presence-Absence	2200	1	(Bachraty et al., 2009)
Ginsburg mud volcano	Seep	Gulf of Cadiz	Presence-Absence	910	3	(Pinheiro et al., 2003)
Green Canyon	Seep	Upper Gulf of Mexico	Abundance	560	3	(D. C. Bergquist et al., 2003)
Guaymas Basin	Vent	Gulf of California	Presence-Absence	1900	1	(Bachraty et al., 2009)
Gulf of Cadiz diapir 1	Seep	Gulf of Cadiz	Presence-Absence	1140	1	(Pinheiro et al., 2003)

Table B4 (continued)

Site	Habitat	Region	Sample Type	Depth (m)	# Samples	Reference
Gulf of Cadiz diapir 2	Seep	Gulf of Cadiz	Presence-Absence	1962	1	(Pinheiro et al., 2003)
Gulf of Cadiz submarine channel	Seep	Gulf of Cadiz	Presence-Absence	845	1	(Pinheiro et al., 2003)
Gulf of Guinea	Seep	Gulf of Guinea	Presence-Absence	400-700	1	(Sibuet & Olu, 1998)
Hakon-Mosby Mud Volcano	Seep	Hakon-Mosby	Presence-Absence	1250	1	(Gebruk et al., 2003)
Hatoma Knoll	Vent	Okinawa Trough	Presence-Absence	1528	1	(Bachraty et al., 2009)
Hikurangi Margin	Seep	New Zealand	Presence-Absence	740-1150	8	(Baco, Rowden, Levin, Smith, & Bowden, 2010)
Hine Hina	Vent	Lau Back-Arc Basin	Presence-Absence	1830	1	(Bachraty et al., 2009)
Hydrate Ridge	Seep	Cascadia Margin	Presence-Absence	770	24	(Sahling, Rickert, Lee, Linke, & Suess, 2002)
Iheya Ridge	Vent	Okinawa Trough	Presence-Absence	1392	1	(Bachraty et al., 2009)
Izena Cauldron	Vent	Okinawa Trough	Presence-Absence	1500	1	(Bachraty et al., 2009)
Jesus Baraza mud volcano	Seep	Gulf of Cadiz	Presence-Absence	1091-1159	2	(Pinheiro et al., 2003)
Kagoshima Bay	Vent	Kagoshima Bay	Presence-Absence	105	1	(Bachraty et al., 2009)
Kaikata Seamount	Vent	Izu-Ogasawara Arc	Presence-Absence	400	1	(Bachraty et al., 2009)
Kairei Vent Field	Vent	Central Indian Ridge	Presence-Absence	2450	1	(Bachraty et al., 2009)

Table B4 (continued)

Site	Habitat	Region	Sample Type	Depth (m)	# Samples	Reference
Kanesu-no-se Bank	Seep	Nankai Trough	Presence-Absence	270-300	1	(Watanabe et al., 2010)
Kodiak	Seep	Alaska	Presence-Absence	4425-4430	2	(Lisa A. Levin & Mendoza, 2007)
Kurile Trench	Seep	Japan Trench	Presence-Absence	3800-6000	1	(Sibuet & Olu, 1998)
Kuroshima Knoll	Seep	Nansei-Shoto Trench	Presence-Absence	636-812	1	(Watanabe et al., 2010)
Laurentian Fan	Seep	Laurentian Fan	Presence-Absence	3800-3900	1	(Sibuet & Olu, 1998)
Logatchev	Vent	Mid-Atlantic Ridge	Presence-Absence	2980	1	(Bachraty et al., 2009)
Loihi Seamount	Vent	Intra-Plate Seamount	Presence-Absence	960	1	(Bachraty et al., 2009)
Lucky Strike	Vent	Mid-Atlantic Ridge	Presence-Absence	1700	2	(Bachraty et al., 2009; Desbruyères et al., 2001)
Magic Mountain	Vent	Explorer Ridge	Presence-Absence	1825	1	(Bachraty et al., 2009)
Mariana Trough	Vent	Mariana Back-Arc Basin	Presence-Absence	2800	1	(Bachraty et al., 2009)
Marmara Sea	Seep	Mediterranean	Presence-Absence	1111-1122	8	(Ritt et al., 2010)
Menez Gwen	Vent	Mid-Atlantic Ridge	Presence-Absence	850	2	(Bachraty et al., 2009; Desbruyères et al., 2001)
Mexico	Seep	Mid-American Trench	Presence-Absence	2500-4000	1	(Sibuet & Olu, 1998)
Middle Valley	Vent	Juan de Fuca	Presence-Absence	2450	1	(Bachraty et al., 2009)

Table B4 (continued)

Site	Habitat	Region	Sample Type	Depth (m)	# Samples	Reference
Minami-Ensei Knoll	Vent	Okinawa Trough	Presence-Absence	705	1	(Bachraty et al., 2009)
Mokuyo Seamount	Vent	Izu-Ogasawara Arc	Presence-Absence	1250	1	(Bachraty et al., 2009)
Monterey Bay	Seep	Monterey Bay	Presence-Absence	600-1000	1	(Sibuet & Olu, 1998)
Monterey Fan Valley	Seep	Monterey Fan Valley	Presence-Absence	3000-3600	1	(Sibuet & Olu, 1998)
Muroto Knoll	Seep	Nankai Trough	Presence-Absence	600	1	(Watanabe et al., 2010)
Mussel Valley	Vent	North-Fiji Back-Arc Basin	Presence-Absence	2700	1	(Bachraty et al., 2009)
Myojin Knoll	Vent	Izu-Ogasawara Arc	Presence-Absence	1300	1	(Bachraty et al., 2009)
Nankai Prism	Seep	Nankai Prism	Presence-Absence	2000	1	(Sibuet & Olu, 1998)
Near Axis of Japan Trench	Seep	Japan Trench	Presence-Absence	7326-7434	1	(Watanabe et al., 2010)
Nikko Seamount	Vent	Izu-Ogasawara Arc	Presence-Absence	450	1	(Bachraty et al., 2009)
Nile Deep Sea Fan	Seep	Mediterranean	Presence-Absence	1154	6	(Ritt et al., 2011)
North California Shelf	Seep	North California	Presence-Absence	450-600	1	(Sibuet & Olu, 1998)
North Carolina Slope	Seep	North Carolina	Presence-Absence	2160	1	(Sibuet & Olu, 1998)
North Iheya Knoll	Vent	Okinawa Trough	Presence-Absence	970	1	(Bachraty et al., 2009)

Table B4 (continued)

Site	Habitat	Region	Sample Type	Depth (m)	# Samples	Reference
Northeastern Taiwan	Vent	Okinawa Arc	Presence-Absence	275	1	(Bachraty et al., 2009)
Oasis	Vent	Southern East Pacific Rise	Abundance	2582	8	(Van Dover, 2002)
Off Hatsushima	Seep	Sagami Bay	Presence-Absence	800-1300	1	(Watanabe et al., 2010)
Off Kikaijima Island	Seep	Nansei-Shoto Trench	Presence-Absence	1400-1500	1	(Watanabe et al., 2010)
Off Kumano	Seep	Nankai Trough	Presence-Absence	2100-3250	3	(Watanabe et al., 2010)
Off Muroto	Seep	Nankai Trough	Presence-Absence	3260-4800	3	(Watanabe et al., 2010)
Off Toi	Seep	Suruga Bay	Presence-Absence	1500-1600	1	(Watanabe et al., 2010)
Okinoyama Bank	Seep	Sagami Bay	Presence-Absence	750-1300	1	(Watanabe et al., 2010)
Olenin mud volcano	Seep	Gulf of Cadiz	Presence-Absence	2614	1	(Pinheiro et al., 2003)
Olimpi Mud Volcano	Seep	Mediterranean	Presence-Absence	2000	2	(Olu-Le Roy et al., 2004)
Omaezaki Spur	Seep	Nankai Trough	Presence-Absence	1100-1200	1	(Watanabe et al., 2010)
Oregon Prism	Seep	Oregon Prism	Presence-Absence	2000-2400	1	(Sibuet & Olu, 1998)
Orenoque	Seep	Barbados Accretionary Prism	Presence-Absence	1700-2000	2	(Cordes et al., 2007)
Pacmanus Complex	Vent	Manus Back-Arc Basin	Presence-Absence	1725	1	(Bachraty et al., 2009)

Table B4 (continued)

Site	Habitat	Region	Sample Type	Depth (m)	# Samples	Reference
Peru	Seep	Peruvian Margin	Presence-Absence	3850	1	(Olu, Duperret, Sibuet, Foucher, & Fiala-Médioni, 1996)
Peru Trench	Seep	Peruvian Margin	Presence-Absence	2300-5100	1	(Sibuet & Olu, 1998)
Rabat mud volcano	Seep	Gulf of Cadiz	Presence-Absence	1060	1	(Pinheiro et al., 2003)
Rainbow	Vent	Mid-Atlantic Ridge	Presence-Absence	2320	2	(Bachraty et al., 2009; Desbruyères et al., 2001)
REGAB Pockmark	Seep	Congo-Angola Margin	Presence-Absence	3170	10	(Olu et al., 2009)
Rehu Marka	Vent	Southern East Pacific Rise	Abundance	2581	7	(Van Dover, 2002)
Riftia Field	Vent	Northern East Pacific Rise	Abundance	2500	4	(Govenar et al., 2005)
Rumble V Seamount	Vent	Kermadec Arc	Presence-Absence	600	1	(Bachraty et al., 2009)
Ryuyo Canyon	Seep	Nankai Trough	Presence-Absence	1000-1100	1	(Watanabe et al., 2010)
Sagami Bay	Seep	Sagami Bay	Presence-Absence	900-1200	1	(Sibuet & Olu, 1998)
Sagami Knoll	Seep	Sagami Bay	Presence-Absence	1400-1500	1	(Watanabe et al., 2010)
Saguaro Field	Vent	Southern East-Pacific Rise	Presence-Absence	2330	1	(Bachraty et al., 2009)
San Clemente Fault	Seep	San Clemente Fault	Presence-Absence	1800	1	(Sibuet & Olu, 1998)

Table B4 (continued)

Site	Habitat	Region	Sample Type	Depth (m)	# Samples	Reference
Sanriku Escarpment	Seep	Japan Trench	Presence-Absence	5343-6809	1	(Watanabe et al., 2010)
Sea Cliff Vent Field	Vent	Gorda Ridge	Presence-Absence	2750	1	(Bachraty et al., 2009)
Senoumi Bank	Seep	Suruga Bay	Presence-Absence	200-400	1	(Watanabe et al., 2010)
Snake Pit	Vent	Mid-Atlantic Ridge	Abundance	3490	13	(Turnipseed et al., 2004)
Snake Pit	Vent	Mid-Atlantic Ridge	Presence-Absence	3490	1	(Bachraty et al., 2009)
Sonora Margin	Seep	Guaymas Basin	Presence-Absence	1550-1600	15	(Portail et al., 2015; Sibuet & Olu, 1998)
Southern Trough	Sedimented Vent	Guaymas Basin	Presence-Absence	1900	7	(Portail et al., 2015)
Student mud volcano	Seep	Gulf of Cadiz	Presence-Absence	940-955	3	(Pinheiro et al., 2003)
Suiyo Seamount	Vent	Izu-Ogasawara Arc	Presence-Absence	1350	1	(Bachraty et al., 2009)
Sumisu Caldera	Vent	Izu-Ogasawara Arc	Presence-Absence	920	1	(Bachraty et al., 2009)
TAG	Vent	Mid-Atlantic Ridge	Presence-Absence	3670	1	(Bachraty et al., 2009)
Tasyo mud volcano	Seep	Gulf of Cadiz	Presence-Absence	1098-1100	2	(Pinheiro et al., 2003)
Tenryu Canyon	Seep	Nankai Trough	Presence-Absence	3600-3855	2	(Sibuet & Olu, 1998; Watanabe et al., 2010)
Tica	Vent	Northern East Pacific Rise	Abundance	2500	4	(Govenar et al., 2005)

Table B4 (continued)

Site	Habitat	Region	Sample Type	Depth (m)	# Samples	Reference
Tokai Thrust	Seep	Nankai Trough	Presence-Absence	2120-2360	1	(Watanabe et al., 2010)
Train Station	Vent	Northern East Pacific Rise	Abundance	2491	8	(Van Dover, 2003)
Tubeworm Site	Seep	Kagoshima Bay	Presence-Absence	80-130	1	(Watanabe et al., 2010)
Unimak	Seep	Alaska	Presence-Absence	3267-3283	2	(Lisa A. Levin & Mendoza, 2007)
Upper Louisiana Slope	Seep	Upper Gulf of Mexico	Presence-Absence	400-1000	1	(Sibuet & Olu, 1998)
Vai Lili	Vent	Lau Back-Arc Basin	Presence-Absence	1707	1	(Bachraty et al., 2009)
Vailulu'u Seamount	Vent	Intra-Plate Seamount	Presence-Absence	700	1	(Bachraty et al., 2009)
Vienna Woods	Vent	Manus Back-Arc Basin	Presence-Absence	2500	1	(Bachraty et al., 2009)
West Kurile Trench	Seep	Japan Trench	Presence-Absence	5131-5785	1	(Watanabe et al., 2010)
White Lady	Vent	North-Fiji Back-Arc Basin	Presence-Absence	1960	1	(Bachraty et al., 2009)
Yukie Ridge	Seep	Nankai Trough	Presence-Absence	1940-2180	1	(Watanabe et al., 2010)
Zenisu Ridge	Seep	Nankai Trough	Presence-Absence	3300	1	(Watanabe et al., 2010)

APPENDIX C

PERMISSION FOR INCLUSION OF COPYRIGHTED MATERIAL

1/22/2018

RightsLink Printable License

SPRINGER NATURE LICENSE TERMS AND CONDITIONS

Jan 22, 2018

This Agreement between Dr. Alanna Durkin ("You") and Springer Nature ("Springer Nature") consists of your license details and the terms and conditions provided by Springer Nature and Copyright Clearance Center.

License Number	4274340747391
License date	Jan 22, 2018
Licensed Content Publisher	Springer Nature
Licensed Content Publication	Naturwissenschaften
Licensed Content Title	Extreme longevity in a deep-sea vestimentiferan tubeworm and its implications for the evolution of life history strategies
Licensed Content Author	Alanna Durkin, Charles R. Fisher, Erik E. Cordes
Licensed Content Date	Jan 1, 2017
Licensed Content Volume	104
Licensed Content Issue	7
Type of Use	Thesis/Dissertation
Requestor type	academic/university or research institute
Format	print and electronic
Portion	full article/chapter
Will you be translating?	no
Circulation/distribution	>50,000
Author of this Springer Nature content	yes
Title	The ecology of deep-sea chemosynthetic ecosystems, from populations to metacommunities
Instructor name	Dr. Erik Cordes
Institution name	Temple University
Expected presentation date	Jan 2018
Portions	Full article
Requestor Location	Dr. Alanna Durkin 1900 N. 12th St. FAIRMOUNT, PA 19121 United States Attn: Dr. Alanna Durkin
Billing Type	Invoice
Billing Address	Dr. Alanna Durkin 1439 Mount Hope Ave. BUCK RUN, PA 17901 United States Attn: Dr. Alanna Durkin

<https://s100.copyright.com/CustomerAdmin/PLF.jsp?ref=2364a9cd-43ea-4129-b3d8-1ff1e6225512>

1/3

Total 0.00 USD

[Terms and Conditions](#)

Springer Nature Terms and Conditions for RightsLink Permissions
Springer Customer Service Centre GmbH (the Licensor) hereby grants you a non-exclusive, world-wide licence to reproduce the material and for the purpose and requirements specified in the attached copy of your order form, and for no other use, subject to the conditions below:

1. The Licensor warrants that it has, to the best of its knowledge, the rights to license reuse of this material. However, you should ensure that the material you are requesting is original to the Licensor and does not carry the copyright of another entity (as credited in the published version).

If the credit line on any part of the material you have requested indicates that it was reprinted or adapted with permission from another source, then you should also seek permission from that source to reuse the material.
2. Where print only permission has been granted for a fee, separate permission must be obtained for any additional electronic re-use.
3. Permission granted free of charge for material in print is also usually granted for any electronic version of that work, provided that the material is incidental to your work as a whole and that the electronic version is essentially equivalent to, or substitutes for, the print version.
4. A licence for 'post on a website' is valid for 12 months from the licence date. This licence does not cover use of full text articles on websites.
5. Where 'reuse in a dissertation/ thesis' has been selected the following terms apply: Print rights for up to 100 copies, electronic rights for use only on a personal website or institutional repository as defined by the Sherpa guideline (www.sherpa.ac.uk/romeo/).
6. Permission granted for books and journals is granted for the lifetime of the first edition and does not apply to second and subsequent editions (except where the first edition permission was granted free of charge or for signatories to the STM Permissions Guidelines <http://www.stm-assoc.org/copyright-legal-affairs/permissions/permissions-guidelines/>), and does not apply for editions in other languages unless additional translation rights have been granted separately in the licence.
7. Rights for additional components such as custom editions and derivatives require additional permission and may be subject to an additional fee. Please apply to Journalpermissions@springernature.com/bookpermissions@springernature.com for these rights.
8. The Licensor's permission must be acknowledged next to the licensed material in print. In electronic form, this acknowledgement must be visible at the same time as the figures/tables/illustrations or abstract, and must be hyperlinked to the journal/book's homepage. Our required acknowledgement format is in the Appendix below.
9. Use of the material for incidental promotional use, minor editing privileges (this does not include cropping, adapting, omitting material or any other changes that affect the meaning, intention or moral rights of the author) and copies for the disabled are permitted under this licence.
10. Minor adaptations of single figures (changes of format, colour and style) do not require the Licensor's approval. However, the adaptation should be credited as shown in Appendix below.

[Appendix — Acknowledgements:](#)

For Journal Content:

Reprinted by permission from [the Licensor]: [Journal Publisher (e.g. Nature/Springer/Palgrave)] [JOURNAL NAME] [REFERENCE CITATION (Article name, Author(s) Name), [COPYRIGHT] (year of publication)]

For Advance Online Publication papers:

Reprinted by permission from [the Licensor]: [Journal Publisher (e.g. Nature/Springer/Palgrave)] [JOURNAL NAME] [REFERENCE CITATION (Article name, Author(s) Name), [COPYRIGHT] (year of publication), advance online publication, day month year (doi: 10.1038/sj.[JOURNAL ACRONYM].)]

For Adaptations/Translations:

Adapted/Translated by permission from [the Licensor]: [Journal Publisher (e.g. Nature/Springer/Palgrave)] [JOURNAL NAME] [REFERENCE CITATION (Article name, Author(s) Name), [COPYRIGHT] (year of publication)]

Note: For any republication from the British Journal of Cancer, the following credit line style applies:

Reprinted/adapted/translated by permission from [the Licensor]: on behalf of Cancer Research UK: : [Journal Publisher (e.g. Nature/Springer/Palgrave)] [JOURNAL NAME] [REFERENCE CITATION (Article name, Author(s) Name), [COPYRIGHT] (year of publication)]

For Advance Online Publication papers:

Reprinted by permission from The [the Licensor]: on behalf of Cancer Research UK: [Journal Publisher (e.g. Nature/Springer/Palgrave)] [JOURNAL NAME] [REFERENCE CITATION (Article name, Author(s) Name), [COPYRIGHT] (year of publication), advance online publication, day month year (doi: 10.1038/sj.[JOURNAL ACRONYM].)]

For Book content:

Reprinted/adapted by permission from [the Licensor]: [Book Publisher (e.g. Palgrave Macmillan, Springer etc) [Book Title] by [Book author(s)] [COPYRIGHT] (year of publication)]

Other Conditions:

Version 1.0

Questions? customercare@copyright.com or +1-855-239-3415 (toll free in the US) or +1-978-646-2777.